DOCTORAL THESIS

Organosolv Lignin: From Characterization to Esterification

Thị Thùy Trân Hồ

TALLINNA TEHNIKAÜLIKOOL
TALLINN UNIVERSITY OF TECHNOLOGY
TALLINN 2026

TALLINN UNIVERSITY OF TECHNOLOGY
DOCTORAL THESIS
8/2026

Organosolv Lignin: From Characterization to Esterification

Thị Thùy Trân Hồ

TAL TECH PRESS

TALLINN UNIVERSITY OF TECHNOLOGY
School of Science
Department of Chemistry and Biotechnology
The dissertation was accepted for the defence of the degree of Doctor of Philosophy in Chemistry on 07/01/2026

Supervisor: Dr. Maria Kulp
Department of Chemistry and Biotechnology
Tallinn University of Technology
Tallinn, Estonia

Co-supervisor: Dr. Yevgen Karpichev
Department of Chemistry and Biotechnology
Tallinn University of Technology
Tallinn, Estonia

Opponents: Dr. Jānis Rižikovs
Biorefinery Laboratory
Latvian State Institute of Wood Chemistry
Riga, Latvia

Prof. Timo Kikas
Institute of Forestry and Engineering
Estonian University of Life Sciences
Tartu, Estonia

Defence of the thesis: 05/02/2026, Tallinn

Declaration:
Hereby I declare that this doctoral thesis, my original investigation and achievement, submitted for the doctoral degree at Tallinn University of Technology has not been submitted for doctoral or equivalent academic degree.

Hồ Thị Thùy Trân (T.Tran Ho)

---
signature

European Union
European Regional
Development Fund

Investing
in your future

ISSN 2585-6898 (publication)
ISBN 978-9916-80-455-1 (publication)
ISSN 2585-6901 (PDF)
ISBN 978-9916-80-456-8 (PDF)
DOI https://doi.org/10.23658/taltech.8/2026
Printed by Koopia Niini & Rauam

Ho, T. T. (2026). *Organosolv Lignin: From Characterization to Esterification* [TalTech Press]. https://doi.org/10.23658/taltech.8/2026

TALLINNA TEHNIKAÜLIKOOL
DOKTORITÖÖ
8/2026

Organosolv ligniin: koostise iseloomustamisest esterdamiseni

Thị Thùy Trân Hồ

TAL TECH
KIRJASTUS

Contents

List of publications

The dissertation has been prepared based on the obtained results from the following publications:

I Piia Jõul*, **T. Tran Ho***, Urve Kallavus, Alar Konist, Kristiina Leiman, Olivia-Stella Salm, Maria Kulp, Mihkel Koel, and Tiit Lukk. Characterization of Organosolv Lignins and Their Application in the Preparation of Aerogels. *Materials* **2022**, *15*, 2861 https://doi.org/10.3390/ma15082861

II **T. Tran Ho**, Olivia-Stella Salm, Tiit Lukk, and Maria Kulp. Utilization of phenolic lignin dimer models for the quantification of monolignols in biomass and in its derived organosolv lignins via thioacidolysis and GC-MS analysis. *Analytical Methods* **2025**, *17*, 3283–3289, https://doi.org/10.1039/D5AY00073D

III Mahendra Kothottil Mohan*, **T. Tran Ho***, Carmen Köster, Oliver Järvik, Maria Kulp, Yevgen Karpichev. Tuning ester derivatives of organosolv vs technical lignin for improved thermoplastic materials. *Faraday Discussions* **2026**, https://doi.org/10.1039/D5FD00068H

* These authors contributed equally

Author's contribution to the publications

Contribution to the papers in this thesis are:

I The author played a significant role in carrying out of experiments for characterization of lignin by NMR, data analysis, preparation and revision of the manuscript.

II The author has conceptualized, carried out all the experiments, analysed the data, prepared and revised the manuscript.

III The author played a significant role in synthesis and characterization of the organosolv lignin esterified via hydroxyl groups, analysis of NMR data and preparation of the manuscript.

Preface

Lignocellulosic biomass (LCB) is a non-edible plant-based feedstock (primarily sourced from forestry residues, agricultural wastes, energy crops) that consists of cellulose, hemicellulose and lignin. The three macropolymers are non- or covalently bonded to form a rigid and supportive platform for plant cell wall. In biorefineries, these lignin-carbohydrate complexes are separated by different methodologies, however regardless of the treatments, sugar products are always prioritized. Meanwhile, lignin is perceived as waste even though it is the highest aromatic compounds containing source in nature and constitutes a significant proportion of LCB. A major setback of lignin arises from its heterogeneity in constituents, bonding motifs, and inevitable structural modification as a consequence of biomass processing. Regarding structural complexity, native lignin is mainly made up of three monolignols, *p*-coumaryl, coniferyl, and sinapyl alcohols, which are transformed into the corresponding *p*-hydroxylphenyl (H), guaiacyl (G), and syringyl (S) units in plant cell wall, with variation in ratios from species to species. Depending on the severity of fractionation process, the downstream lignin experiences different degrees of depolymerization and repolymerization, leading to the formation of a newly arranged network with respect to the native. Due to the intrinsic complexity of lignin presents in either native or product forms, the study of its structure is always an essential step prior to fully unleashing its potential and maximizing efficiency of biorefineries, and thus never being outdated.

To contribute to the ongoing effort of understanding lignin, three types of biomass representing hardwood (aspen chips), softwood (pine sawdust), non-woody (barley straw) and their lignin samples extracted by organic solvent pulping process (organosolv) were opted as the main objects throughout the study. Within the scope of characterization, nuclear magnetic resonance (NMR), 1D (^{31}P) and 2D (heteronuclear single quantum coherence) were applied to quantify hydroxyl contents, and elucidate interlinkages and subunits in organosolv lignins, respectively (**Paper I**). Further details about the monolignols concentration in biomasses and their organosolv lignins were quantitatively analysed by thioacidolysis coupled with GC-MS, in which the challenging aspect of lignin's authentic standard was resolved (**Paper II**).

The study continued to shift from characterization to its modification and its impact on thermal and mechanical properties of the composites manufactured with polylactic acid (PLA). Particularly, esterification was carried out using two approaches: one targeted modification of the hydroxyl groups of lignin, and the other introduced ester groups onto the lignin's aromatic rings while retaining hydrogen bonding. The fascinating outcomes of esterification at different positions within the lignin structure influenced the composite's properties (**Paper III**).

In addition to the published articles, the results of this research have been communicated internationally at several conferences held in Estonia, Finland, and Greece.

Abbreviations

^{31}P NMR	Phosphorous nuclear magnetic resonance
BAEP	Benzoic esterified lignin by chloromethylation
BF_3	Boron trifluoride diethyl etherate
BSTFA, 1% TMCS	*N,O*-Bis(-trimethylsilyl)trifluoroacetamide containing 1% trimethylchlorosilane
C12	C12 hydroxyl-esterified lignin
C16	C16 hydroxyl-esterified lignin
C8	C8 hydroxyl-esterified lignin
CML	Chloromethylated lignin
DOL	1,4-dioxane extracted lignin
DSC	Differential scanning calorimetry
DTG	Derivative thermogravimetry
EI	Electron ionization
EIC	Extracted ion chromatogram
EOL	Ethanol extracted lignin
FTIR	Fourier transform infrared spectroscopy
G	Guaiacyl unit
GC-FID	Gas chromatography-flame ionization detector
GGE	Guaiacylglycerol-β-guaiacyl ether
H	*p*-hydroxylphenyl unit
HLE	C14 esterified hydrolysis lignin by chloromethylation
HSQC	Heteronuclear single quantum coherence
IDL	Instrumental detection limit
IQL	Instrumental quantification limit
IS	Internal standard
LCB	Lignocellulosic biomass
LCC	Lignin-carbohydrate complexes
LMCs	Phenolic lignin model compounds
LOQ	Limits of quantification
LTM MACH	Low thermal mass modular accelerated column heater
MSD	Mass selective detector
NHND	endo-*N*-hydroxy-5-norbornene-2,3-dicarboximide
NMR	Nuclear magnetic resonance
PLA	Polylactic acid
R	Recovery
RRF	Relative response factor
RSD	Relative standard deviation
S	Syringyl unit

SGE	Syringylglycerol-β-guaiacyl
TEA	Triethylamine
TGA	Thermogravimetric analysis
THF	Tetrahydrofuran
TIC	Total ion chromatogram
TMDP	2-chloro-4,4,5,5-tetramethyl-1,3,2-dioxaphospholane
ΔCp	Specific heat capacity

1 Literature overview

The review provides a brief introduction to lignocellulosic biomass by clarifying its definition, sources, compositions, and applications in biorefineries. In the following sections, the background for the three articles is presented.

1.1 Lignocellulosic biomass

In human history, the discovery of fire by our ancestors million years ago has been a crucial milestone marking the initial usage of lignocellulosic biomass (LCB) for energy by combustion, along with the construction and textile applications [1], [2]. During the industrial revolution, the utilization of this renewable feedstock has been extensively advanced since the development of chemical bleaching and fermentation technologies was successfully applied in the paper industry, and biofuel production, respectively [1], [3]. Nowadays, the exhaustion of fossil-based resources due to overexploitation and the alarming increase in greenhouse gases emissions demand the finding of alternatives that could alleviate the stress and aid the development of a sustainable living world. To address the issue, one of the possible solutions is to shift our reliance on fossil feedstocks to LCB, which is outstandingly noted for its renewability and abundance [2].

The term LCB was coined to describe a group of non-food biomasses originating from energy crops, grasses, agricultural residues, forestry waste, and papermaking by-products [4]. 'Lignocellulose' is a compound word merging the prefix – 'lignin' and the suffix – 'cellulose', which are the key compositions present in the biomass belonging to this category [1]. In fact, the secondary plant cell wall of LCB is a rigid network that is built from three main components namely, cellulose, hemicellulose, and lignin (Figure 1) [5]. These three biopolymers coexist at varying ratios depending on the botanical origin and are non- or covalently interconnected to form a structural support for the plant [4]. Overall, LCB contains 40–50% of cellulose, 20–30% of hemicellulose, 18–35% of lignin, and a minor portion of other components (e.g., extractives, minerals) [6].

Cellulose is a semi-crystalline homopolymer consisting of approximately 7,000 to 15,000 D-glucose monomer units linked by β-(1→4) glycosidic bonds in equatorial configuration [1]. The orientation of cellulose chains is primarily driven by the hydrogen bonding and Van der Waals interactions leading to the formation of microfibrils, which play an important role in the architecture of the cell structure [5]–[7]. On the other hand, hemicellulose is an amorphous heteropolymer made up of 70 to 200 different sugar monomers including xylose, arabinose, galactose, glucose and mannose [1]. The distribution of these monosaccharides is highly dependent on biomass species [4]. Hemicellulose backbone is built by pentoses or hexoses linked by β-(1→4) linkages, akin to cellulose; however, it is a non-linear polysaccharide due to the additional pendant groups (e.g., monosaccharides, uronic acids, and acetyl groups) branching off the main polymer chain [5], [8]. In the matrix of secondary cell wall, hemicellulose was found to be strongly adsorbed onto the surface of cellulose bundles via non-covalent bonding, thus improving the mechanical strength and flexibility [9], [10]. Additionally, the spatial arrangement of hemicellulose around cellulose fibrils is crucial for augmenting the proximity between cellulose and lignin [9].

Lignin is the main non-carbohydrate component found in plant cell wall. It is a complex polyphenolic polymer that is constructed from three fundamental phenylpropanoid-derived monolignols: *p*-coumaryl, coniferyl, and sinapyl alcohols [11]. Lignification

sequentially occurs in three steps: the biosynthesis of monolignols, the translocation of the resulting monomer precursors from cytosol to cell wall, and the radical coupling of oxidative monolignols [12]–[14]. Upon completion of the lignification process, three monolignols are converted into *p*-hydroxyphenyl (H), guaiacyl (G), and siringyl (S) units corresponding to their origins, *p*-coumaryl, coniferyl, and sinapyl alcohols, respectively. In nature, the feature of polymeric lignin is strictly defined by plant species [8], [15]. Softwood lignin mainly derives from G units with the minority of others, while hardwood lignin is principally constructed from S and G units [4], [6]. By contrast, grass lignin contains all three and other unconventional monolignols [8], [16], [17]. Unlike holocellulose (cellulose and hemicellulose), lignin units are crosslinked by different key bonding motifs, such as β-O-4', β-β', β-5', and dibenzodioxocin that resulted from combinatorial polymerization in the secondary cell wall (Figure 1) [8], [15], [18]. The Greek notations (α, β, γ) indicate three carbon atoms in the propyl chain starting from the carbon directly attached to the aromatic ring. Among the interlinkages, aryl-ether bonds (β-O-4') were recorded to be the most prevalent regardless of the biomass sources (up to 50% in softwood, 62% in hardwood, and 84% in non-woody biomass) [8]. Lignin is embedded in the polysaccharide matrix by the formation of ether and ester bonds with hemicellulose, resulting in lignin-carbohydrate complexes (LCC) [19], [20]. These covalent bonds are formed between the hydroxyl or carboxylic groups of carbohydrates and the α-hydroxyl of lignin sidechain or C-4 position in the benzene ring [8], [20], [21]. The nature of this hybrid structure reinforces the mechanical strength of the cell wall, provides the antibacterial properties, and contributes to the recalcitrance of biomass [22], [23]. However, LCC poses challenges for secondary biorefineries where individual constituents need to be efficiently separated for valorisation [19], [24].

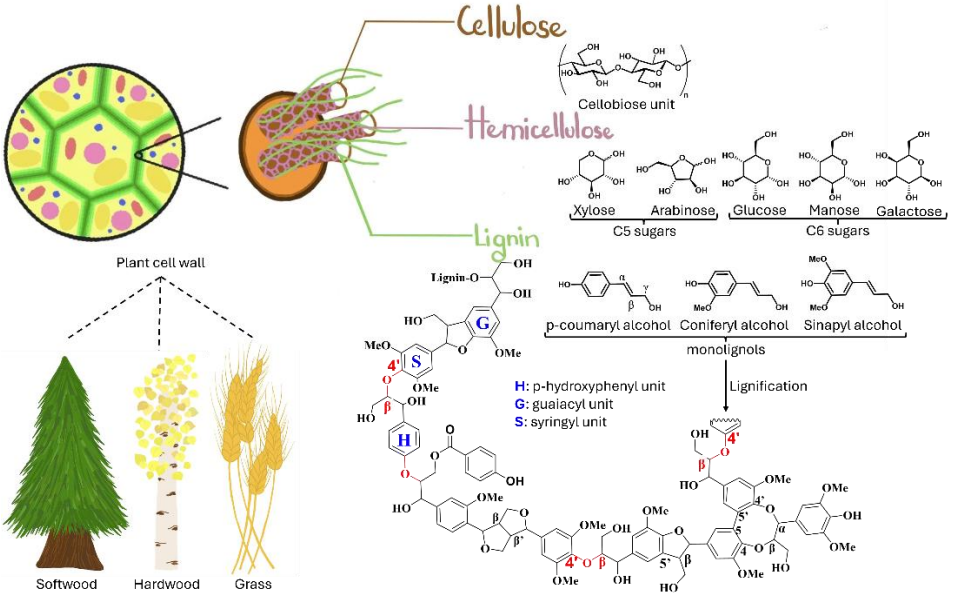

Figure 1. *Illustration of lignocellulosic biomass compositions, cellulose, hemicellulose, lignin, and their monomer units that compose each biopolymer. An additional demonstration of lignin polymer is sketched with typical bonding motifs (β-O-4', β-β', β-5', and dibenzodioxocin).*

Regarding lignocellulose applications, the value of individual component is considered separately [25]. Fibrous cellulose material significantly contributes to paper, textile, and packaging industries. Furthermore, cellulose-derived nanomaterials are widely employed for energy storage, photovoltaic devices and drug delivery [26], [27]. Hemicellulose is a promising material for the food industry, and the production of bioethanol and other chemicals (e.g., sorbitol, xylitol, and 2,3-butanediol) [25], [28]. Among all, lignin valorisation remains challenging due to its heterogeneity. In paper mills, a large portion of lignin is burned for energy, while part of it is recovered for higher-value added applications, biomedicine, biochemicals (e.g., vanillin, phenolic derivatives) and bio-based products (e.g., plastic filler, bitumen, phenolic resin) [8], [25], [29]. Fortunately, with the ongoing intensive research in lignin valorisation, it is envisioned that lignin would play a significant role in biorefineries [30].

1.2 Characterization of organosolv lignin by NMR

Organosolv lignin is a type of technical lignin that is produced as a byproduct in the bioethanol industry [31]. It is named after the process called organosolv that uses a wide range of organic solvents (alcohols [32], organic acids [33], ethers [34], esters [35], or ketones [36]), at elevated temperature, with or without the presence of inorganic acid or base as a catalyst to release lignin from the recalcitrant lignocellulosic biomass cell wall. The industrial scale of organosolv technique was initially introduced in the 1990s, known as Alcell treatment, followed by other scale-ups progressively developed until nowadays [37]. Organosolv process produces lignin with a variety of structural features depending on the severity factor, meaning lignin's physiochemical properties can be tuned according to the extraction condition [38].

Several advantages have been marked down for organosolv pulping, such as high yield of enzymatic treatment for cellulosic pulp, high purity and free-sulfur lignin production, and possible recovery of solvent for the next use [37], [39], [40]. On the other hand, the concept also faces some hurdles, mainly related to the operating expense. This cost-ineffective issue lies in the price of the solvent, the extensive washing process before submitting cellulose-rich pulp to the enzymatic treatment, and expensive equipment due to the volatile nature of the organic solvent [37]. Among biomass treatment methods, organosolv pulping is one of the most effective for preserving the native structure of lignin [8]. This type of lignin could be extracted from the biomass with the least modification and thus closest to its native state. For that reason, organosolv lignin is usually favorable for structural elucidation studies [41], [42].

In lignin chemistry, spectroscopic methods are indispensable tools for investigating the structure of lignin [43]. For example, one, and two-dimensional nuclear magnetic resonance (NMR) techniques are widely employed for this purpose. The principle of NMR method is based on the resonance of radio frequency of nucleus that has spin quantum number differs from zero (e.g., ^{1}H, ^{13}C, ^{31}P) in the presence of a strong external magnetic field. As nuclei resonate, the magnetic moment is perturbed from its equilibrium state, and its unique frequency decay when coming back to the initial position is dependent on chemical environment or electron density around nuclei. This phenomenon is known as chemical shift (ppm), which is characteristic and meaningful for structural elucidation. The application of ^{31}P NMR and 2D-heteronuclear single quantum coherence (2D-HSQC) in lignin field is well-known for quantification of hydroxyl content and lignin units, interunit linkages studies, respectively [44]. Nowadays, the most widely used ^{31}P experiment was developed by Argyropoulus et al [45]. It requires lignin derivatization

with appropriate phosphitylation reagent (e.g., 2-chloro-4,4,5,5-tetramethyl-1,3,2-dioxaphospholane) prior to the analysis. The phosphorous-derivatized lignin exhibited well-resolved signals corresponding to different origins, including aliphatic, carboxylic, or phenolic hydroxyl groups. With an appropriate internal standard, the method enables quantitative determination of their concentrations [44]. In addition to ^{31}P, HSQC experiment shows correlation of the protons that are directly connected to the carbon atoms. Such information is greatly useful for understanding the units and interlinkages that remained in lignin after treatment process as well as its biomass origin [43].

Apparently, the variety source of biomass and the extraction conditions are two key factors that influence the structure of lignin. To contribute to the existing knowledge of lignin, **Paper I** devoted NMR techniques to study organosolv lignin. Structural characterization was performed for a total of six samples that fractionated from three representative biomasses (e.g., softwood – pine sawdust, hardwood – aspen chips, and non-woody – barley straw) using two organic solvent systems, ethanol and 1,4-dioxane under dilute acidic condition. The information about hydroxyl content, and the subunits/interlinkages was revealed by ^{31}P, and 2D-HSQC, respectively. A thorough discussion about the different observations in terms of biomass origin and the impact of used solvent will be provided.

1.3 Quantifying uncondensed monolignols using thioacidolysis followed by GC-MS analysis

As has been discussed, the intrinsic complexity of lignin is attributed to the diversity of monolignols and bonding motifs. Additionally, due to the biomass treatment process, lignin is inevitably facing structural modification, which adds difficulties to valorizing this macromolecule. Therefore, gaining knowledge of the structure of lignin is a crucial first step prior to extracting its maximum value. To unravel the intricate polymeric network of lignin, data from different analytical techniques must be acquired. In addition to NMR methods for structural analysis (e.g., ^{31}P for hydroxyl content, and 2D-HSQC for subunits, and interlinkages characterization), thioacidolysis coupled with gas chromatography-mass spectrometry (GC-MS) is an essential tool for revealing another facet of lignin: the concentration of uncondensed monolignols.

Under acidic organosolv pulping conditions, lignin depolymerization occurs simultaneously with repolymerization, which is known as condensation (Figure 2) [46], [47]. This undesirable reaction is initiated by the hydrolysis of ether bonds generating carbocations at C_α. These highly reactive species can easily react with other electron-rich carbon atoms in the benzene ring of another lignin monomers, forming new stable C-C bonds. As a result, more condensed fragments are obtained in isolated lignin compared to its native counterparts, which adversely influences the upgradation [48], [49]. Monitoring and controlling lignin's condensation is undoubtedly essential for further valorizing lignin into value-added chemicals [50].

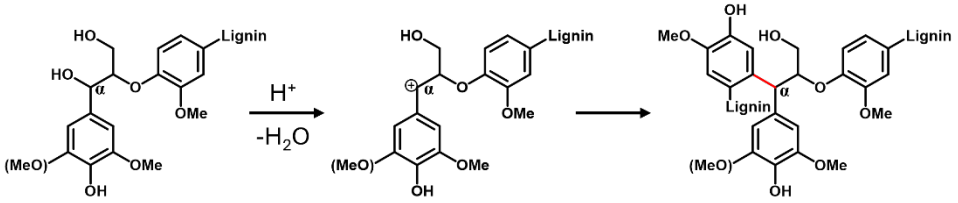

Figure 2. *The elimination of water via formation of carbocation at α-position of lignin sidechain under acidic condition, followed by new carbon-carbon bond (red) formation during condensation reaction.*

Thioacidolysis method was firstly developed by Lapierre in 1985 [51]. Since then, it has been widely used as the diagnostic test for lignin. A mixture of ethanethiol dissolved in 1,4-dioxane and boron trifluoride (BF_3) etherate was used as the depolymerization reagent to efficiently and selectively break down lignin macromolecule into its constituent subunits (H, G, and S) that interconnect via β-O-4' linkages [19], [51], [52]. The resulting monomers were then derivatized and analyzed by GC-MS (Figure 3). The interpretation of data obtained from this method is straightforward. A higher recovery monolignol yield indicates the better preservation of labile β-O-4' bonds. In other words, the given extraction condition produces lignin that is more suitable for high value-added applications.

Throughout decades, scientists have been focusing on improving throughput of the method [53]–[59]. The refinement initially focused on minimizing the amount of starting material and thioacidolysis reagent used. This optimization reduced tenfold of chemicals needed compared to the conventional method, facilitating the thioethylated purification process [54], [57]. The workup procedure was then considered to replace chlorinated solvents with ethyl acetate or diethyl ether for the liquid-liquid extraction of thioethylated monomers [54], [56]. The introduction of Low Thermal Mass Modular Accelerated Column Heater (LTM MACH) coupled with gas chromatography-flame ionization detector (GC-FID) by Harman-Ware significantly decreased the acquisition time to five minutes per analysis [56]. Recently, the development of multi-reaction monitoring (MRM) mode of MS detectors has contributed to the success of analyzing monolignols at ppb concentration level [59]. Despite all efforts, the method still faced hurdles, arising from the time-consuming liquid extraction workup. To tackle this, the protocol was redesigned by F. Chen and colleagues to eliminate this tedious step without compromising results [58].

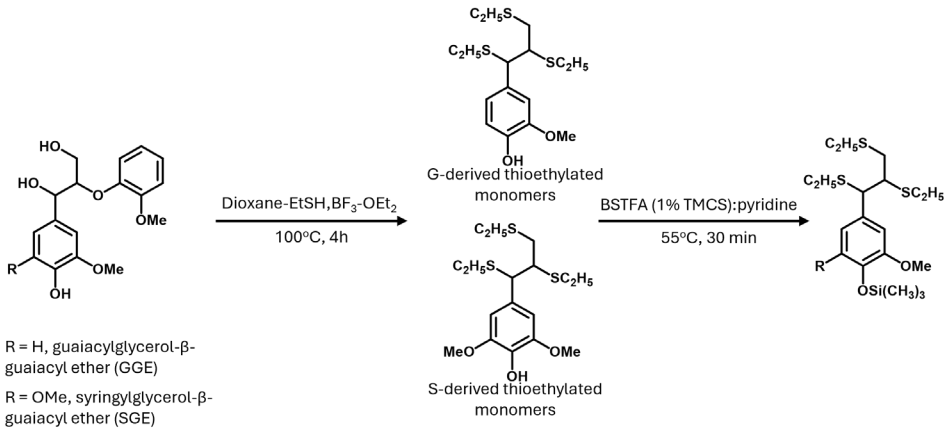

Figure 3. *Thioacidolysis and derivatization reactions scheme of lignin.*

Since lignin is a macromolecule, whose structure substantially varies among biomass species, it is uncommon to have a lignin's standard for thioacidolysis study. This limitation motivated Yue's group to propose the syntheses of thioethylated monolignols from which the relative response factors (RRFs) were calculated against the internal standard (IS) [60]:

$$\text{RRF} = \frac{\frac{W_S}{A_S}}{\frac{W_{IS}}{A_{IS}}} \qquad (1)$$

where W_S and W_{IS} represent the mass or concentration of thioacidolysis-derived monomers and the used internal standard, respectively, while A_S and A_{IS} are their corresponding peak areas. The obtained RRFs were successfully applied to quantify uncondensed monolignols in different biomasses. However, the fundamental limitation of RRF approach is the requirement for pure analyte, which needs to be synthesized, purified and characterized through several steps. Thus, the approach may not be feasible for all laboratories. Additionally, RRF is a conditionally dependent parameter that can experience significant fluctuation due to small changes in, for example, the choice of IS, the sample preparation, the instrument, the operation condition, or other variables, leading to an increase in the uncertainty in analytical results [61], [62]. Based on these considerations, it is concluded that the pre-determined RRFs cannot be applied across laboratories for quantitative measurements without the availability of pure analytes.

Despite all the efforts for thioacidolysis/GC-MS improvement, the lack of lignin standard for the quantification of non-condensed monolignols remains challenging for the field. In this thesis, **Paper II** proposed a solution to overcome the tedious lab work for the syntheses of lignin-derived thioethylated monomers. Here, the application of two phenolic lignin model compounds (LMCs) (Figure 3), guaiacylglycerol-β-guaiacyl ether (GGE), and syringylglycerol-β-guaiacyl ether (SGE) were studied as lignin's standards for the quantification of monolignols. This potential usage of model compounds has not yet been reported elsewhere. The validated LMC-based method was applied for the quantification of monolignols in virgin biomass, and in the extracted lignin samples.

1.4 Esterification of lignin and its composites with PLA

The intrinsic heterogeneity of lignin hampers its utilization in high-value applications at the top of the valorisation hierarchy (e.g., fine chemicals, phenol derivatives, carbon fibres) compared to low-value usage (e.g., energy) [63]. On the other hand, lignin possesses captivating structure with high aromaticity and abundant hydroxyl groups offering tremendous potential in polymer industry [64]–[67]. It can impart improved thermomechanical stability, antioxidant, antibacterial, and UV-resistance properties, and more importantly it is plentiful and low cost [65], [68], [69]. From this point of view, lignin is a promising alternative to replace petroleum-based polymers, alleviating our reliance on fossil-based resources concurrently accelerating the innovation in biopolymers.

However, a high-density crosslinked structure and the rigidity of lignin due to hydrogen bonding, π-π stacking and van der Waals interactions have been reported to adversely affect its compatibility with other commercial polymers [64], [67]. These self-interactions often cause lignin to aggregate, thus getting expelled from the polymer matrix. Microscopic examination has shown that at the same blending ratio, unmodified kraft lignin samples showed uneven distribution in polypropylene matrix, while esterified lignin (e.g., with maleic anhydride) exerted more uniform behaviour [70]. The same trend was observed for polyethylene composite in which non-modified lignin agglomerated into large particles and was immiscible with polymer matrix, while butyrated lignin showed markedly improved compatibility [71]. Additional evidence was recorded that unmodified lignin's aggregation led to phase separation when blending with polybutylene succinate, which was attributed to poor interfacial interaction compared to those modified ones [72]. Molecular dynamics simulations have shown that disruption of hydrogen bonding was one of the fundamental reasons preventing lignin from agglomeration in polylactic acid (PLA) blends [73]. Generally, modification endows lignin derivatives with greater flexibility, compatibility with commercial polymers, better solubility in organic solvents, and improved processability [74]. Therefore, a successful incorporation of lignin into polymeric materials necessitates chemical modification, commonly esterification [74].

In practice, the abundance of hydroxyl groups in lignin structure can be conveniently exploited for such purposes [75], [76]. Direct esterification could be carried out with carboxylic acids [77]–[79], acid anhydrides [80], or acid chlorides [81], [82] in the presence of suitable catalyst, or by a solventless approach – reactive extrusion [72]. In addition to that our recent proposal for a greener esterification strategy of lignin tends to preserve hydroxyl groups by the introduction of a new proactive centre onto the aromatic rings [83]. The resultant intermediates, chloromethylated lignin (CML), possesses highly reactive sites that are preference for several functionalization possibilities. One of which is esterification using carboxylic acid. Interestingly, with the maintenance of hydrogen bonding, the functionalized materials have been studied for PLA composite in which up to 30% by weight of tetradecanoic acid-esterified lignin was successfully blended with PLA without any phase separation observed [84].

Although lignin esterification for making PLA composites is not novel, a comprehensive review of how different modification pathways impact the final materials has not yet been concluded. In this thesis, **Paper III** firstly focused on the synthesis and characterization of hydroxyl-esterified lignins using FTIR and ^{31}P NMR. Esterified lignins obtained from two distinct approaches: (i) direct esterification with acid chloride, and (ii) chloromethylation followed by esterification with carboxylic acid, were evaluated for preparation of PLA

composites. A comprehensive study of thermal and mechanical properties (conducted by DSC and TGA) of esterified lignin-PLA composites will be thoroughly discussed. This study underscores the importance of choosing a specific lignin modification approach to tailor the thermomechanical properties of PLA composites – an aspect that has not yet been investigated.

2 Research Objectives

This work is focused on giving an in-depth understanding of the solvent choice in organosolv fractionation influencing lignin's structure and revealing the two possible esterification pathways of lignin in tailoring properties of polylactic acid (PLA) composites.

The specific aims of this dissertation were:

- To investigate the structural differences in organosolv lignin extracted by ethanol and 1,4-dioxane from three different biomass sources: hardwood (aspen), softwood (pine) and grass (barley straw). To apply ^{31}P-NMR and HSQC techniques for elucidation of the changes in content of hydroxyl groups and β-O-4' linkages depending on the used solvent, and the lignin subunits.
- To address the lack of suitable lignin standards for thioacidolysis coupled with GC–MS by developing a calibration strategy based on commercially available phenolic lignin dimer model compounds, guaiacylglycerol-β-guaiacyl ether (GGE) and syringylglycerol-β-guaiacyl ether (SGE), as substitutes for authentic standards, thereby avoiding the need for synthetic thioethylated monomer standards and RRF-based quantification. The study further aimed to validate this LMC-based method (e.g., calibration performance and analytical reliability) and apply it to quantify uncondensed G- and S-derived monolignols in native biomass and corresponding organosolv lignin, enabling comparison of monolignol yields across biomass types and extraction conditions.
- To investigate the effect of two different approaches of organosolv lignin esterification (hydroxyl-esterified lignin versus chloromethylated lignin followed by esterification) on thermomechanical properties of modified lignin and PLA-lignin composites; to prepare lignin esters via a one-step route by esterifying the available hydroxyl groups of organosolv pine lignin using fatty acid chlorides, and characterize the products by FTIR and ^{31}P NMR; to evaluate and compare their thermal and mechanical properties by DSC, TGA and mechanical testing.

3 Experimental

3.1 Chemicals and materials

Raw biomass was kindly provided by company and research groups, located in Estonia: aspen wood chips was provided by Estonian Cell AS, pine sawdust was obtained from TalTech Laboratory of wood technology, barley straw was obtained from Estonian University of Life Sciences. All the resources were dried in an oven at 50 °C (remaining moisture up to 8%), followed by grinding prior to use.

The following chemicals were used in the study: ethanol (%), hydrochloric acid, sodium hydroxide, chloroform, $CDCl_3$, tetrahydrofuran (THF), pyridine (99.8%, anhydrous), bisphenol E (≥ 98%, analytical grade), boron trifluoride diethyl etherate (BF_3), ethanethiol (97%), molecular sieves (3Å) were purchased from Sigma-Aldrich (Germany); DMSO-d_6, endo-*N*-hydroxy-5-norbornene-2,3-dicarboximide (NHND), chromium (III) acetylacetonate, 2-chloro-4,4,5,5-tetramethyl-1,3,2-dioxaphospholane (TMDP, 95%); guaiacylglycerol-β-guaiacyl ether (GGE, 97%, TCI, Tokyo), syringylglycerol-β-guaiacyl ether (SGE, 96%, BLDpharm, Germany), 1,4-dioxane (analytical grade, ≥ 99.8%, Fisher); N,O-Bis(-trimethylsilyl)trifluoroacetamide containing 1.0% trimethylchlorosilane (BSTFA, 1.0% TMCS), triethylamine (TEA), octanoyl chloride (99%), lauroyl chloride (98%), palmitoyl chloride (98%) and sodium bicarbonate ($NaHCO_3$) were obtained from Thermo Fisher Scientific, Germany. Deionized water was generated in-house by Millipore S.A purification system.

3.2 Organosolv extraction

The obtained materials by this procedure were employed as the main objects of characterization study in **Papers I and II**. Organosolv delignification was investigated by using two solvents, ethanol and 1,4-dioxane. Particularly, 50.0 g of dried biomass was weighted into a 2.0 L roundbottom flask containing 1.5 L of organic solvent with 0.28 M of HCl. The system was kept refluxed, and mechanical stirring for 6h. Upon completion, the separation of leftover biomass and supernatant was done by Buchner filtration. The biomass was washed three times with 50 mL of the same solvent for extraction. The lignin-rich supernatant was collected and evaporated by a rotovap until obtaining the concentrated liquor. Organosolv lignin was recovered by precipitation in an excess of ultrapure water with virgorously stirring. The precipitated lignin was gathered and washed with water three times by centrifugation at 4200 rpm. The resultant lignin was dried in a convection oven at 30 ^{0}C for 24h, the extraction yield of lignin was calculated as following:

$$\%\ Lignin\ yield = \frac{W_{extracted\ lignin}}{W_{lignin\ in\ biomass}} \times 100 \quad (2)$$

3.3 Nuclear magnetic resonance (NMR)

In **Papers I and III**, phosphorous NMR (^{31}P NMR) was used to quantify hydroxyl contents of lignin. Firstly, about 25.0 mg of lignin sample was weighed into a 1.5 mL Eppendorf tube, followed by pipetting 500.0 µL of pyridine/$CDCl_3$ (1.6:1 v/v, named as solution I). The tube was vortexed to completely dissolve lignin. Next, 100.0 µL of endo-*N*-hydroxy-5-norbornene-2,3-dicarboximide (NHND, internal standard) was prepared in solution I at the concentration of 20.0 mg/mL, was added. Then, 100.0 µL of the relaxation reagent, chromium (III) acetylacetonate (approximately 5.0 mg/mL) prepared in solution I, was

pipetted into the same tube. Lastly, the mixture was derivatized with 70.0 µL of 2-chloro-4,4,5,5-tetramethyl-1,3,2-dioxaphospholane (TMDP), phosphitylation reagent, and reacted for 15 minutes. About 600.0 µL of derivatized lignin was transferred to NMR tube ready for the submission. The data acquisition was obtained by Bruker 400 MHz spectrometer that equipped with 5mm BBO BB-1H/D probe. The spectra were recorded at 25 °C with inverse gated decoupling pulse sequence (zgig), 768 number of scans, 10s for relaxation delay. The data analysis was assisted by TopSpin 4.0.8. The quantification of aliphatic, aromatic, and carboxylic hydroxyl groups was calculated as follows:

$$OH\ (mmol/g) = \frac{I_{OH} \times C_{NHND}}{I_{NHND} \times m_{lignin}} \qquad (3)$$

where I_{OH} is the integral of hydroxyl groups, I_{NHND} is the integral of internal standard adjusted to 1.0, C_{NHND} is the concentration of internal standard in the prepared NMR sample (mmol), m_{lignin} is the dried weight of lignin sample get phosphitylated (g).

In **Paper I**, HSQC experiment was performed by 500 MHz Agilent DD2 spectrometer that equipped with an inverse detection probe. The data was acquired by the standard multiplicity edited HSQC pulse sequence with adiabatic pulses in ^{13}C channel. The two-dimensional data was acquired with 256 increments (64 scans/increment) in f1 dimension with 20,000 Hz spectral width. The f2-dimension was zero filled to 2000 points, whereas the f1 was linear predicted to 512 points followed by zero filling to 1000 points. Fourier transformation was applied before the application of gaussian window in both dimensions. In **Paper III**, the HSQC pulse sequence, hsqcetgpsisp2.2 was opted with four scans for the analysis of hydrolysis lignin and its derivatives by Bruker Avance III 800 MHz spectrometer.

3.4 Fourier transform infrared spectroscopy (FT - IR)

The infrared spectra of lignin samples were performed by IRTracer-100 (Shimadzu, Japan). The diffuse reflection mode was applied for the measurement in which the sample was prepared by mixing with KBr and recorded from 4000 cm^{-1} to 400 cm^{-1} with 80 scans. The post-measurement processing was done using Lab Solutions software.

3.5 Quantification of non-condensed monolignols

Thioacidolysis reagent was freshly prepared by firstly adding 10 mL of 1,4-dioxane in a 25 mL volumetric flask. Next, 6.25 mL of BF_3 and 2.5 mL of ethanethiol were pipetted into the same container. 1.5 mL of internal standard stock solution of bisphenol E (concentration of 2.0 mg/mL prepared in 1,4-dioxane) was added. Lastly, volume was filled to 25 mL by adding 1,4-dioxane. Notably, 1,4-dioxane was kept in molecular sieve 3Å to minimize the water content prior to using.

Preparation of calibrations from lignin model compounds (LMCs, GGE and SGE): 10.0 mg of each LMC was dissolved in 5.0 mL of 1,4-dioxane, marked as stock solution. A series of working solutions was prepared by accurately pipetting 10, 20, 50, 100, 150, 200, 250 µL from stock solution into a 1.5 mL vials. Subsequently, the vials were set up for drying under nitrogen gas before subjecting it to thioacidolysis reaction.

Thioacidolysis procedure was adapted from [58], was applied for calibration and lignin sample preparation with modifications. In brief, 2.0–3.0 mg of biomass, or organosolv lignin was weighed into a 1.5 mL aluminium cap vial. Then, 1.0 mL of the prepared

thioacidolysis cocktail was added to the vial, which was tightly sealed. The reaction was carried out for 4h, at 100 °C set up by MULTIVAP (12 positions, JXDC-10 model, China) with quick vortex required every hour. After completion, the vials were left to cool down at room temperature. Meanwhile, a set of vials was pipetted with 190.0 µL of saturated $NaHCO_3$. Next, 400.0 µL of reaction mixture was transferred into these prepared vials to quench the reaction, mixing by pipette two times. After quenching, the vials were dried under nitrogen gas at 55 °C by the same MULTIVAP equipped with the gas distribution system.

Derivatization of thioethylated samples with 200.0 µL BSTFA (1.0% TMCS): pyridine (1:1, v/v) was performed at 55 °C for 30 minutes and a quick vortex in the end, was required prior to submitting to GC. The silylated sample was transferred into a GC vial containing a 400 µL micro insert and sealed. Each standard point was prepared in triplicate, while biomass and lignin samples were prepared in duplicate.

GC-MS analysis

Agilent Technologies 7890A instrument equipped with Agilent 5975C VL mass selective detector (MSD), using electron ionization (EI) mode in combination with quadrupole mass analyser. An ultra-inert split liner (Agilent Technologies, 5190-2295) was used. A Phenomenex ZB-5plus capillary column (30 m x ID 0.25 mm, film thickness 0.25 µm) was used for the analysis. The operating parameters were as follows: the GC inlet temperature was kept at 250 °C; the oven temperature started at 100 °C, held for 1 min, next increased to 300 °C incrementally at 25 °C/min and held for 3 min. The temperature of MSD transfer line, MS quadrupole, and ion source were set at 280 °C, 150 °C, and 230 °C, respectively. The energy was applied for EI at 70 eV. The signals were recorded by a full scanning mode across the range from 30 to 500 *m/z* starting after solvent delay 6.5 min. The quantification was based on the extracted ion chromatogram (EIC) that extracting characteristic fragments: 343 *m/z* for bisphenol E (internal standard), 269 *m/z* for uncondensed G-derived monolignols, and 299 *m/z* for S-derived monolignols. The interpretation was assisted by MSD Chem-Station F.01.03.2357 software.

Method validation

Instrumental detection limit (IDL) and quantification limit (IQL) were estimated as the ratio of residual standard deviation of the regression line (standard deviation of y-intercept) and the slope, multiplied by 3.3 for IDL and 10 for IQL. According to the methodology, limits of quantification (LOQ) for both G and S monomers were calculated in µmol per gram of lignin, and µmol per g of Klason lignin in case of biomass. Precision and trueness were evaluated based on spiked samples (n = 8) prepared on the matrix of barley straw biomass, which is enriched in G and S monolignols. Trueness was calculated as the absolute difference between the experimental recovery and 100%, while precision was indicated as relative standard deviation (RSD%). The recovery (R%) was calculated (equation 4) by taking total concentration of target analyte in spiked sample ($C_{recovered}$, µmol) excluding the inherent amount of that in the biomass matrix ($C_{non\text{-}spiked}$, µmol), followed by comparing to the known spiked concentration (C_{spiked}, µmol) of LMCs.

$$R\% = \frac{C_{recovered} - C_{non-spiked}}{C_{spiked}} \times 100 \qquad (4)$$

3.6 Esterification of lignin via hydroxyl groups

In **Paper III**, the esterification of lignin via hydroxyl groups using fatty acid chloride was prepared as follows: 1.0 g of organosolv pine lignin was weighed into a 100 mL round bottom flask, followed by adding 10.0 mL of dry THF; next, triethylamine (1.5 equivalent to total OH groups, 2.87 mmol/g of lignin Appendix 1, Table 2) was added and mixed by magnetic stirrer for 10 minutes. The flask was then stabilised in a cold bath for 10 minutes, and subsequently, 1.5 equivalent to total hydroxyls of fatty acid chloride (367.0 µL of C8, 506.0 µL of C12, or 657.0 µL of C16) was added dropwise. The reaction was carried out at room temperature, vigorously stirring for 4 hours. After esterification, 50 mL of $CHCl_3$ was added to the flask, and the mixture was transferred to a separatory funnel. Next, liquid-liquid extraction was performed with 30 mL of 5% sodium hydroxide to hydrolyse the unreacted fatty acid chloride. The esterified lignin remaining in the organic layer was collected, and solvent evaporated using a rotavapor. The final material was washed three times with 50 mL of ethanol to remove undesired byproducts, followed by freeze-drying overnight to remove solvent residue.

The setup parameters for differential scanning calorimetry (DSC), thermogravimetry analysis (TGA), mechanical testing, and preparation of PLA/esterified lignin films by solvent casting were provided in Appendix 3 (materials and methods), carried out by Dr. M. K. Mohan. The data obtained from these techniques will be discussed in Section 4.3 of the thesis.

4 Results and discussions

The main results were compiled from three publications and were presented and discussed in the following order: (i) the application of 1D and 2D NMR to characterize the structure of lignin extracted using ethanol, and 1,4-dioxane; (ii) The utilization of lignin model compounds (LMCs) as substitutes of authentic standards to quantify uncondensed monolignols by thioacidolysis coupled with GC-MS. This approach applied to biomass and organosolv extracted lignin samples; (iii) the dissertation summarized how differences in lignin esterification pathways (e.g., direct esterification via hydroxy groups versus indirect modification through chloromethylation followed by esterification) influenced the thermal properties and mechanical strength of lignin-PLA composite.

4.1 Characterization of organosolv lignin by NMR

Paper I focused on the results of the total hydroxyl content quantified by ^{31}P NMR experiment together with the details of lignin's substructure and inter-unit linkages revealed by HSQC.

4.1.1 Total hydroxyl quantification by ^{31}P NMR

The quantification of free hydroxyl groups in lignin was achieved by ^{31}P NMR analysis. Figure 4 illustrates a representative spectrum of organosolv lignin where IS (NHND) signal was calibrated at 151.8 ppm and its integral was normalized to 1.0. The derivatized lignin shows the well-resolved peaks related to aliphatic, syringyl (S-OH), guaiacyl (G-OH), *p*-hydroxylphenyl (H-OH), and carboxylic acid (R-COOH) groups.

The concentrations of free hydroxyl groups were evaluated for six organosolv lignin samples isolated from softwood (pine sawdust), hardwood (aspen chips), and non-woody biomass (barley straw) by using ethanol (EOL), and 1,4-dioxane (DOL). The quantification results (Table 1) were achieved based on the known concentration of IS and the peak integral of targeted -OH group relative to IS. To include the condensed phenolic hydroxyls (or C5-substituted OH) that appear on both sides of syringyl hydroxyl signal, the additional integral of aromatic hydroxyl groups from 137.0 ppm to 144.0 ppm was added [85].

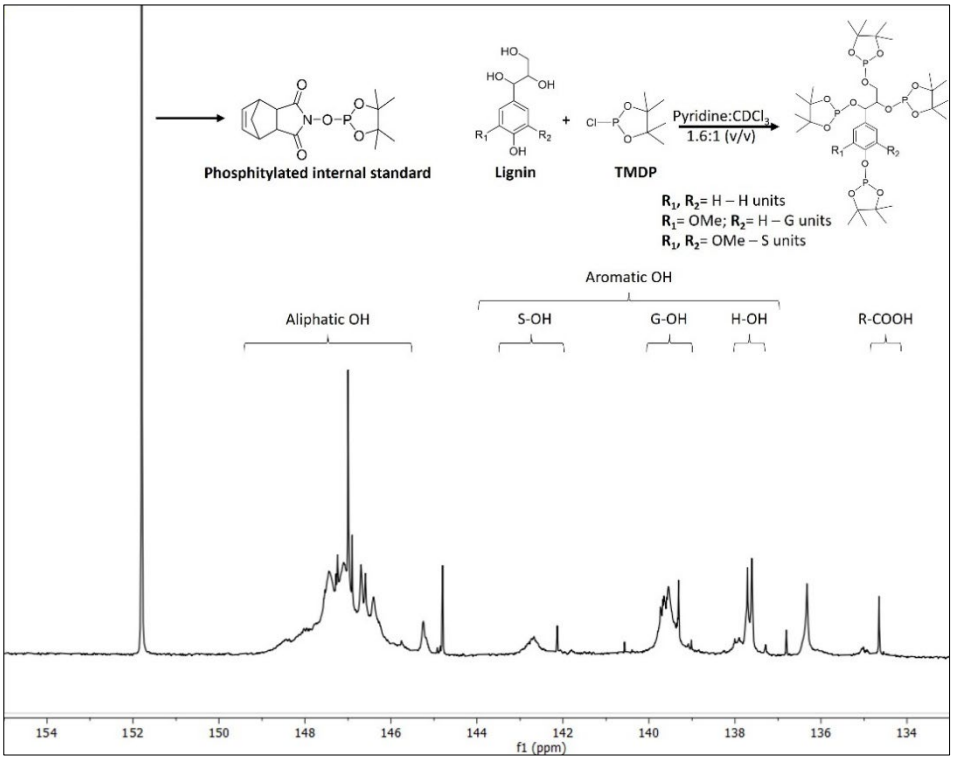

Figure 4. *A representative ^{31}P NMR spectrum of ethanol extracted barley biomass that derivatized with TMDP in the presence of NHND as an internal standard.*

Table 1*. Hydroxyl content (mmol OH /g) in studied lignin samples determined by quantitative ^{31}P NMR analysis. Chemical shifts (ppm) are presented for lignin extracted from hardwood (aspen), grass (barley straw), and softwood (pine) using ethanol (EOL) and 1,4-dioxane (DOL). Characteristic chemical shifts are assigned to the different types of the hydroxyl groups in lignin.*

Chemical shift (ppm)	Types of OH	Aspen		Barley		Pine	
		EOL	DOL	EOL	DOL	EOL	DOL
149.0-145.5	**Aliphatic OH**	2.38	1.50	2.08	0.94	1.90	1.61
143.5-142.0	**Syringyl OH**	0.35	1.32	0.11	0.53	ND	ND
140.2-139.0	**Guaiacyl OH**	0.47	0.55	0.48	0.62	0.73	1.35
138.0-137.5	***p*-hydroxyphenyl**	0.23	0.12	0.23	0.16	0.08	0.07
134.74-134.5	**Carboxylic acid**	0.05	0.20	0.02	0.25	0.04	0.15
144.0-137.0	**Aromatic OH**	1.14	2.49	0.92	1.76	0.97	2.59

Overall, the organosolv lignin samples fractionated by two different solvents show a significant difference in the distribution of functional groups. Regardless of the biomass source, the concentration of hydroxyl groups originating from aliphatic side chains was higher in all lignin samples extracted using ethanol, than in those extracted using 1,4-dioxane. This observation indicates that lignin structure was better preserved when ethanol was used, whereas the lower aliphatic OH content in DOL suggests that more severe fragmentation occurred when the biomass was treated with 1,4-dioxane [47], [86]. In contrast to ethanol extraction, delignification in 1,4-dioxane resulted in a higher lignin yield (Appendix 1, Table 1) and produced lignin fragments with a higher phenolic content. These phenomena could be explained by the more extensive cleavage of aryl-ether bonds during organosolv isolation in 1,4-dioxane compared with ethanol. In plant cell wall, these bonds are formed between lignin and polysaccharides. Therefore, cleaving these linkages is the main driving force for liberating lignin from the recalcitrant biomass matrix; consequently, the more frequently this cleavage occurs, the higher the lignin yield. This process results in the formation of new phenolic groups within the lignin network, as also evidenced in the previous studies [87]–[89].

In addition to the dependence of lignin structure on extraction conditions, botanical origin also plays a crucial role in determining the abundance of hydroxyl groups. For instance, organosolv-isolated aspen lignin exhibited a higher syringyl OH content than barley lignin, and none was detected in pine lignin. The highest amount was attributed to Aspen-DOL (1.32 mmol OH g^{-1} of dried lignin), which was about ten times higher than the contribution from *p*-hydroxyphenyl units (0.12 mmol OH g^{-1} of dried lignin) in the same batch. In contrast, the phenolic content in organsolv pine lignin originated predominantly from guaiacyl units, reaching 1.35 mmol OH g^{-1} of dried lignin in Pine-DOL. In case of barley biomass, all three main monolignol-derived units in lignin (H-, G-, and S- units) contributed to the total phenolic content, with a slightly higher concentration of G-OH. These results are consistent with well-established differences in lignin composition: hardwoods generally exhibit higher S/G ratio than softwoods, while grasses contain all three units (H, G, S) [8], [75], [90].

4.1.2 Elucidation of lignin substructures and interlinkages using HSQC

To gain an in-depth understanding of lignin structure, a heteronuclear single quantum coherence (HSQC) experiment was employed. HSQC is a two-dimensional NMR technique that provides information about correlations between directly bonded hydrogen and carbon atoms. Thanks to an additional dimension of ^{13}C, overlapping signals in 1D proton spectrum can be well resolved based on differences in the chemical shifts of the attached carbons, and vice versa [91], [92]. In this study, HSQC was employed to qualitatively elucidate the structure of lignin extracted using two different solvents, thereby revealing the detailed structural features of the fragments as well as the interunit linkages. Data interpretation was based on the two most informative regions: (i) oxygenated aliphatic sidechain (δC/δH 100.0–40.0/6.0–2.5 ppm), and (ii) aromatic/unsaturated region (δC/δH 150.0–100/8.0–6.0 ppm). The assignment of cross signals was referenced to the literature [90], [93]–[98].

The recorded oxygenated aliphatic region (δC/δH 100.0–40.0/6.0–2.5 ppm) of six samples is shown in Figure 5. As expected, methoxy groups – the most abundant functional group in lignin – are clearly observed in all spectra, with intense signals at δC/δH 55.5/3.7 ppm. Under acidic hydrolysis treatment, the cleavage of α- and β-aryl ether bonds are the main mechanisms that liberate lignin from the recalcitrant matrix of

lignocellulosic cell wall. However, the occurrence of ether bonds breakdown at α-position is favoured over the β-position due to the lower bond dissociation energy, 80–118 kJ mol^{-1} compared to 150 kJ mol^{-1} [47], [88]. Consequently, there is a formation of intermediate α-carbocation, which readily reacts with nucleophilic ethanol present as a solvent [96]. Hence, in all ethanol-extracted lignin (Figure 5A, C, E), ethoxylation took place at α-position of β-O-4' substructure (A'), was clearly visible at δC/δH 63.6/3.3 ppm. The presence of other dominant linkage motifs, such as β-O-4' without α-ethoxylation (A), β-β resinol (B), phenylcoumaran (C), and cinnamyl alcohol end-group (I) was detected in all EOL samples. However, signals corresponding to resinol fragments (B) were not detectable in pinewood lignin (Figure 5E). Additionally, softwood lignin, characterized by a low S/G ratio, shows aryl-ether bonds primarily between G-units (Figure 5E), whereas in hardwood and non-woody biomass these bonds are also formed between S-units (Figure 5A, C).

Intriguingly, by switching solvent from protic (ethanol) to aprotic (1,4-dioxane), a series of cross peaks originating from β-O-4' bonds (present in both substructures A and A') experienced a profound decrease in all DOL-spectra (Figure 5B, D, F). This observation could be possibly explained by two facts: (i) the higher boiling point of 1,4-dioxane, which allowed the pulping system to operate at higher temperature, assisting in the cleavage of β-O-4' bonds [99]; (ii) the solubility of lignin in 1,4-dioxane was discovered to be greater than in ethanol thanks to the dominant solvent-molecule interaction via van der Waals force [100], which facilitated the extraction process resulting in lower density of β-O-4' bonds in the obtained lignin.

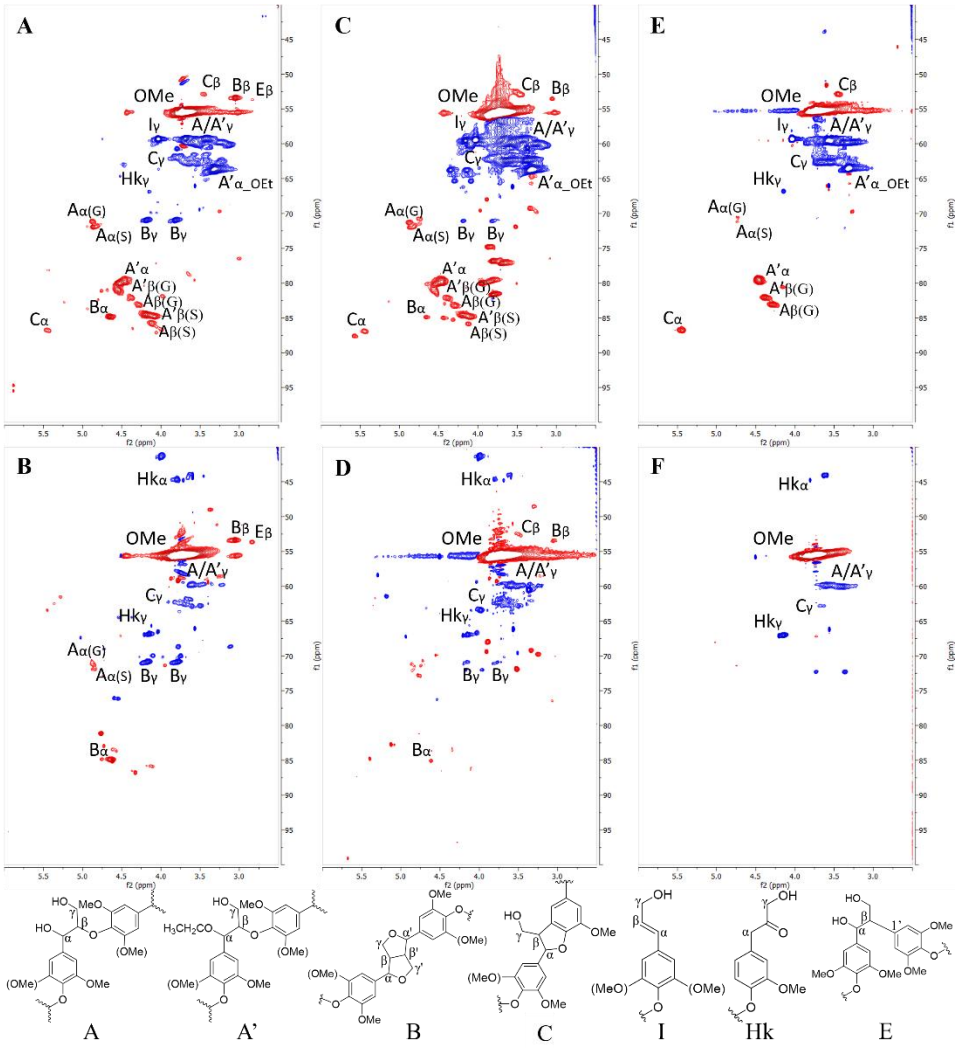

Figure 5. *HSQC spectra of oxygenated aliphatic side chain of six organosolv lignin samples, (A, B) Aspen-EOL, DOL; (C, D) Barley-EOL, DOL; (E, F) Pine-EOL, DOL. Their assigned fragments are illustrated accordingly (A)* β*-O-4' alkyl-aryl ethers; (A')* β*-O-4' alkyl-aryl ethers with ethoxylation at α-position; (B)* β*-*β*' resinols; (C)* β*-5' phenylcoumarans; (I) cinnamyl alcohol-end groups; (Hk) Hibbert's ketone-end groups; (E)* β*-1' linkage. Red cross peaks indicate -CH₃ and -CH, while blue ones are -CH₂.*

Furthermore, in all DOL spectra, the formation of Hibbert's ketones (Hk), a known consequence of delignification under acidic conditions, was observed by the detection of its $C_{\alpha,\gamma}$-$H_{\alpha,\gamma}$, whereas only C_γ-H_γ signal was detected in EOL [96], [101]. It is likely that the intensity of Hk (C_α-H_α) cross peak in EOL was adversely affected by the aggressive ethoxylation at α-position in the excess of ethanol, which has been previously discussed. The other linkages were also present, such as cinamyl alcohol end-groups (I) mostly in EOL, and β-1′ (E) only in aspen lignin (Figure 5A, B).

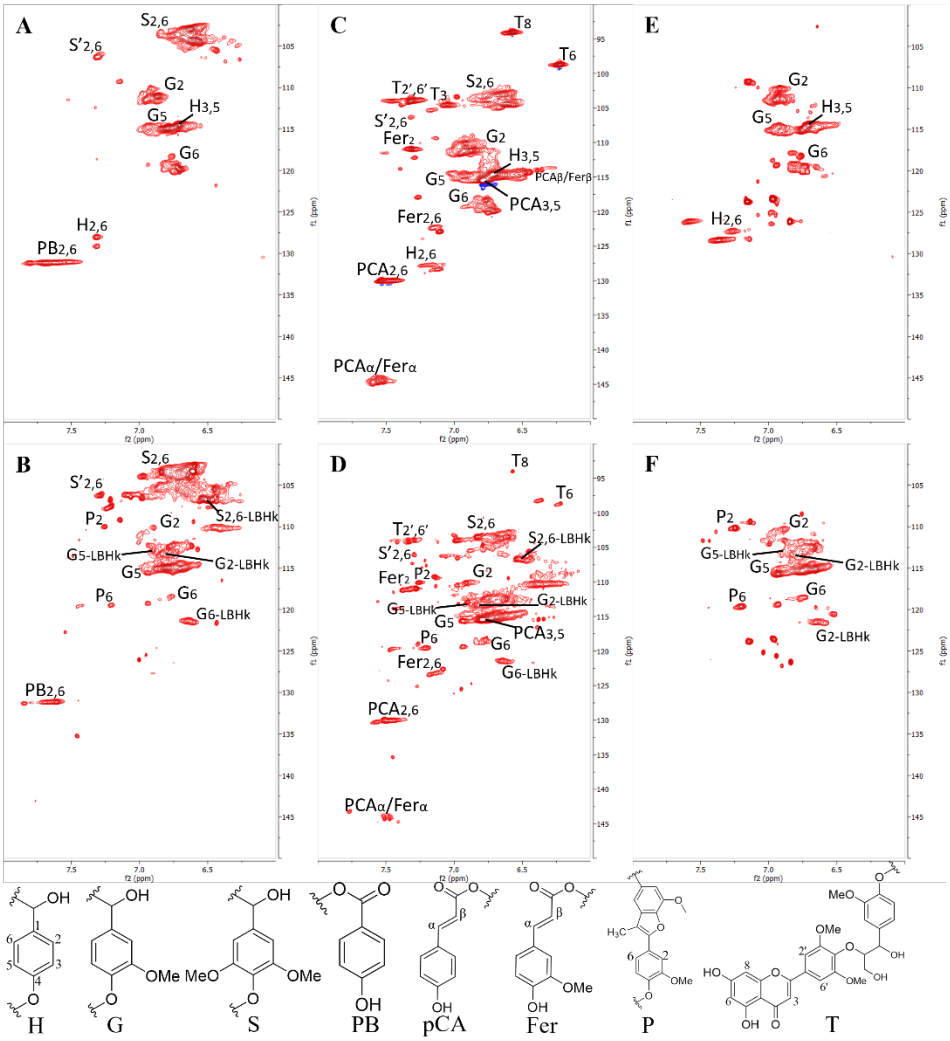

Figure 6. *HSQC spectra of aromatic/unsaturated region of six organosolv lignin samples, (A, B) Aspen-EOL, DOL; (C, D) Barley-EOL, DOL; (E, F) Pine-EOL, DOL. Their assigned fragments are illustrated accordingly (H) p-hydroxyphenyl units; (G) guaiacyl units; (S) syringyl units; (T) tricin; (PB) p-hydroxybenzoate; (pCA) p-coumarates; (Fer) ferulates; (P) methyl-substituted phenylcoumaran. Red cross peaks indicate -CH.*

Figure 6 represents the aromatic/unsaturated region (δC/δH 150.0–100/8.0–6.0 ppm) of the HSQC spectra, where the detail information about monolignols as well as their distributions in different types of biomasses are disclosed. The intense cross peaks of guaiacyl (G) and syringyl (S) units emerged from the spectrum of hardwood (aspen, Figure 6A, B) and non-woody biomasses (barley straw, Figure 6C, D). Notably, S-contained lignin experienced oxidation to some extent at C_α-OH to form C_α=O ($S'_{2,6}$) [86], [102]. In addition to that, an important feature of aspen lignin was recognized by the acylated monolignol, *p*-hydroxybenzoate (PB) that bound to lignin sidechain at C_γ-position as the result of natural acylation, followed by lignification in the plant cell wall [103]. Likewise, the two distinguish monolignol esters conjugated with *p*-coumarates

(pCA) and ferulates (Fer) were abundantly found in grass-derived lignin [93], [95], [102]. Along with these two unconventional lignin precursors (pCA and Fer), another signature flavone-type structure, tricin (T) was well-incorporated and noticed in lignin network [17], [104].

In contrast to aspen- and barley-types lignin, the extract from pine demonstrated the least number of correlations and thus displayed the simplest HSQC spectrum (Figure 6E, F). Particularly, the noticeable amounts of H- and G- monolignols were present, while S-units were not detectable. These observations are in good agreement with the previous ^{31}P NMR data where syringyl-OH groups were not detected.

It is noteworthy that the second, third, fifth, and sixth aromatic protons of H-ring faded from the treatment with 1,4-dioxane, which is the indicative of high degree of condensation or repolymerization during acidic organosolv fractionation. For Hibbert's ketone (Hk) fragments, conventional assignment is based on the sidechain signals $C_{\alpha,\gamma}$-$H_{\alpha,\gamma}$, thanks to the work of Miles-Barrett and co-workers [98], who synthesized lignin analogues containing Hk moieties, since then, the structure of Hibbert's ketones has been elucidated in greater detail. As a result, more information can be extracted in the aromatic area of HSQC spectrum, G-/S- units that bound to Hk (noted as $S_{2,6}$-LBHK, G_2-LBHK, G_5-LBHK, G_6-LBHK) were assigned at δ_C/δ_H 106.67/6.53, 113.31/6.84, 112.89/6.90, and 121.36/6.64 ppm respectively. Apart from the above-mentioned subunits, methyl-substituted phenylcoumaran (P) were successfully confirmed by Faleva et al [90] and present in dioxane lignin (Figure 6B, D, F) in the present study.

4.2 Quantification of uncondensed monolignols by GC-MS

Paper II underscores the capability of two phenolic dimers acting as lignin standards for the analysis (Scheme 1). Validation of the method and the variation in monolignols contents in biomass and lignin samples are discussed.

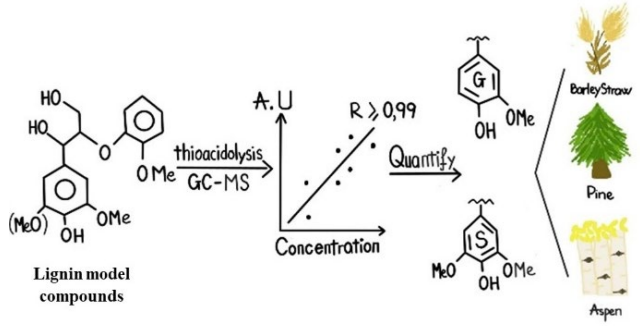

Scheme 1. *The scheme of using LMCs for non-condensed monolignols analysis using thioacidolysis/GS-MS method. The quantification was carried out for three types of lignocellulosic biomass and their organosolv fractionated lignin.*

4.2.1 Calibration using lignin model compounds (LMCs)

Unlike other chemical analytes, it is nearly impossible to have an analytical standard for lignin due to the diversity of compositions and the inevitable rearrangement of its structure (e.g., depolymerization, condensation, oxidation and modification of functional groups) after being pretreated [42]. Hence, identifying suitable compounds that can serve as substitutes for authentic lignin standards is crucial for the field, particularly for

the analysis of non-condensed monolignols by thioacidolysis, followed by GC-MS quantification. The idea initiated us to explore the feasibility of using commercially available reference dimer models (GGE and SGE) in the preparation of calibration curve for quantification of uncondensed S- and G- monolignols in biomass as well as in its resultant lignin (Figure 3). This approach simplifies the procedure compared to earlier methods that used relative response factors (RRFs) to quantify monolignol concentrations. The latter requires multiple steps, including synthesis (at least five steps starting from arylglycerol monomers), purification, and characterization, to obtain pure thioethylated monomers, from which RRFs can be accurately determined [56], [59], [60]. It is obvious that the synthesis procedure of such substances is not only time-consuming, but also requires certain expertise, and advanced instruments.

Instead, our study proposed the application of model compounds as the alternatives to standards, providing several advantages for the analysis: (i) physical appearance of LMCs are powder, making them easier to handle and prepare compared to the highly viscous thioethylated products, which require more attention [60]; (ii) the structure of LMCs inherently carries important features that are representative of lignin. For instance, each compound is composed of non-condensed phenolic monomer that linked to another aromatic subunit via β-O-4' bond, which is selectively thioacidolysis-depolymerized into the targeted analytes; (iii) the conversion of LMCs into the corresponding thioethylated monomers was efficient and maintained stable efficiency across the investigated dynamic range, ensuring the consistent results; (iv) this approach is convenient and readily applicable to various laboratories, particularly for routine analysis and optimization. In this study, the values of RRFs were not aimed to be provided due to the challenges of determining the precise thioacidolysis yield.

The stacked total ion chromatogram (TIC) of two derivatized thioethylated products released from LMCs, lignin and raw biomass samples, is presented in Figure 7. For the analysis, the standard solution was prepared individually so that the two TICs (Figure 7A, B) could give a visual demonstration of how well all the peaks were resolved, including the chosen IS (bisphenol E), G- and S-monomers released from GGE and SGE compounds, respectively. The inherent impurities of the used dimers may give rise to the alien peaks (marked as asterisks); however, they do not interfere or overlap with the targeted analytes. Furthermore, based on the reported data of synthesized lignin-derived thioacidolysis monomers [60], the identity of thioacidolysis depolymerization products originated from our chosen phenolic model compounds were firmly confirmed by their characteristic splitting peak shapes due to the mixture of diastereomers, erythro- and threo-; and their fragmentation patterns resulted from the mass spectrometry (Figure 8). The obtained chromatograms and mass spectra underscore the choice of LMCs as the best fit analogues to analytical standards for non-condensed monolignols quantification. Because they exhibited the capability of yielding analytes of interest via thioacidolysis without any concerned interfering degraded products. The follow-up TICs of monolignols released from organosolv lignin and lignocellulosic biomasses are shown in Figure 7C-F. As expected, the native monolignols yielded from biomass (Figure 7D-F) resulting the more complicated baseline compared to the ones from lignin itself (Figure 7C) which were cleaned from carbohydrates, and extractives.

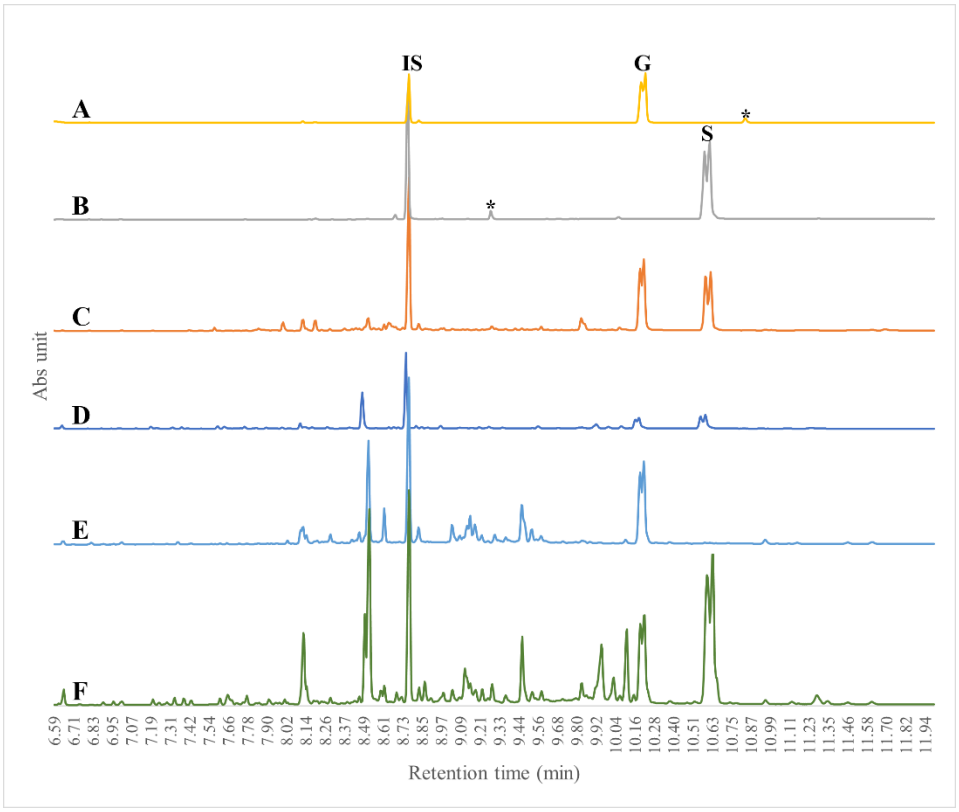

Figure 7. *TIC of: thioethylated G-, S- (A, B) released from phenolic model compound. The following are TIC of: ethanol organosolv lignin extracted from barley straw (C); raw biomass barley (D), pine (E), and aspen (F).*

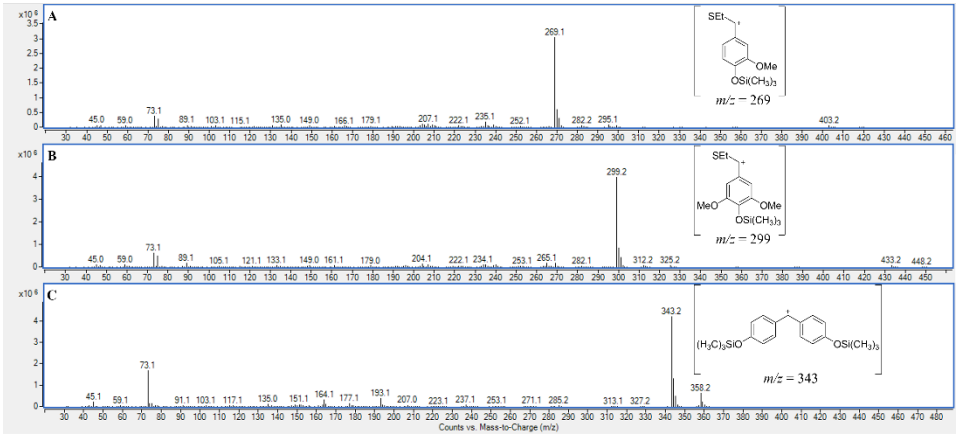

Figure 8. *Mass spectra of GGE-derived thioacidolysis monomer (A), SGE-derived thioethylated monomer (B), and the bisphenol E (C) presented with their chosen quantification fragments, 269.0, 299.0, and 343.0 (m/z), respectively.*

For quantification, peaks were integrated based on their retention times in the total ion chromatogram (TIC) and confirmed using extracted ion chromatograms (EICs). The selected ions *m/z* 343, 269, and 299 correspond to the internal standard (IS), G monomers, and S monomers, respectively. To confirm the presence of analytes in the real samples, the qualitative information was validated based on mass spectra and their relative retention times that closely align with those of the standard with the average tolerance less than 0.5%, satisfying the performance criteria required for GC-MS method [105].

Table 2 summarizes thioacidolysis method performance characteristics. For calibration, LMC standards were subjected to thioacidolysis, followed by derivatization and GC-MS analysis. Obtained peak area ratios of targeted analytes (G-, S-monolignols) to IS were plotted against the initial concentrations of LMCs to create the calibration curves. To minimize the random error due to the sample preparation, each standard point of calibration was prepared in triplicate, and their mean values of peak area were considered. As the results, both model compounds exhibited adequate linearity within the dynamic range (regression coefficients, $R^2 \geq 0.99$), regression error less than 7.5%. The high correlation coefficients achieved from two phenolic dimers were comparable to those created from aryl glycerol monomers that reported in the previous study [56], [59]. The results indicate that the structural features of LMCs did not disrupt their proficiency in terms of yielding thioethylated monomers as the simpler monomers. Moreover, the linearity implies the consistency of thioacidolysis and derivatization yields across the investigated concentration range. The identical preparation protocol was applied to pretreat the real samples before GC-MS quantitation.

Table 2. *Calibration and validation statistics of thioacidolysis/GC-MS method, including linearity, instrumental quantification limit (IQL), limit of quantification (LOQ), precision, and trueness.*

Linearity range (µmol/mL)	Regression error (%)	IQL* (µg/mL)	LOQ (µmol/g of lignin)	Precision (RSD, %)	Trueness (%)
G: 0.25-3.10 R^2 = 0.9900	7.1	48.1	30.0	9.0	11.1
S: 0.11-2.82 R^2 = 0.9970	5.4	43.6	25.0	10.5	2.9

**IQL was expressed in mass units based on the base fragments of GGE and SGE, which are 269, 299 m/z, respectively.*

IDL (GGE: 0.059 µmol mL^{-1}, SGE: 0.048 µmol mL^{-1}), IQL (GGE: 0.179 µmol mL^{-1}, SGE: 0.146 µmol mL^{-1}) were estimated based on the close-to-zero concentration range (for instance, 0.2-1.2 µmol mL^{-1} for G-monomer, 0.1–0.6 µmol mL^{-1} for S-monomer) where the ratio of residual standard deviation of regression line to the slope was calculated and multiplied by 3.3 for IDL, and 10 for IQL. LOQ of the method was calculated by taking into consideration of the initial mass and dilution factor. As the results, the minimal concentration required for quantification was 30.0 (µmol/g of lignin) for G-monolignols, and 25.0 (µmol/g of lignin) for S-monolignols, ensuring the quantitative estimation of these analytes in biomass and lignin samples.

The recovery test is one of the key factors for method validation and essential to assess the applicability of any analytical method to the real samples. Herein, for the first time the test was carried out on the complex matrix of biomass (e.g., barley straw)

via eight independent spiked samples (n = 8), with the concentration was spiked at 0.39 µmol mL^{-1} of GGE, and 0.56 µmol mL^{-1} of SGE. Based on that, the accuracy of the entire procedure (including two major steps, thioacidolysis and derivatization) were expressed as precision (RSD%), trueness, and mean recovery for each model compound. In terms of precision, RSD% was obtained 9% for GGE, and slightly higher 10.5% for SGE. The recovery yield was achieved 88.9% for GGE, and 97.1% for SGE. The deviation of the mean recovery values to the spiked concentration reflects the trueness of the method, which was calculated 11.1% for GGE, and 2.9% for SGE. Taking root sum of squares of precision and trueness, we obtained the so-called combined uncertainty, approximately 14.3% (GGE), and 10.9% (SGE). The validation statistics indicate that the developed method was qualified for the analysis purpose. Indeed, the utilization of LMCs approach eases the monolignols quantification by overcoming the needs for synthetic standard substances, which are achieved by the time-consuming and costly procedure. The proposed method is thus justified and feasible for all the lignin-related analytical laboratories in terms of routine analysis and method optimization.

4.2.2 Uncondensed monolignols content in native and organosolv lignins

Constructed calibration lines were applied to quantify the non-condensed phenolic G and S monomers in three representative types of lignocellulosic biomass: hardwood (aspen chips), softwood (pine sawdust), grass (barley straw); and their corresponding organosolv-fractionated lignins. Theoretically, it is anticipated that there would be a significant variation in lignin's compositions due to the difference in biomass resources and treatment conditions. The structural changes of lignin are reflected by thioacidolysis monomer yields presented in Table 3. The total monolignol yields were expressed based on the Klason lignin content in the studied biomasses (e.g., 28.6% in aspen, 22.4% in barley, 37.0% in pine). The sum of phenolic G- and S-monomers yield in biomass was 2294, 1017, 1076 (µmol/g of Klason lignin), recorded for aspen, barley, and pine, respectively. As expected for softwood lignin, S-derived thioacidolysis monomers were present only in small amounts in pine. In contrast, a substantial amount of G-derived thioacidolysis monomers (1037 µmol/g of Klason lignin) was quantified in pine. This was relatively close to the published data where the RRFs of pure synthetic standards applied for the calculation (1020 µmol/g of Klason lignin [60]). The content of the thioacidolysis derivatives originated from S-units was negligible (39.3 µmol/g of Klason lignin). The minor portion of phenolic S-monomers in pine biomass was reinforced by the pyrolysis/GC-MS data where they were detected under different forms of pyrolysis degraded products [90]. By contrast, the yield of characteristic S units in aspen wood was 1335 µmol/g of Klason lignin, the highest among three biomasses. This value is comparable to that reported using synthetic thioethylated S monomers (1342 µmol/g of Klason lignin) [60]. However, the overall S/G ratio of 1.39 was lower than the published data due to difference in the detected amount of G-monomers [60], [106]. Furthermore, lignin composition in the grass-type biomass barley straw was reported here for the first time. The S/G ratio was 1.12, and the yields of uncondensed S and G monomers were 538 and 479 µmol/g of Klason lignin, respectively. The ratio is close to the value of 1.0 indicates the equal distribution of G and S units in this type of biomass.

To clarify the impact of treatment condition on lignin condensed structure, thioacidolysis analyses were further conducted for the organosolv samples (Table 3). In comparison with the native lignin presenting in biomass, the extracted ones show a drastic decline in β-O-4' interconnected condensation-free monolignols. The results

support two key features of organosolv delignification: (i) the breakdown of α/β-O-4' linkage is the main driving force to liberate lignin from the lignin-carbohydrate complexes; (ii) repolymerization or condensation is one of the unavoidable consequences when the performance occurring under acidic organosolv condition [107], [108].

Table 3. *Monomer yields from thioacidolysis (µmol/g of Klason lignin) in lignocellulosic materials and their organosolv lignin samples (n = 2).*

Biomass	**S (± SD)**	**G (± SD)**	**S/G**
Aspen	1335 (± 87)	959 (± 8)	1.39
Barley	538 (± 112)	479 (± 11)	1.12
Pine	39.3 (± 0.3)	1037 (± 201)	0.04
Organosolv lignin	**S (± SD)**	**G (± SD)**	**S/G**
Aspen-EOL	902 (± 4)	339 (± 24)	2.66
Aspen-DOL	380 (± 14)	102 (± 0.1)	3.72
Barley-EOL	413 (± 7)	491 (± 14)	0.84
Barley-DOL	109 (± 2)	39.3 (± 6)	2.77
Pine-EOL	37 (± 4)	802 (± 9)	0.05
Pine-DOL	34 (± 2)	175 (± 14)	0.20

It is noteworthy that the recovery rates of non-condensed monomers were greater for all ethanol organosolv lignin compared to those obtained from 1,4-dioxane. This observation proved the efficiency of using ethanol for the extraction in terms of β-O-4' bond preservation, which is beneficial for the subsequent chemical valorisation. While using 1,4-dioxane resulted in better extraction yield, but on the other hand, the disruption of β-O-4' linkages was more remarkable leading to the formation of rigid or condensed lignin structure through repolymerization. These thioacidolysis findings are consistent with our prior knowledge achieved by the HSQC-NMR spectra (**Paper I**) where the abundance of aryl-ether bond cross signals experienced a sharp decline when the fractionation operated with 1,4-dioxane as solvent.

Additionally, a noticeable number of G-units underwent irreversible condensation compared to S-units. The results of this study show that there was almost a tenfold reduction in non-condensed phenolic G-monomers content that still connected via β-O-4' bond compared to their origins in all DOLs, whereas a maximum fivefold decrease in concentration of S-monomers was observed in the same batch. This phenomenon could be explained by the faster formation and higher reactivity of benzylic carbocation derived from G-unit than S-unit, which make this active moiety easier to participate in

either cleavage or condensation with other electron-rich aromatic carbon atoms [46], [109], [110]. As the results, the lower concentration of non-condensed G units was determined after the fractionation. It is evident that even for highly condensed lignin samples, such as 1,4-dioxane-extracted lignin, the thioacidolysis protocol remained effective for analysis. Bringing these results together, it can be concluded that there is a trade-off between lignin yield and the preservation of lignin's native structure during extraction. If the goal is lignin valorisation the latter should be prioritized.

4.3 Esterification of lignin and study of PLA-lignin composites

The main aim of this study is to elucidate how different esterification approaches could have impact on the resulting lignin and its composites with PLA. Discussions of **Paper III** focus on the one-step esterification via available hydroxyl groups in organosolv pine lignin using fatty acid chloride (Scheme 2, top) and their characterizations using FT-IR, ^{31}P NMR. Subsequently, the modified lignin was blended with PLA and compared with those composites made up of the two-step modification process (Scheme 2, bottom). This comparison was based on thermal and mechanical properties that attained by DSC and TGA techniques.

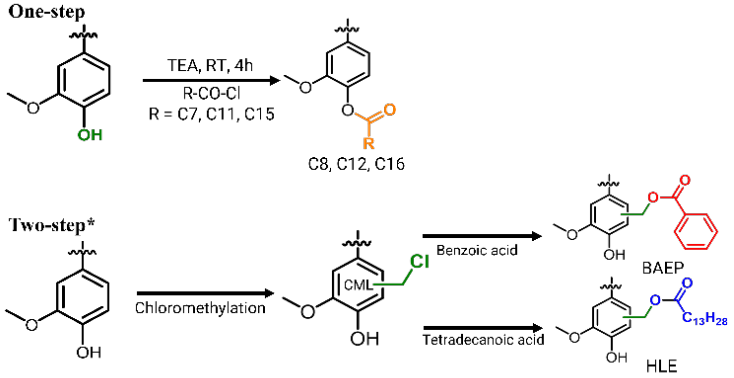

Scheme 2. *Two pathways of lignin esterification: one-step synthesis esterifying the available hydroxyl groups of lignin using fatty acid chloride (top); two-step synthesis firstly introduces new active site, secondly esterifying with carboxylic acid (bottom). (*) The detail of synthesis is provided in Appendix 3 and is not discussed here.*

4.3.1 Characterization of hydroxyl-esterified lignin

The one-step synthesis pathway of lignin esterification was carried out with octanoyl – C8, lauroyl – C12, palmitoyl – C16 chlorides. The successful modification was initially confirmed by FTIR (Figure 9). Two new absorbance bands at 1760 and 1740 cm^{-1} are assigned for the formation of ester linkages between the acid chloride and phenolic and aliphatic hydroxyl groups, resulting in aromatic and aliphatic ester, respectively [111]. The work-up steps completely removed the unreacted acyl chloride, which could be easily monitored by the complete absence of the carbonyl chloride (CO-Cl) stretching band at 1800 cm^{-1}. The broaden stretching band of hydroxyl groups at 3440 cm^{-1} decline remarkably in all the modified lignin derivatives, indicating the consumption of those functional groups during the reaction. The bands at 2922 and 2850 cm^{-1} correspond to the C-H stretching vibrations slightly increase due to the attachment of long alkyl chain

originated from the fatty acid. Another crucial confirmation of the saturated alkyl chain grafted onto lignin was spotted at the fingerprint region, 721 cm^{-1} – the band corresponding to the CH_2 rocking vibration [112]. The study revealed that the lengthier the hydrocarbon chain is, the stronger the signal could be detected, which explains the appearance of more intensive peak in the spectra of C16-modified lignin (Figure 9D) than those of the shorter chains (Figure 9B, C). The distortion of the region ranging from 1060 to 1170 cm^{-1} can be attributed to the overlap of C-O deformation in secondary alcohol/aliphatic ester and C-O ether stretching of lignin together with a decrease in the primary alcohol C-O stretching band (1028 cm^{-1}), providing a compelling proof of the esterification [111], [113], [114].

Apart from the necessary structural changes because of the chemical modification, it should be noted some bands representing the core structure of lignin in FTIR. For instance, the intense band at 1510 cm^{-1} is from the characteristic polymeric backbone vibration of lignin, and the absorbance at 1595 cm^{-1} arises from the aromatic skeletal vibration with carbonyl stretching [115]. The peak at 1459 cm^{-1} is assigned to the C-H deformation asymmetric [116]. In addition to that, monolignol compositions are also partially recognizable in FTIR spectra, such as the signal at 1263 cm^{-1} corresponds to the C-O and C-O-C stretching of phenol and ether linkages in lignin, which are mostly derived from H-unit, while the G-aromatic ring vibration was noticed at 1214 cm^{-1} associated with C-C, C-O, and C=O stretching [113]. These features firmly verify the identity of pine lignin as a softwood type. The FTIR spectrum of all the PLA composites with esterified lignin (30%) are shown in Appendix 3 (Figure 3d) in conjunction with the interpretation.

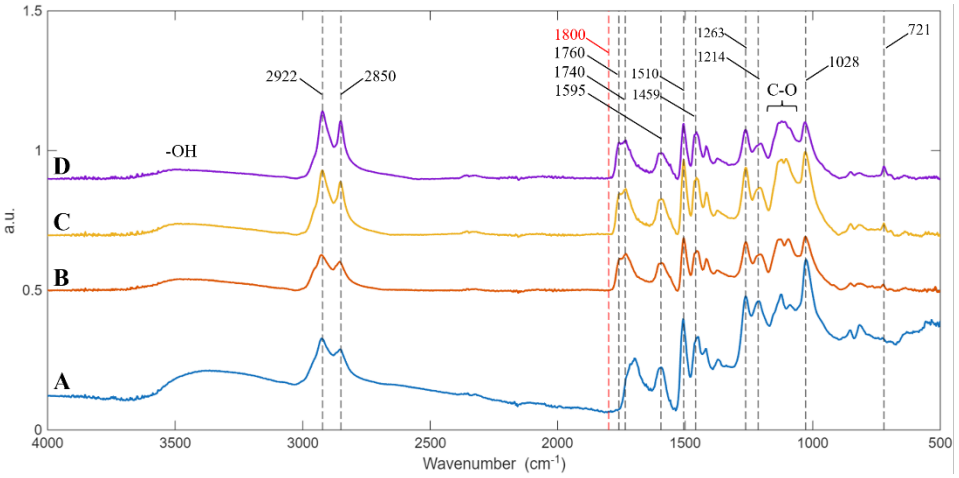

Figure 9. *FTIR spectra of the unmodified pine organosolv lignin (A) in comparison with the hydroxyl-esterified derivatives C8 (B), C12 (C), C16 (D).*

To further characterize hydroxyl-esterified lignin, ^{31}P NMR was employed. The experiment was additionally used for the study of the esterified lignin obtained from the two-step esterification route (Scheme 2, bottom). For those purposes, the starting material, C16-esterified, chloromethylated and its corresponding benzoic-esterified organosolv pine lignin samples were examined (Figure 10). All the spectra were calibrated at IS signal (151.8 ppm) prior to the analysis. As a G/H type lignin, the predominant phenolic OH arises from those units detected in the unmodified lignin (Figure 10A, 137.5–140.2 ppm). As anticipated, these functional groups reduced sharply

after the modification by the one-step esterification approach, meanwhile the aliphatic hydroxyls experienced a subtle decrease. This observation was consistent with the previous study, where the higher reactivity of phenolic hydroxyl groups toward esterification was observed compared to their aliphatic counterparts under the similar reaction condition [117].

In chloromethylated lignin (Figure 10C), the preservation of OH groups were evident from the pronounced shift of hydroxyl groups originating from G-units (around 139.0 ppm) towards the region associated with condensed phenolic OH (or C5/C6-substituted aromatic OH), ranging from 140.0 to 144.0 ppm, rather than a complete absence as observed in the first case scenario. The shifting could be rationalized by two reasons: (i) the introduction of new active sites (e.g., chloromethyl) to the aromatic backbone resembles the structural feature of lignin condensed fragments; (ii) the electronegativity of chloride atoms contributes to the deficiency in electron density of the aromatic rings causing the downfield shift indicated by higher chemical shift value. Later, the grafting of benzoic acid was successfully confirmed by an upfield shift of the peak (Figure 10D). The aromatic hydroxyl signal coming from benzoic-esterified lignin was present in a lower frequency region (approximately at 142.4 ppm) possibly due to the weaker electron-withdrawing effect of the ester bond formation with benzoic acids compared to the chloride atoms in their precursor (chloromethylated lignin, CML). The appearance of this signal was still detected within the boundary of the condensed phenolic region.

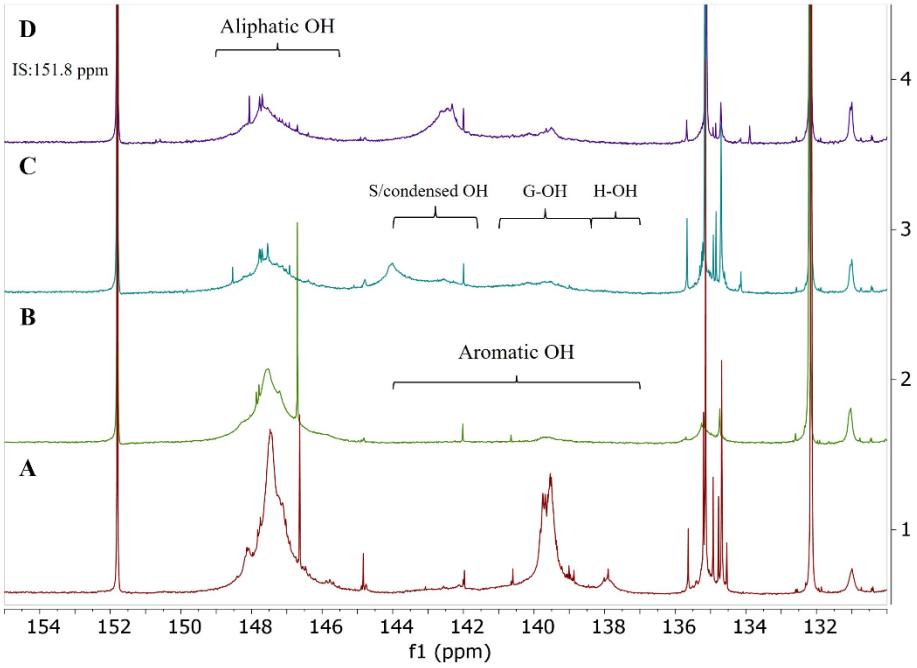

Figure 10. *^{31}P NMR spectra of starting material – organosolv pine lignin (A); C16-ester derivative modified via OH of lignin, C16 (B), chloromethylated lignin, CML (C), and benzoic ester lignin, BAEP (D).*

4.3.2 Thermal properties of esterified lignin and PLA composites

The thermal and mechanical profiling (Figure 11) were studied for the composites made up of PLA and 10–30% by weight of esterified lignin synthesized from the hydroxyl-esterification approach (presented in this work) and from the two-step protocol – chloromethylation followed by esterification using benzoic acid and tetradecanoic acid resulting in BAEP and HLE, respectively (carried out by Dr. M. K. Mohan). Overall, the blended polymeric materials exhibited variation in glass transition temperature (Tg) compared to pristine PLA (Figure 11A). The composites containing C8 and C12-esterified lignin exhibited Tg values close to PLA with a negligible fluctuation, for example, the values displayed around 60 to 62 °C. An increase in alkyl chain length up to C16 significantly reduced the Tg to 55 °C for modified lignin content of 20%. By contrast, the two-step protocol resulted the materials (BAEP and HLE) that could enhance the thermal performance of the composites, which was confirmed by elevated Tg by approximately 18 °C at the maximum load 30%. These results demonstrated two distinguished trends: (i) lignin esterification via hydroxyl groups was resulted in strong plasticization effect, which lowered Tg of the composites [118], [119]; (ii) attachment of the ester moieties via two-step protocol allowed to keep lignin hydroxy groups intact, which facilitated hydrogen bonding and thus tended to the elevated Tg values [120].

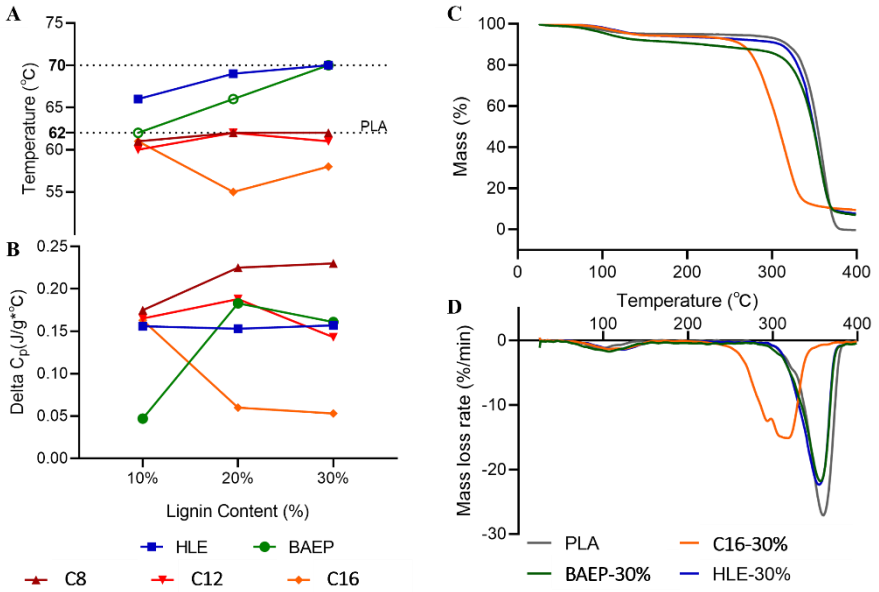

Figure 11. *Thermal properties of esterified lignin/PLA composites and neat PLA measured by DSC: glass transition temperature (A); delta Cp (B). Mass loss profile of the composite materials versus pure PLA achieved by thermogravimetric, TGA (C) and its differential thermogravimetric curve, DTG (D).*

Depending on the blending ratio and type of lignin derivative, Figure 11B shows various trends in ΔCp (specific heat capacity), which represents the change in the amount of thermal energy required to raise the temperature of one unit of mass by one degree at the glass transition stage of the material. The higher magnitude of ΔCp, by definition, corresponds to the increase in molecular mobility within the amorphous region during

the transition from a rigid, glassy to a softer, rubbery state, and vice versa. Notably, at the same concentration of hydroxyl-esterified lignin loaded into the PLA matrix, ΔCp sharply declined with the increasing of the carbon chain length substituent. This behaviour confirms that the compatibility between PLA and lignin modified with long alkyl chain ester was better than with the short chain esterified lignin. The former potentially led to a higher crystalline fraction or smaller amount of amorphous region of the material, hence decreasing ΔCp [119], [121]. On the other hand, BAEP/PLA composites demonstrate a sudden jump in ΔCp from the ratio of 10 to 20% indicating the flexibility of polymer chain in the amorphous region. This phenomenon could be explained by the interchain spacing effect. In this instance, due to differences in the conformation of benzene rings and PLA, the polymer chains were not as tightly packed as in the case of C16. Consequently, the increased free volume facilitated molecular movement, resulting in a larger change in heat capacity [122]. Even though the substituted alkyl chain length was comparable to C16, HLE-blended polymers showed no noticeable change in ΔCp at all loading levels, which underscores the significant impact of the modification approach on thermal behaviour of the composites.

To compare the thermal stability among the blended polymers, the study narrows down to three representatives, including PLA+C16, PLA+BAEP, and PLA+HLE (70:30 %w/w). Figure 11C displays the thermogravimetric data where all the materials were initially observed mass loss began at 80 °C, which was ascribed to the evaporation of moisture residue. As the temperature increased, PLA+BAEP gradually decomposed, while PLA+C16 shows the onset degradation temperature at approximately 245 °C, and PLA+HLE exhibited at a higher temperature of 300 °C. The differential thermogravimetric curves of the investigated materials (Figure 11D) illustrate the variation in the mass loss rate with respect to temperature. As anticipated, the consumption of hydroxyl groups during the direct esterification pathway weakens hydrogen bonding, resulting in a significant degradation of PLA+C16 at above 300 °C. Meanwhile, those blends made up of esterified lignin synthesized from the chloromethylation protocol experienced the highest mass loss rate at around 350 °C, which was moderately close to pristine PLA. These results reinforce the valuable presence of lignin hydroxyl groups for the manufacture of PLA composite in terms of thermal stability.

4.3.3 Mechanical properties of esterified lignin and PLA composites

The tensile test results of PLA and its composites with lignin esters (C16, BAEP, and HLE) 30% incorporated, are presented in Figure 12. All the blended products exhibit lower maximum load compared to neat PLA whose resistance could be up to 15.2 N prior to its fracture (Figure 12A). It is noteworthy that PLA+C16 withstood the highest force (10.3 N) among all the tested materials (Figure 12A), however the obtained ultimate tensile strength value for the same composite was lower than that of PLA+HLE in terms of cross-sectional area (Figure 12B). These inconsistent results possibly caused by the unidentical thickness of the films. Due to the difference in structural feature of the benzene rings from BAEP and PLA, the resultant composite PLA+BAEP (30%) was recorded with the lowest load and tensile stress, which were indicative of the weak interfacial interaction and less efficient stress transfer between polymer chains.

In contrast to the maximum load, the tensile extension enhanced upon the addition of ester lignin regardless of how they were modified (Figure 12C). The value represents the ductility of the material, which decreases in the order PLA+C16 (5.0 mm) > PLA+HLE > PLA+BAEP > PLA (2.5 mm). These results reflect that the intrinsic brittleness of PLA could

be potentially adjusted by adding esterified lignin. Additionally, the obtained values highlight the strong plasticization effect of hydroxyl-esterified C16 facilitating the movement of the polymer chain, thereby enhancing ductile property of the composite [76]. On the other hand, the elastic or Young's modulus (Figure 12D) describes material stiffness showing that the stiffest polymer composite was PLA+HLE, remarkably higher than neat PLA. In other words, the incorporation of 30% HLE into PLA matrix moderately improved the ductility, simultaneously enhanced the overall strength of the polymeric material thanks to the preservation of hydroxyl groups. Consequently, due to lack of intermolecular interactions, such as hydrogen bonding, the Young's modulus of PLA+C16 was comparatively low to PLA+HLE.

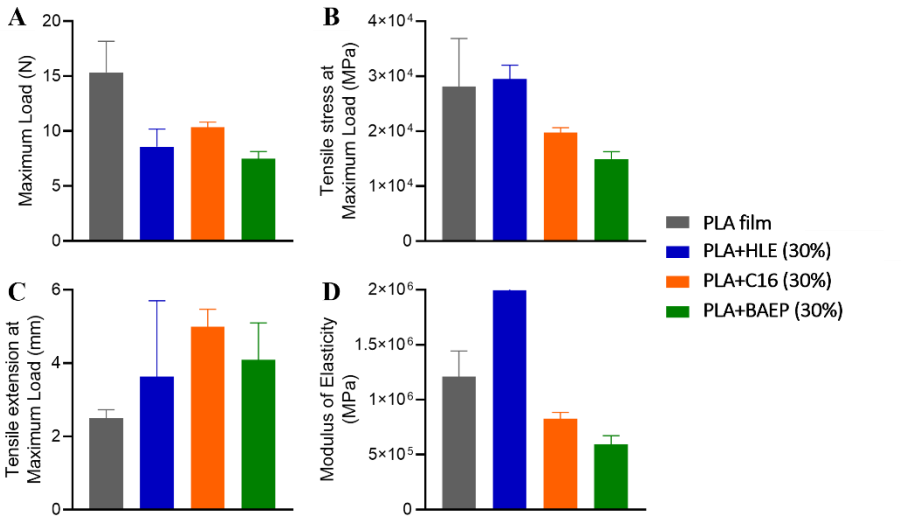

Figure 12. *Mechanical properties of esterified lignin/PLA composites reflected by maximum load (A), tensile stress at maximum load (B), tensile extension at maximum load (C), and Young's modulus (D).*

Overall, the impact of opting the esterification pathway of lignin is clearly indicated in the PLA composites characteristics. The exploitation of hydroxyl groups during esterification resulting in the composites with lower glass transition, and tensile modulus, however with improvement in elasticity. In other words, the esterified lignin synthesized from this approach exert a strong plasticization effect. By contrast, the retained hydroxyl groups attained in chloromethylation approach resulting in the additives that could increase thermal stability and mechanical strength.

5 Conclusions

This research elucidated how solvent choice influenced the structure of native and organosolv lignin (hydroxyl-group contents, subunit composition, interunit linkages, and the yield of uncondensed monolignols), as determined by NMR and thioacidolysis coupled with GC-MS. This study also demonstrated that the esterification strategy used for lignin modification has a strong impact on the properties of PLA–lignin composites, highlighting the importance of selecting an appropriate modification route to tailor composite performance.

The primary conclusions are summarized as follows:

- Solvent choice controls the extent of organosolv lignin depolymerization and functional-group profile. Under acidic organosolv conditions, 1,4-dioxane promoted more extensive β-O-4' cleavage, giving higher aromatic -OH and lower aliphatic -OH contents (and higher lignin recovery), whereas ethanol better preserved lignin closer to its native structure.
- Practical, broadly applicable calibration standards were validated for thioacidolysis/GC–MS quantification of uncondensed monolignols. Two lignin model compounds enabled reliable quantification, showing that uncondensed S/G monolignols are higher in native biomass than in organosolv lignin, and lower in DOLs than in EOLs, while avoiding the need for multi-step synthesis of thioethylated monomer standards.
- The choice of lignin esterification protocol is a key factor for tuning PLA–lignin composite performance. C16 hydroxyl-esterified lignin acted mainly as a plasticizer (lower glass transition, higher elasticity at 30 wt%), whereas two-step esterification that retained hydrogen bonding in BAEP and HLE composites with PLA, increased the thermal stability and stiffness of PLA composites at the same loading.

References

[1] M. D. Smith, 'An Abbreviated Historical and Structural Introduction to Lignocellulose', *ACS Symposium Series*, vol. 1338, pp. 1–15, 2019, doi: 10.1021/bk-2019-1338.ch001.

[2] H. Chen, 'Lignocellulose biorefinery engineering', in *Lignocellulose Biorefinery Engineering*, Elsevier, 2015, pp. 1–17. doi: 10.1016/b978-0-08-100135-6.00001-6.

[3] A. Yousuf, D. Pirozzi, and F. Sannino, 'Fundamentals of lignocellulosic biomass', in *Lignocellulosic Biomass to Liquid Biofuels*, Elsevier, 2019, pp. 1–15. doi: 10.1016/B978-0-12-815936-1.00001-0.

[4] B. Segers, P. Nimmegeers, M. Spiller, G. Tofani, E. Jasiukaitytė-Grojzdek, E. Dace, T. Kikas, J. M. Marchetti, M. Rajić, G. Yildiz, and P. Billen, 'Lignocellulosic biomass valorisation: a review of feedstocks, processes and potential value chains and their implications for the decision-making process', *RSC Sustainability*, vol. 2, no. 12. Royal Society of Chemistry, pp. 3730–3749, Oct. 10, 2024. doi: 10.1039/d4su00342j.

[5] G. Guerriero, J. F. Hausman, J. Strauss, H. Ertan, and K. S. Siddiqui, 'Lignocellulosic biomass: Biosynthesis, degradation, and industrial utilization', *Engineering in Life Sciences*, vol. 16, no. 1. Wiley-VCH Verlag, pp. 1–16, Jan. 01, 2016. doi: 10.1002/elsc.201400196.

[6] J. Bueno Moron, G. P. M. van Klink, and G. J. M. Gruter, 'Lignocellulose saccharification: historical insights and recent industrial advancements towards 2nd generation sugars', *RSC Sustainability*, vol. 3, no. 3. Royal Society of Chemistry, pp. 1170–1211, Jan. 27, 2025. doi: 10.1039/d4su00600c.

[7] L. N. Trentin, A. C. S. Alcântara, C. G. T. Batista, and M. S. Skaf, 'Unraveling the Mechanical Behavior of Softwood Secondary Cell Walls through Atomistic Simulations', *Biomacromolecules*, vol. 26, no. 6, pp. 3395–3409, Jun. 2025, doi: 10.1021/acs.biomac.4c01806.

[8] F. Brienza, D. Cannella, D. Montesdeoca, I. Cybulska, and D. P. Debecker, 'A guide to lignin valorization in biorefineries: traditional, recent, and forthcoming approaches to convert raw lignocellulose into valuable materials and chemicals', *RSC Sustainability*, vol. 2, no. 1. Royal Society of Chemistry, pp. 37–90, Nov. 09, 2023. doi: 10.1039/d3su00140g.

[9] J. Berglund, D. Mikkelsen, B. M. Flanagan, S. Dhital, S. Gaunitz, G. Henriksson, M. E. Lindström, G. E. Yakubov, M. J. Gidley, and F. Vilaplana, 'Wood hemicelluloses exert distinct biomechanical contributions to cellulose fibrillar networks', *Nat Commun*, vol. 11, no. 1, Dec. 2020, doi: 10.1038/s41467-020-18390-z.

[10] J. Berglund, T. Angles d'Ortoli, F. Vilaplana, G. Widmalm, M. Bergenstråhle-Wohlert, M. Lawoko, G. Henriksson, M. Lindström, and J. Wohlert, 'A molecular dynamics study of the effect of glycosidic linkage type in the hemicellulose backbone on the molecular chain flexibility', *Plant Journal*, vol. 88, no. 1, pp. 56–70, Oct. 2016, doi: 10.1111/tpj.13259.

[11] C. W. Lahive, P. C. J. Kamer, C. S. Lancefield, and P. J. Deuss, 'An Introduction to Model Compounds of Lignin Linking Motifs; Synthesis and Selection Considerations for Reactivity Studies', *ChemSusChem*, vol. 13, no. 17. Wiley-VCH Verlag, pp. 4238–4265, Sep. 07, 2020. doi: 10.1002/cssc.202000989.

[12] C. J. Liu, 'Deciphering the enigma of lignification: Precursor transport, oxidation, and the topochemistry of lignin assembly', in *Molecular Plant*, Oxford University Press, 2012, pp. 304–317. doi: 10.1093/mp/ssr121.

[13] R. Vanholme, B. Demedts, K. Morreel, J. Ralph, and W. Boerjan, 'Lignin biosynthesis and structure', *Plant Physiol*, vol. 153, no. 3, pp. 895–905, 2010, doi: 10.1104/pp.110.155119.

[14] Y. Tobimatsu and M. Schuetz, 'Lignin polymerization: how do plants manage the chemistry so well?', *Current Opinion in Biotechnology*, vol. 56. Elsevier Ltd, pp. 75–81, Apr. 01, 2019. doi: 10.1016/j.copbio.2018.10.001.

[15] J. Ralph, C. Lapierre, and W. Boerjan, 'Lignin structure and its engineering', *Current Opinion in Biotechnology*, vol. 56. Elsevier Ltd, pp. 240–249, Apr. 01, 2019. doi: 10.1016/j.copbio.2019.02.019.

[16] Y. Mottiar, S. D. Karlen, R. E. Goacher, J. Ralph, and S. D. Mansfield, 'Metabolic engineering of p-hydroxybenzoate in poplar lignin', *Plant Biotechnol J*, vol. 21, no. 1, pp. 176–188, Jan. 2023, doi: 10.1111/pbi.13935.

[17] J. C. Del Río, J. Rencoret, A. Gutiérrez, T. Elder, H. Kim, and J. Ralph, 'Lignin Monomers from beyond the Canonical Monolignol Biosynthetic Pathway: Another Brick in the Wall', *ACS Sustainable Chemistry and Engineering*, vol. 8, no. 13. American Chemical Society, pp. 4997–5012, Apr. 06, 2020. doi: 10.1021/acssuschemeng.0c01109.

[18] L. Yan, A. J. Huertas-Alonso, H. Liu, L. Dai, C. Si, and M. H. Sipponen, 'Lignin polymerization: towards high-performance materials', *Chemical Society Reviews*, vol. 54, no. 14. Royal Society of Chemistry, pp. 6634–6651, Jun. 10, 2025. doi: 10.1039/d4cs01044b.

[19] C. G. Yoo, X. Meng, Y. Pu, and A. J. Ragauskas, 'The critical role of lignin in lignocellulosic biomass conversion and recent pretreatment strategies: A comprehensive review', *Bioresource Technology*, vol. 301. Elsevier Ltd, Apr. 01, 2020. doi: 10.1016/j.biortech.2020.122784.

[20] Y. Zhao, U. Shakeel, M. Saif Ur Rehman, H. Li, X. Xu, and J. Xu, 'Lignin-carbohydrate complexes (LCCs) and its role in biorefinery', *Journal of Cleaner Production*, vol. 253. Elsevier Ltd, Apr. 20, 2020. doi: 10.1016/j.jclepro.2020.120076.

[21] H. Nishimura, A. Kamiya, T. Nagata, M. Katahira, and T. Watanabe, 'Direct evidence for α ether linkage between lignin and carbohydrates in wood cell walls', *Sci Rep*, vol. 8, no. 1, Dec. 2018, doi: 10.1038/s41598-018-24328-9.

[22] M. Li, Y. Pu, and A. J. Ragauskas, 'Current understanding of the correlation of lignin structure with biomass recalcitrance', *Frontiers in Chemistry*, vol. 4, no. NOV. Frontiers Media S. A, 2016. doi: 10.3389/fchem.2016.00045.

[23] M. Lee, H. S. Jeon, S. H. Kim, J. H. Chung, D. Roppolo, H. Lee, H. J. Cho, Y. Tobimatsu, J. Ralph, and O. K. Park, 'Lignin-based barrier restricts pathogens to the infection site and confers resistance in plants', *EMBO J*, vol. 38, no. 23, Dec. 2019, doi: 10.15252/embj.2019101948.

[24] A. Zoghlami and G. Paës, 'Lignocellulosic Biomass: Understanding Recalcitrance and Predicting Hydrolysis', *Frontiers in Chemistry*, vol. 7. Frontiers Media S.A., Dec. 18, 2019. doi: 10.3389/fchem.2019.00874.

[25] D. B. Sulis, N. Lavoine, H. Sederoff, X. Jiang, B. M. Marques, K. Lan, C. Cofre-Vega, R. Barrangou, and J. P. Wang, 'Advances in lignocellulosic feedstocks for bioenergy and bioproducts', *Nature Communications* , vol. 16, no. 1. Nature Research, Dec. 01, 2025. doi: 10.1038/s41467-025-56472-y.

[26] C. Zhen, H. Sun, M. Ma, T. Mu, and M. Garcia-Vaquero, 'Applications of modified lignocellulose and its composites prepared by different pretreatments in biomedicine: A review', *International Journal of Biological Macromolecules*, vol. 301. Elsevier B.V., Apr. 01, 2025. doi: 10.1016/j.ijbiomac.2025.140347.

[27] J. A. Okolie, S. Nanda, A. K. Dalai, and J. A. Kozinski, 'Chemistry and Specialty Industrial Applications of Lignocellulosic Biomass', *Waste and Biomass Valorization*, vol. 12, no. 5. Springer Science and Business Media B.V., pp. 2145–2169, May 01, 2021. doi: 10.1007/s12649-020-01123-0.

[28] S. R. Mathura, A. C. Landázuri, F. Mathura, A. G. Andrade Sosa, and L. M. Orejuela-Escobar, 'Hemicelluloses from bioresidues and their applications in the food industry - towards an advanced bioeconomy and a sustainable global value chain of chemicals and materials', *Sustainable Food Technology*, vol. 2, no. 5. Royal Society of Chemistry, pp. 1183–1205, Jul. 02, 2024. doi: 10.1039/d4fb00035h.

[29] J. Zhao, M. Zhu, W. Jin, J. Zhang, G. Fan, Y. Feng, Z. Li, S. Wang, J. S. Lee, G. Luan, Z. Dong, and Y. Li, 'A comprehensive review of unlocking the potential of lignin-derived biomaterials: from lignin structure to biomedical application', *Journal of Nanobiotechnology* , vol. 23, no. 1. BioMed Central Ltd, Dec. 01, 2025. doi: 10.1186/s12951-025-03604-7.

[30] H. Luo and M. M. Abu-Omar, 'Chemicals From Lignin', in *Encyclopedia of Sustainable Technologies*, Elsevier, 2017, pp. 573–585. doi: 10.1016/B978-0-12-409548-9.10235-0.

[31] T. Li and S. Takkellapati, 'The current and emerging sources of technical lignins and their applications', *Biofuels, Bioproducts and Biorefining*, vol. 12, no. 5, pp. 756–787, Sep. 2018, doi: 10.1002/bbb.1913.

[32] D. S. Zijlstra, C. W. Lahive, C. A. Analbers, M. B. Figueirêdo, Z. Wang, C. S. Lancefield, and P. J. Deuss, 'Mild Organosolv Lignin Extraction with Alcohols: The Importance of Benzylic Alkoxylation', *ACS Sustain Chem Eng*, vol. 8, no. 13, pp. 5119–5131, Apr. 2020, doi: 10.1021/acssuschemeng.9b07222.

[33] N. Cachet and B. Benjelloun-Mlayah, 'Comparison of Organic Acid-based Organosolv Lignins Extracted from the Residues of Five Annual Crops', *Bioresources*, vol. 16(4), no. Lignins, pp. 7966–7990, 2021.

[34] V. Ponnuchamy, O. Gordobil, R. H. Diaz, A. Sandak, and J. Sandak, 'Fractionation of lignin using organic solvents: A combined experimental and theoretical study', *Int J Biol Macromol*, vol. 168, pp. 792–805, Jan. 2021, doi: 10.1016/j.ijbiomac.2020.11.139.

[35] Sen Ma, W. Li, H. Liu, Z. Li, X. Tang, L. Lin, and X. Zeng, 'Ethyl acetate fractionation improved the homogeneity and purity of CAOSA-extracted lignin', *Ind Crops Prod*, vol. 219, Nov. 2024, doi: 10.1016/j.indcrop.2024.118957.

[36] C. G. Boeriu, F. I. Fiţigău, R. J. A. Gosselink, A. E. Frissen, J. Stoutjesdijk, and F. Peter, 'Fractionation of five technical lignins by selective extraction in green solvents and characterisation of isolated fractions', *Ind Crops Prod*, vol. 62, pp. 481–490, Dec. 2014, doi: 10.1016/j.indcrop.2014.09.019.

[37] G. Tofani, E. Jasiukaitytė-Grojzdek, M. Grilc, and B. Likozar, 'Organosolv biorefinery: resource-based process optimisation, pilot technology scale-up and economics', *Green Chemistry*, vol. 26, no. 1. Royal Society of Chemistry, pp. 186–201, Nov. 21, 2023. doi: 10.1039/d3gc03274d.

[38] S. Sandner and M. Kienberger, 'Tuning organosolv lignin properties through the cooking process: A meta-analysis', *Industrial Crops and Products*, vol. 232. Elsevier B.V., Sep. 15, 2025. doi: 10.1016/j.indcrop.2025.121247.

[39] A. A. Vaidya, K. D. Murton, D. A. Smith, and G. Dedual, 'A review on organosolv pretreatment of softwood with a focus on enzymatic hydrolysis of cellulose', *Biomass Conversion and Biorefinery*, vol. 12, no. 11. Springer Science and Business Media Deutschland GmbH, pp. 5427–5442, Nov. 01, 2022. doi: 10.1007/s13399-022-02373-9.

[40] M. Parot, D. Rodrigue, and T. Stevanovic, 'High purity softwood lignin obtained by an eco-friendly organosolv process', *Bioresour Technol Rep*, vol. 17, Feb. 2022, doi: 10.1016/j.biteb.2021.100880.

[41] T. P. Wang, H. Li, J. M. Yuan, W. X. Li, K. Li, Y. B. Huang, L. P. Xiao, and Q. Lu, 'Structures and pyrolytic characteristics of organosolv lignins from typical softwood, hardwood and herbaceous biomass', *Ind Crops Prod*, vol. 171, Nov. 2021, doi: 10.1016/j.indcrop.2021.113912.

[42] N. Obrzut, R. Hickmott, L. Shure, and K. A. Gray, 'The effects of lignin source and extraction on the composition and properties of biorefined depolymerization products', *RSC Sustainability*, vol. 1, no. 9, pp. 2328–2340, Oct. 2023, doi: 10.1039/d3su00262d.

[43] N. M. Stark, D. J. Yelle, and U. P. Agarwal, 'Techniques for Characterizing Lignin', in *Lignin in Polymer Composites*, Elsevier Inc., 2016, pp. 49–66. doi: 10.1016/B978-0-323-35565-0.00004-7.

[44] Y. Pu, S. Cao, and A. J. Ragauskas, 'Application of quantitative 31P NMR in biomass lignin and biofuel precursors characterization', *Energy and Environmental Science*, vol. 4, no. 9. pp. 3154–3166, Sep. 2011. doi: 10.1039/c1ee01201k.

[45] A. Granata and D. S. Argyropoulos, '2-Chloro-4,4,5,5-tetramethyl-1,3,2-dioxaphospholane, a Reagent for the Accurate Determination of the Uncondensed and Condensed Phenolic Moieties in Lignins', *J Agric Food Chem*, vol. 43, pp. 1538–1544, 1995, [Online]. Available: https://pubs.acs.org/sharingguidelines

[46] M. R. Sturgeon, S. Kim, K. Lawrence, R. S. Paton, S. C. Chmely, M. Nimlos, T. D. Foust, and G. T. Beckham, 'A Mechanistic investigation of acid-catalyzed cleavage of aryl-ether linkages: Implications for lignin depolymerization in acidic environments', *ACS Sustain Chem Eng*, vol. 2, no. 3, pp. 472–485, Mar. 2014, doi: 10.1021/sc400384w.

[47] P. Sannigrahi, A. J. Ragauskas, and S. J. Miller, 'Lignin structural modifications resulting from ethanol organosolv treatment of Loblolly pine', in *Energy and Fuels*, Jan. 2010, pp. 683–689. doi: 10.1021/ef900845t.

[48] D. G. Brandner, J. Gracia Vitoria, J. K. Kenny, J. R. Bussard, J. H. Jang, S. P. Woodworth, K. Vanbroekhoven, Y. Román-Leshkov, and G. T. Beckham, 'Lignin Extraction and Condensation as a Function of Temperature, Residence Time, and Solvent System in Flow-through Reactors', *ACS Sustain Chem Eng*, vol. 13, no. 31, pp. 12573–12582, Aug. 2025, doi: 10.1021/acssuschemeng.5c04198.

[49] A. Antczak, A. Skręta, A. Kamińska-Dwórznicka, K. Rząd, and A. Matwijczuk, 'Study on the Structure of Lignin Isolated from Wood Under Acidic Conditions', *Molecules*, vol. 30, no. 24, p. 4705, Dec. 2025, doi: 10.3390/molecules30244705.

[50] K. H. Kim and C. S. Kim, 'Recent efforts to prevent undesirable reactions from fractionation to depolymerization of lignin: Toward maximizing the value from lignin', *Frontiers in Energy Research*, vol. 6, no. SEP. Frontiers Media S.A., Sep. 11, 2018. doi: 10.3389/fenrg.2018.00092.

[51] C. Lapierre, B. Monties, C. Rolando, C. Lapierre, B. Monties, and C. Rolando, 'Thioacidolysis of lignin: Comparison with acidolysis', *Journal of Wood Chemistry and Technology*, vol. 5, no. 2, pp. 277–292, Jan. 1985, doi: 10.1080/02773818508085193.

[52] C. Lapierre, B. Monties, and C. Rolando, 'Thioacidolysis of Poplar Lignins: Identification of Monomeric Syringyl Products and Chracterization of Guaiacyl-Syringyl Lignin Fractions', *Holzforschung*, vol. 113, pp. 113–118, 1986.

[53] C. Rolando, B. Monties, and C. Lapierre, 'New insights into the molecular architecture of hardwood lignins by chemical degradative methods', *Research on chemical intermediate*, vol. 21, pp. 397–412, 1995, doi: 10.1007/978-3-642-74065-7_23.

[54] A. R. Robinson and S. D. Mansfield, 'Rapid analysis of poplar lignin monomer composition by a streamlined thioacidolysis procedure and near-infrared reflectance-based prediction modeling', *Plant Journal*, vol. 58, no. 4, pp. 706–714, May 2009, doi: 10.1111/j.1365-313X.2009.03808.x.

[55] M. Yamamura, T. Hattori, S. Suzuki, D. Shibata, and T. Umezawa, 'Microscale thioacidolysis method for the rapid analysis of β-O-4 substructures in lignin', *Plant Biotechnology*, vol. 29, no. 4, pp. 419–423, 2012, doi: 10.5511/plantbiotechnology.12.0627a.

[56] A. E. Harman-Ware, C. Foster, R. M. Happs, C. Doeppke, K. Meunier, J. Gehan, F. Yue, F. Lu, and M. F. Davis, 'A thioacidolysis method tailored for higher-throughput quantitative analysis of lignin monomers', *Biotechnol J*, vol. 11, no. 10, pp. 1268–1273, 2016, doi: 10.1002/biot.201600266.

[57] Q. Qi, J. Hu, L. Qu, X. Jiang, Y. Gai, S. A. Valenzuela, and L. Qi, 'Rapid, simplified microscale quantitative analysis of lignin H/G/S composition with GC–MS in glass ampules and glass capillaries', *MethodsX*, vol. 6, pp. 2592–2600, Jan. 2019, doi: 10.1016/j.mex.2019.11.005.

[58] F. Chen, C. Zhuo, X. Xiao, T. H. Pendergast, and K. M. Devos, 'A rapid thioacidolysis method for biomass lignin composition and tricin analysis', *Biotechnol Biofuels*, vol. 14, no. 1, pp. 1–9, 2021, doi: 10.1186/s13068-020-01865-y.

[59] L. Yang, J. Wang, C. Wang, F. Yue, and F. Lu, 'A tailored fast thioacidolysis method incorporating multi-reaction monitoring mode of GC-MS for higher sensitivity on lignin monomer quantification', *Holzforschung*, vol. 76, no. 7, pp. 604–610, Jul. 2022, doi: 10.1515/hf-2021-0224.

[60] F. Yue, F. Lu, R. C. Sun, and J. Ralph, 'Syntheses of lignin-derived thioacidolysis monomers and their uses as quantitation standards', *J Agric Food Chem*, vol. 60, no. 4, pp. 922–928, 2012, doi: 10.1021/jf204481x.

[61] T. Capoun and J. Krykorkova, 'Internal Standards for Quantitative Analysis of Chemical Warfare Agents by the GC/MS Method: Nerve Agents', *J Anal Methods Chem*, vol. 2020, 2020, doi: 10.1155/2020/8857210.

[62] A. Korban, R. Čabala, V. Egorov, Z. Bosáková, and S. Charapitsa, 'Evaluation of the variation in relative response factors of GC-MS analysis with the internal standard methods: Application for the alcoholic products quality control', *Talanta*, vol. 246, Aug. 2022, doi: 10.1016/j.talanta.2022.123518.

[63] M. Margarida Martins, F. Carvalheiro, and F. Gírio, 'An overview of lignin pathways of valorization: from isolation to refining and conversion into value-added products', *Biomass Conversion and Biorefinery*, vol. 14, no. 3. Springer Science and Business Media Deutschland GmbH, pp. 3183–3207, Feb. 01, 2024. doi: 10.1007/s13399-022-02701-z.

[64] A. Nagardeolekar, M. Ovadias, P. Dongre, and B. Bujanovic, 'Prospects and Challenges of Using Lignin for Thermoplastic Materials', in *ACS Symposium Series*, vol. 1377, American Chemical Society, 2021, pp. 231–271. doi: 10.1021/bk-2021-1377.ch010.

[65] C. Vasile and M. Baican, 'Lignins as Promising Renewable Biopolymers and Bioactive Compounds for High-Performance Materials', *Polymers*, vol. 15, no. 15. Multidisciplinary Digital Publishing Institute (MDPI), Aug. 01, 2023. doi: 10.3390/polym15153177.

[66] L. A. Zevallos Torres, A. Lorenci Woiciechowski, V. O. de Andrade Tanobe, S. G. Karp, L. C. Guimarães Lorenci, C. Faulds, and C. R. Soccol, 'Lignin as a potential source of high-added value compounds: A review', *Journal of Cleaner Production*, vol. 263. Elsevier Ltd, Aug. 01, 2020. doi: 10.1016/j.jclepro.2020.121499.

[67] 'Lignin as Green Filler in Polymer Composites: Development Methods, Characteristics, and Potential Applications', *Advances in Materials Science and Engineering*, vol. 2022. Hindawi Limited, 2022. doi: 10.1155/2022/1363481.

[68] N. I. Jeffri, N. F. Mohammad Rawi, M. H. Mohamad Kassim, and C. K. Abdullah, 'Unlocking the potential: Evolving role of technical lignin in diverse applications and overcoming challenges', *International Journal of Biological Macromolecules*, vol. 274. Elsevier B.V., Aug. 01, 2024. doi: 10.1016/j.ijbiomac.2024.133506.

[69] A. J. Basbasan, B. Hararak, C. Winotapun, W. Wanmolee, P. Leelaphiwat, K. Boonruang, W. Chinsirikul, and V. Chonhenchob, 'Emerging challenges on viability and commercialization of lignin in biobased polymers for food packaging: A review', *Food Packaging and Shelf Life*, vol. 34. Elsevier Ltd, Dec. 01, 2022. doi: 10.1016/j.fpsl.2022.100969.

[70] R. R. de Sousa Junior, G. E. S. Garcia, M. P. da Silva Bisneto, L. G. de Freitas, T. B. Hubmann, T. M. Coutinho, and D. J. dos Santos, 'Thermo-Mechanical Properties of Polypropylene Blends with Esterified Lignin', *AppliedChem*, vol. 5, no. 1, Mar. 2025, doi: 10.3390/appliedchem5010003.

[71] L. Dehne, C. Vila, B. Saake, and K. U. Schwarz, 'Esterification of Kraft lignin as a method to improve structural and mechanical properties of lignin-polyethylene blends', *J Appl Polym Sci*, vol. 134, no. 11, Mar. 2017, doi: 10.1002/app.44582.

[72] E. M. Garcia, P. Nousiainen, U. Hyväkkö, and M. Österberg, 'Solventless Production of Thermoplastic Lignin Esters for Polymer Blends and Elastomers via Reactive Extrusion', *ACS Sustain Chem Eng*, vol. 13, no. 30, pp. 12198–12209, Aug. 2025, doi: 10.1021/acssuschemeng.5c04676.

[73] E. S. Esakkimuthu, V. Ponnuchamy, M. H. Sipponen, and D. DeVallance, 'Elucidating intermolecular forces to improve compatibility of kraft lignin in poly(lactic acid)', *Front Chem*, vol. 12, 2024, doi: 10.3389/fchem.2024.1347147.

[74] M. Parit and Z. Jiang, 'Towards lignin derived thermoplastic polymers', *International Journal of Biological Macromolecules*, vol. 165. Elsevier B.V., pp. 3180–3197, Dec. 15, 2020. doi: 10.1016/j.ijbiomac.2020.09.173.

[75] V. Georgs, H. Piili, J. Gustafsson, and C. Xu, 'A critical review on lignin structure, chemistry, and modification towards utilisation in additive manufacturing of lignin-based composites', *Ind Crops Prod*, vol. 233, Oct. 2025, doi: 10.1016/j.indcrop.2025.121416.

[76] K. Komisarz, T. M. Majka, and K. Pielichowski, 'Chemical and Physical Modification of Lignin for Green Polymeric Composite Materials', *Materials*, vol. 16, no. 1. MDPI, Jan. 01, 2023. doi: 10.3390/ma16010016.

[77] L. Y. Liu, S. Chen, L. Ji, S. K. Jang, and S. Renneckar, 'One-pot route to convert technical lignin into versatile lignin esters for tailored bioplastics and sustainable materials', *Green Chemistry*, vol. 23, no. 12, pp. 4567–4579, Jun. 2021, doi: 10.1039/d1gc01033f.

[78] O. R. Agede and M. C. Thies, 'Interlinking Lignin Molecules with Citric Acid: The Effect of Reaction Conditions on Lignin Properties', *ChemSusChem*, vol. 18, no. 14, Jul. 2025, doi: 10.1002/cssc.202500311.

[79] G. Resende, G. D. Azevedo, F. Souto, and V. Calado, 'Chemical Modification of Softwood Kraft Lignin with Succinic Acid', *ACS Omega*, vol. 9, no. 52, pp. 50945–50956, Dec. 2024, doi: 10.1021/acsomega.4c03127.

[80] R. R. de Sousa Junior, G. E. S. Garcia, M. P. da Silva Bisneto, L. G. de Freitas, T. B. Hubmann, T. M. Coutinho, and D. J. dos Santos, 'Thermo-Mechanical Properties of Polypropylene Blends with Esterified Lignin', *AppliedChem*, vol. 5, no. 1, Mar. 2025, doi: 10.3390/appliedchem5010003.

[81] O. Gordobil, E. Robles, I. Egüés, and J. Labidi, 'Lignin-ester derivatives as novel thermoplastic materials', *RSC Adv*, vol. 6, no. 90, pp. 86909–86917, 2016, doi: 10.1039/c6ra20238a.

[82] C. Libretti, L. Santos Correa, and M. A. R. Meier, 'From waste to resource: advancements in sustainable lignin modification', *Green Chemistry*, vol. 26, no. 8. Royal Society of Chemistry, pp. 4358–4386, Mar. 20, 2024. doi: 10.1039/d4gc00745j.

[83] M. K. Mohan, O. Silenko, I. Krasnou, O. Volobujeva, M. Kulp, M. Ošeka, T. Lukk, and Y. Karpichev, 'Chloromethylation of Lignin as a Route to Functional Material with Catalytic Properties in Cross-Coupling and Click Reactions', *ChemSusChem*, vol. 17, no. 8, Apr. 2024, doi: 10.1002/cssc.202301588.

[84] M. K. Mohan, I. Krasnou, T. Lukk, and Y. Karpichev, 'Novel Softwood Lignin Esters as Advanced Filler to PLA for 3D Printing', *ACS Omega*, 2024, doi: 10.1021/acsomega.4c06680.

[85] X. Meng, C. Crestini, H. Ben, N. Hao, Y. Pu, A. J. Ragauskas, and D. S. Argyropoulos, 'Determination of hydroxyl groups in biorefinery resources via quantitative 31P NMR spectroscopy', *Nat Protoc*, vol. 14, no. 9, pp. 2627–2647, Sep. 2019, doi: 10.1038/s41596-019-0191-1.

[86] P. Paulsen Thoresen, H. Lange, C. Crestini, U. Rova, L. Matsakas, and P. Christakopoulos, 'Characterization of Organosolv Birch Lignins: Toward Application-Specific Lignin Production', *ACS Omega*, vol. 6, no. 6, pp. 4374–4385, Feb. 2021, doi: 10.1021/acsomega.0c05719.

[87] X. Wei, Y. Liu, Y. Luo, Z. Shen, S. Wang, M. Li, and L. Zhang, 'Effect of organosolv extraction on the structure and antioxidant activity of eucalyptus kraft lignin', *Int J Biol Macromol*, vol. 187, pp. 462–470, Sep. 2021, doi: 10.1016/j.ijbiomac.2021.07.082.

[88] E. Jasiukaitytė-Grojzdek, M. Huš, M. Grilc, and B. Likozar, 'Acid-catalysed α-O-4 aryl-ether bond cleavage in methanol/(aqueous) ethanol: understanding depolymerisation of a lignin model compound during organosolv pretreatment', *Sci Rep*, vol. 10, no. 1, Dec. 2020, doi: 10.1038/s41598-020-67787-9.

[89] G. H. Kim and B. H. Um, 'Fractionation and characterization of lignins from Miscanthus via organosolv and soda pulping for biorefinery applications', *Int J Biol Macromol*, vol. 158, pp. 443–451, Sep. 2020, doi: 10.1016/j.ijbiomac.2020.04.229.

[90] A. V. Faleva, A. Y. Kozhevnikov, S. A. Pokryshkin, D. I. Falev, S. L. Shestakov, and J. A. Popova, 'Structural characteristics of different softwood lignins according to 1D and 2D NMR spectroscopy', *Journal of Wood Chemistry and Technology*, vol. 40, no. 3, pp. 178–189, May 2020, doi: 10.1080/02773813.2020.1722702.

[91] J. L. Wen, S. L. Sun, B. L. Xue, and R. C. Sun, 'Recent advances in characterization of lignin polymer by solution-state nuclear magnetic resonance (NMR) methodology', *Materials*, vol. 6, no. 1. pp. 359–391, 2013. doi: 10.3390/ma6010359.

[92] M. Sette, H. Lange, and C. Crestini, 'Quantitative HSQC analyses of lignin: A practical comparison', *Comput Struct Biotechnol J*, vol. 6, no. 7, p. e201303016, 2013, doi: 10.5936/csbj.201303016.

[93] S. Constant, H. L. J. Wienk, A. E. Frissen, P. De Peinder, R. Boelens, D. S. Van Es, R. J. H. Grisel, B. M. Weckhuysen, W. J. J. Huijgen, R. J. A. Gosselink, and P. C. A. Bruijnincx, 'New insights into the structure and composition of technical lignins: A comparative characterisation study', *Green Chemistry*, vol. 18, no. 9, pp. 2651–2665, 2016, doi: 10.1039/c5gc03043a.

[94] M. Yáñez-S, B. Matsuhiro, C. Nuñez, S. Pan, C. A. Hubbell, P. Sannigrahi, and A. J. Ragauskas, 'Physicochemical characterization of ethanol organosolv lignin (EOL) from Eucalyptus globulus: Effect of extraction conditions on the molecular structure', *Polymer Degradation and Stability*, vol. 110. Elsevier Ltd, pp. 184–194, 2014. doi: 10.1016/j.polymdegradstab.2014.08.026.

[95] J. C. Del Río, J. Rencoret, P. Prinsen, Á. T. Martínez, J. Ralph, and A. Gutiérrez, 'Structural characterization of wheat straw lignin as revealed by analytical pyrolysis, 2D-NMR, and reductive cleavage methods', *J Agric Food Chem*, vol. 60, no. 23, pp. 5922–5935, Jun. 2012, doi: 10.1021/jf301002n.

[96] S. Bauer, H. Sorek, V. D. Mitchell, A. B. Ibáñez, and D. E. Wemmer, 'Characterization of Miscanthus giganteus lignin isolated by ethanol organosolv process under reflux condition', *J Agric Food Chem*, vol. 60, no. 33, pp. 8203–8212, Aug. 2012, doi: 10.1021/jf302409d.

[97] P. Wang, Y. Fu, Z. Shao, F. Zhang, and M. Qin, 'Structural changes to Aspen wood lignin during autohydrolysis pretreatment', *Bioresources*, vol. 11, no. 2, pp. 4086–4103, 2016.

[98] D. M. Miles-Barrett, A. R. Neal, C. Hand, J. R. D. Montgomery, I. Panovic, O. S. Ojo, C. S. Lancefield, D. B. Cordes, A. M. Z. Slawin, T. Lebl, and N. J. Westwood, 'The synthesis and analysis of lignin-bound Hibbert ketone structures in technical lignins', *Org Biomol Chem*, vol. 14, no. 42, pp. 10023–10030, 2016, doi: 10.1039/c6ob01915c.

[99] S. Sandner and M. Kienberger, 'Tuning organosolv lignin properties through the cooking process: A meta-analysis', *Industrial Crops and Products*, vol. 232. Elsevier B.V., Sep. 15, 2025. doi: 10.1016/j.indcrop.2025.121247.

[100] G. Li, Y. Sang, X. Li, H. Chen, and Y. Li, 'Solvolysis of enzymatic hydrolysis lignin in fuel compatible solvents', *Chem Eng Sci*, vol. 310, May 2025, doi: 10.1016/j.ces.2025.121549.

[101] R. El Hage, N. Brosse, P. Sannigrahi, and A. Ragauskas, 'Effects of process severity on the chemical structure of Miscanthus ethanol organosolv lignin', *Polym Degrad Stab*, vol. 95, no. 6, pp. 997–1003, Jun. 2010, doi: 10.1016/j.polymdegradstab.2010.03.012.

[102] H. Kim and J. Ralph, 'Solution-state 2D NMR of ball-milled plant cell wall gels in DMSO-d 6/pyridine-d5', *Org Biomol Chem*, vol. 8, no. 3, pp. 576–591, 2010, doi: 10.1039/b916070a.

[103] Y. Mottiar, S. D. Karlen, R. E. Goacher, J. Ralph, and S. D. Mansfield, 'Metabolic engineering of p-hydroxybenzoate in poplar lignin', *Plant Biotechnol J*, vol. 21, no. 1, pp. 176–188, Jan. 2023, doi: 10.1111/pbi.13935.

[104] J. C. Del Río, J. Rencoret, P. Prinsen, Á. T. Martínez, J. Ralph, and A. Gutiérrez, 'Structural characterization of wheat straw lignin as revealed by analytical pyrolysis, 2D-NMR, and reductive cleavage methods', *J Agric Food Chem*, vol. 60, no. 23, pp. 5922–5935, Jun. 2012, doi: 10.1021/jf301002n.

[105] European Commission, '2002/657/EC: Commission Decision of 12 August 2002 implementing Council Directive 96/23/EC concerning the performance of analytical methods and the interpretation of results', *Official Journal of European Communities*, 2002.

[106] M. Christiernin, A. B. Ohlsson, T. Berglund, and G. Henriksson, 'Lignin isolated from primary walls of hybrid aspen cell cultures indicates significant differences in lignin structure between primary and secondary cell wall', *Plant Physiology and Biochemistry*, vol. 43, no. 8, pp. 777–785, Aug. 2005, doi: 10.1016/j.plaphy.2005.07.007.

[107] J. Bergrath, J. Rumpf, R. Burger, X. T. Do, M. Wirtz, and M. Schulze, 'Beyond Yield Optimization: The Impact of Organosolv Process Parameters on Lignin Structure', *Macromolecular Materials and Engineering*, vol. 308, no. 10. John Wiley and Sons Inc, Oct. 01, 2023. doi: 10.1002/mame.202300093.

[108] M. Žula, E. Jasiukaitytė-Grojzdek, M. Grilc, and B. Likozar, 'Understanding acid-catalysed lignin depolymerisation process by model aromatic compound reaction kinetics', *Chemical Engineering Journal*, vol. 455, Jan. 2023, doi: 10.1016/j.cej.2022.140912.

[109] K. Shimada, S. Hosoya, and T. Ikeda, 'Condensation reactions of softwood and hardwood lignin model compounds under organic acid cooking conditions', *Journal of Wood Chemistry and Technology*, vol. 17, no. 1–2, pp. 57–72, 1997, doi: 10.1080/02773819708003118.

[110] X. Mu, Z. Han, C. Liu, and D. Zhang, 'Mechanistic Insights into Formaldehyde-Blocked Lignin Condensation: A DFT Study', *Journal of Physical Chemistry C*, vol. 123, no. 14, pp. 8640–8648, Apr. 2019, doi: 10.1021/acs.jpcc.9b00247.

[111] K. A. Y. Koivu, H. Sadeghifar, P. A. Nousiainen, D. S. Argyropoulos, and J. Sipilä, 'Effect of Fatty Acid Esterification on the Thermal Properties of Softwood Kraft Lignin', *ACS Sustain Chem Eng*, vol. 4, no. 10, pp. 5238–5247, Oct. 2016, doi: 10.1021/acssuschemeng.6b01048.

[112] A. Filopoulou, S. Vlachou, and S. C. Boyatzis, 'Fatty acids and their metal salts: A review of their infrared spectra in light of their presence in cultural heritage', *Molecules*, vol. 26, no. 19, Oct. 2021, doi: 10.3390/molecules26196005.

[113] Z. Liu, Y. Hou, S. Hu, and Y. Li, 'Possible dissolution mechanism of alkali lignin in lactic acid-choline chloride under mild conditions', *RSC Adv*, vol. 10, no. 67, pp. 40649–40657, Nov. 2020, doi: 10.1039/d0ra07808e.

[114] I. Anugwom, V. Lahtela, M. Kallioinen, and T. Kärki, 'Lignin as a functional additive in a biocomposite: Influence on mechanical properties of polylactic acid composites', *Ind Crops Prod*, vol. 140, Nov. 2019, doi: 10.1016/j.indcrop.2019.111704.

[115] M. Tanase-Opedal and J. Ruwoldt, 'Organosolv Lignin as a Green Sizing Agent for Thermoformed Pulp Products', *ACS Omega*, vol. 7, no. 50, pp. 46583–46593, Dec. 2022, doi: 10.1021/acsomega.2c05416.

[116] N. Cachet, S. Camy, B. Benjelloun-Mlayah, J. S. Condoret, and M. Delmas, 'Esterification of organosolv lignin under supercritical conditions', *Ind Crops Prod*, vol. 58, pp. 287–297, 2014, doi: 10.1016/j.indcrop.2014.03.039.

[117] T. Xu, A. V. Riazanova, P. A. Lindén, G. Henriksson, L. D. Söderberg, O. Gordobil, and O. Sevastyanova, 'Engineering of Industrial Kraft Lignin: The Role of Esterification Methods in Lignin Nanoparticle Self-Assembly', *Biomacromolecules*, vol. 26, no. 9, pp. 5727–5739, Sep. 2025, doi: 10.1021/acs.biomac.5c00507.

[118] Å. Henrik-Klemens, U. Edlund, G. Westman, and A. Larsson, 'Dynamic Mechanical Analysis of Plasticized and Esterified Native, Residual, and Technical Lignins: Compatibility and Glass Transition', *ACS Sustain Chem Eng*, vol. 13, no. 4, pp. 1648–1656, Feb. 2025, doi: 10.1021/acssuschemeng.4c08391.

[119] A. Greco, F. Ferrari, and A. Maffezzoli, 'Thermal analysis of poly(lactic acid) plasticized by cardanol derivatives', *J Therm Anal Calorim*, vol. 134, no. 1, pp. 559–565, Oct. 2018, doi: 10.1007/s10973-018-7059-4.

[120] P. González Cortes, R. Araya-Hermosilla, K. Wrighton-Araneda, D. Cortés-Arriagada, F. Picchioni, F. Yan, P. Rudolf, R. K. Bose, and F. Quero, 'Effect of intermolecular interactions on the glass transition temperature of chemically modified alternating polyketones', *Mater Today Chem*, vol. 34, Dec. 2023, doi: 10.1016/j.mtchem.2023.101771.

[121] A. Greco, F. Ferrari, and A. Maffezzoli, 'Mechanical properties of poly(lactid acid) plasticized by cardanol derivatives', *Polym Degrad Stab*, vol. 159, pp. 199–204, Jan. 2019, doi: 10.1016/j.polymdegradstab.2018.11.028.

[122] Q. Zhang, X. Chen, B. Zhang, T. Zhang, W. Lu, Z. Chen, Z. Liu, S. H. Kim, B. Donovan, R. J. Warzoha, E. D. Gomez, J. Bernholc, and Q. M. Zhang, 'High-temperature polymers with record-high breakdown strength enabled by rationally designed chain-packing behavior in blends', *Matter*, vol. 4, no. 7, pp. 2448–2459, Jul. 2021, doi: 10.1016/j.matt.2021.04.026.

Acknowledgements

This research was completed at Tallinn University of Technology under division of Chemistry and Biotechnology department with the supporting grant from Estonian Research Council (RESTA11, TEM-TA49).

From my point of view, the journey of doctoral study is best described as a 'marathon' in which I am forever grateful for the opportunity to stand at the starting line given by my supervisors, Dr. Maria Kulp, Dr. Tiit Lukk and Dr. Yevgen Karpichev. This ticket opened the door to the world that the 18th version of me could never have imagined fitting myself in; certainly, without your support along the way I would never have made it to the finishing line. Thank you for your presence and guidance, which substantially contributed to the success of my study. I am deeply thankful for your assistance in making the 'impossible(s)' possible.

I would like to express my gratitude to Dr. Indrek Reile and Dr. Marina Kudrjašova for their valuable discussions on NMR data analysis.

In the pursuit of my doctoral degree, I have never been alone, and this has never been a solo journey. Throughout the time, it would be hard for me to imagine going through all of ups and downs without my awesome lab mates. Thank you Piia for being there for me without hesitation whenever I need someone to talk to; your kindness is absolutely the most precious light that I could hold on to in those darkest moments. Thank you Hegne for all the hugs that you have been generously giving me; they may seem as ordinary as greetings but for me those hugs are more than enough to warm myself up inside out. Thank you, Eve-Ly, Kairit for always giving me the feeling of being included and heard. Thank you Maarja for being such a cool company that I have been always enjoying spending time with you. Thank you Pille-Riin for all the advice that helped me tackle all the questions I had at the beginning of my journey. Thank you Kristiina for your help that made my starting at the lab much easier. Thank you Darja for the coffee times that we spent together, and your deep listening to all my Taurus' talk. Thank you, Mahendra for being such a nice collaborator at work and a good friend in life. Kannan, there is no doubt about your pure friendship has made my life fulfilled in Estonia, thank you for being my 'go-to' buddies who have been staying shoulder to shoulder with me no matter what situations I was going through; you are like an extra golden medal that I have got and treasured for the rest of my life. Moreover, I would like to thank the department with their effort to improve PhD's life in all possible ways, and all the 'hello(s)' and 'smile(s)' that I have received from all Taltech'ers – those are as valuable as espresso shots that I always crave for on the daily basis.

Apart from the supporting system I have gained in Estonia, I am always grateful for having the 'online' system across countries, and continents. Thank you Shuang for having my back as always, every time we met felt like a go-home experience. Thank you for all friends whom I have met in Umeå, your companionship is exceptionally invaluable and meaningful that helped me having a perfect kick-start for my very first adventure of being abroad. Thank you for all my friends in Vietnam, despite the difference in time zone and my business, you have been always available for my nostalgic calls, and on behalf of me been there for my family's needs. I am deeply grateful that you all have chosen to stay in my circle.

The thankful speech could not be completed without expressing my heartfelt gratitude to my high school chemistry teacher, Trinh Dinh Thao; and my bachelor supervisor, Phan Thi Xuan. For many years and tons of reasons, you are the most

influential in my academic career. All the knowledge you have taught me is by far the most valuable things that I could never gotten from the books. Because those wisdoms are not only theories more than that the passion and compassion you have passed down shaping me into a scientist and a human being today.

I believe in all languages, the most beautiful word is 'family', which is translated as 'gia đình' in Vietnamese. Day by day, I have never stopped wishing to be born again in the same family in the next life. Perhaps I am the youngest, and therefore the luckiest-for my life to be filled with LOVE.

I have an amazing Sister (chị Na), who is also my best friend, and adviser for life. Her interest in books has had a tremendous impact on how I became a reader, without that passion for reading, my academic journey would not have progressed this far. Your wisdom is a treasure that I always admire. Thank you for your artwork in all my work and never complained about the deadlines I was facing. Thank you for being such a wonderful package comes all at once with the free lifetime subscription <3.

Thật sự không thể ngờ ngày hôm nay có thể viết vài dòng để cám ơn Ba, Mẹ trong chính cuốn luận văn tốt nghiệp tiến sĩ của con. Cám ơn Ba vì từ nhỏ đã luôn rèn luyện con sự ngăn nắp, gọn gàng, những tính cách làm nên nền tảng của con bây giờ. Cám ơn Ba vì đã chọn cách để lại những kỷ niệm đẹp theo cách rất riêng của mình. Cám ơn Mẹ, nếu không có Mẹ có lẽ con đã không đủ can đảm để nộp đơn phỏng vấn đi du học Umeå vào năm ấy. Cám ơn Mẹ vì đã luôn có niềm tin nơi con, thứ mà dường như giúp con vượt qua mọi trở ngại trên hành trình dài hơn nửa thập kỷ này. Cám ơn Mẹ dù trải qua bao nắng mưa vẫn luôn cố gắng dành những điều tốt đẹp nhất cho hai chị em con. Như con đã hứa, con tốt nghiệp rồi nhé!

Bé Ni luôn cảm thấy mình là đứa trẻ may mắn khi được ông, bà, chú, bác yêu thương. Tình yêu đó luôn là lá chắn giúp con dù có thế nào cũng có thể vững chân tiến về phía trước. Cám ơn gia đình mình vì đã luôn yêu thương và tự hào về con như vậy.

To beautifully end this part, I would like to give myself credit for not giving up, for being a soldier! More than a title, I am proud of the person I have become.

PHD = **P**ersistent, **H**umble, **D**etermined

What a ride!!!

This thesis is dedicated to my Grandma, and my Dad!

Abstract

Organosolv Lignin: From Characterization to Esterification

In nature, lignin is a repository of aromatic compounds composed of three primary phenylpropanoid monomers: *p*-coumaryl, coniferyl and sinapyl alcohols. It occurs in lignocellulosic biomass in conjunction with cellulose and hemicellulose forming a rigid supporting framework for plant cell wall. Despite the valuable chemical potential of lignin, its valorisation remains challenging in biorefineries. A key limitation is its structural heterogeneity, which varies significantly among species, and depends strongly on the severity of fractionation process. Therefore, a holistic understanding of lignin structure before and after biomass processing is essential for effective valorisation.

This dissertation addresses two important aspects of lignin: structural characterization (**Paper I, II**) and chemical modification for thermoplastic application (**Paper III**). The structural composition of organosolv lignin, fractionated using ethanol, or 1,4-dioxane and derived from three classes of biomass (e.g., hardwood – aspen chips, softwood – pine sawdust, and grass – barley straw) was investigated using nuclear magnetic resonance spectroscopy and thioacidolysis followed by gas chromatography – mass spectrometry. To further advance the understanding of how lignin can be used to tailor the properties of polylactic acid (PLA) composites, the esterification of organosolv pine and hydrolysis birch lignin using different protocols was investigated.

In **Paper I**, a comprehensive spectroscopic comparison was conducted on six organosolv lignins extracted from three biomass sources. Regardless of the botanical origins, phosphorus NMR (^{31}P-NMR) revealed that all 1,4-dioxane extracted lignins (DOLs) exhibited lower aliphatic hydroxyl and higher phenolic hydroxyl contents compared to ethanol-derived lignins (EOLs). The transformation of lignin sidechain into different arrangements and the formation of new aromatic hydroxyl groups resulted from lignin depolymerization through cleavage of aryl-ether bonds (α/β-O-4’). This observation was cemented by the heteronuclear single quantum coherence (HSQC) spectra, which showed a drastic decrease in the cross signals of β-O-4’ in DOLs. In other words, there was an extreme event of lignin depolymerization when using 1,4-dioxane for delignification; meanwhile, ethanol-based extraction resulted in lignin with a slightly modified structure (ethoxylation at C_α), and higher β-O-4’ content. The latter would be beneficial for the subsequent conversion of lignin into valuable monophenols.

In **Paper II**, the lack of suitable lignin standards for quantifying uncondensed monolignols analysis was addressed by proposing two commercially available phenolic lignin dimer model compounds (guaiacylglycerol-β-guaiacyl ether – GGE, syringylglycerol-β-guaiacyl ether – SGE) as calibration standards for thioacidolysis coupled with GC–MS. Quantification was performed by integrating peaks using TIC retention times and confirming them with EICs (*m/z* 343 for the internal standard, 269 for G-derived monomers, and 299 for S-derived monomers), with analyte identity verified by mass spectra and retention-time matching. The method showed strong calibration performance ($R^2 \geq 0.99$) and good accuracy based on recovery experiments (88.9% for GGE and 97.1% for SGE). Finally, the validated approach was applied to biomass and organosolv lignin samples, revealing higher uncondensed monolignol contents in native biomass than in extracted lignin samples, with lower values in DOLs compared to EOLs.

In **Paper III**, the focus of the study shifted from characterization to lignin modification. Specifically, two lignin esterification approaches were compared and their effects on polylactic acid (PLA) composites at a maximum lignin loading of 30% were evaluated. In

the first approach, conventional esterification of lignin hydroxyl groups with fatty acid chlorides (e.g., octanoyl – C8, lauroyl – C12, palmitoyl – C16 chlorides) produced materials with a pronounced plasticization effect, most evident for the longest substitution alkyl chain (C16). 30% of C16-esterified lignin blended polymer possesses better elasticity and lower thermal stability compared to pristine PLA. On the other hand, esterification concurrently retaining hydrogen bonds in lignin was carried out by the introduction of new active sites on the aromatic rings by chloromethylation and subsequent esterification using carboxylic acids (e.g., benzoic, tetradecanoic acids). The second approach produced modified lignin that increased the thermal resistance threshold and stiffness of the composites compared with the hydroxyl-esterified lignin at the same loading.

In conclusion, the findings of this thesis revealed the relationship between the extraction solvents and organosolv lignin's composition characterized by NMR and GC-MS methods. In addition, the study demonstrated that the choice of esterification site on lignin is critical for tailoring the thermochemical properties of PLA composites. These findings provide new insights into lignin valorisation and support its use in developing higher value-added, economically attractive, and environmentally friendly bio-based materials.

Lühikokkuvõte

Organosolv ligniin: koostise iseloomustamisest esterdamiseni

Looduses on ligniin aromaatsete ühendite varamu, mis koosneb kolmest peamisest fenüülpropanoidsest monomeerist: p-kumaarüül-, koniferiil- ja sinapüülalkoholist. Ligniin esineb lignotselluloosses biomassis koos tselluloosi ja hemitselluloosiga, moodustades taimeraku seinale jäiga tugiraamistiku. Hoolimata ligniini väärtuslikust keemilisest potentsiaalist on selle väärindamine endiselt keerukas. Üheks peamiseks piiranguks on ligniini struktuuri heterogeensus, mis sõltub oluliselt biomassi päritolust ja fraktsioneerimisprotsessi intensiivsusest. Seetõttu on ligniini tõhusaks väärindamiseks hädavajalik terviklik arusaam selle struktuurist enne ja pärast biomassi töötlemist.

Käesolev uurimitöö käsitleb kahte olulist aspekti, mis on seotud ligniini väärindamisega: organosolv ligniini struktuuri iseloomustamist (I ja II artikkel) ning selle keemilist modifitseerimist termoplastiliste rakenduste jaoks (III artikkel). Töös uuriti etanooli ja 1,4-dioksaaniga kolmest erinevast biomassist (lehtpuit, okaspuit ja rohttaimed) ekstraheeritud ligniini struktuuri ja koostist, kasutades tuumamagnetresonantsspektroskoopiat (NMR) ja tioatsidolüüsiga gaasikromatograafia–massispektromeetriat (GC–MS). Et paremini mõista, kuidas ligniini saab kasutada polülaktiidhappe (PLA) komposiitide omaduste reguleerimiseks, uuriti organosolv-männist ja hüdrolüüsi teel saadud kase ligniini esterifitseerimist rakendades erinevaid protokolle.

I artiklis põhjalikult analüüsiti struktuurset koostist kuuele organosolv-ligniinile, mis ekstraheeriti kolme liiki biomassist. Sõltumata botaanilisest päritolust näitas fosfor-NMR (^{31}P-NMR), et kõik 1,4-dioksaaniga ekstraheeritud ligniinid (DOL-id) sisaldasid vähem alifaatseid hüdroksüülrühmi ja rohkem fenoolseid hüdroksüülrühmi kui etanoolipõhised ligniinid (EOL-id). Ligniini külgahela funktsionaliseerimine ning uute aromaatsete hüdroksüülrühmade teke tulenes ligniini depolümerisatsioonist arüül-eetersidemete (α/β-O-4') lõhustumise kaudu. Seda kinnitasid HSQC spektrid, milles DOL-proovides täheldati β-O-4' signaalide märkimisväärset vähenemist. Teisisõnu põhjustas delignifikatsioon 1,4-dioksaanis ulatusliku depolümerisatsiooni, samas kui etanoolipõhine ekstraheerimine andis vaid kergelt modifitseeritud struktuuriga (Cα-etoksüülimine) ja suurema β-O-4' sisaldusega ligniini. Viimane on soodne ligniini edasiseks muundamiseks väärtuslikeks monofenoolideks.

II artiklis lahendati kvanitatiivseks analüüsiks vajalike ligniini standardite puudumine kondenseerumata monolignoolide kasutusele võtuga. Näidati, et tioatsidolüüsiga kombineeritud GC–MS analüüsiks sobivad kalibreerimisstandarditena kaks kommertsiaalselt kättesaadavat fenoolset ligniini dimeer-mudelühendit (guaiatsüülglütserool-β-guaiatsüül-eeter – GGE ja süüriingüülglütserool-β-guaiatsüül-eeter – SGE). Analüütide identifitseerimine ja kvantifitseerimine teostati piikide integraalide järgi, kasutades TIC-i retentsiooniaegu ning ainete massi-laengu suhteid; analüütide identiteet kinnitati massispektrite ja retentsiooniaegade abil. Arendatud ja valideeritud meetod näitas tugevat sõltuvust signaali ja monolignoolide kontsentratsiooni vahel ($R^2 \geq 0,99$) ning head täpsust rikastamismiskatsete põhjal (88,9% GGE ja 97,1% SGE puhul). Lõpuks rakendati valideeritud analüüsimeetodit biomassi- ja organosolv-ligniinide analüüsil, mille tulemused näitasid, et kondenseerumata monolignoolide sisaldus oli algses biomassis suurem kui ekstraheeritud ligniinides ning DOL-ides madalam kui EOL-ides.

III artiklis nihkus töö fookus ligniini iseloomustamiselt ligniini modifitseerimisele. Võrreldi kahte ligniini esterdamise meetodit ning hinnati nende mõju polülaktiidhappe (PLA) komposiitidele. Esimesel juhul esterdati ligniini hüdroksüülrühmad rasvhapete kloriididega (oktanoüül – C8, lauroüül – C12 ja palmitoüül – C16 kloriidid), mille tulemusel saadi plastilised materjalid . See efekt avaldus kõige selgemalt pikima alküülahela (C16) rasvhapete kasutamise korral. 30% C16-esterdatud ligniiniga PLA-komposiit oli suurema elastsusega, kuid madalama termilise stabiilsusega võrreldes puhta PLA-ga. Seejärel viidi läbi esterdamine viisil, mis säilitas ligniinis vesiniksidemed: areenidele lisati klorometüülimisega uued reaktiivsed rühmad ning seejärel teostati esterdamine karboksüülhapetega (bensoe- ja tetradekaanhape). See teine lähenemine andis modifitseeritud ligniinid, mis tõstsid komposiitide termilist vastupidavust ja jäikust võrreldes hüdroksüülrühmade kaudu esterdatud ligniinidega sama ligniini vahekorra juures komposiidis.

Kokkuvõttes näitasid käesoleva väitekirja tulemused seost ekstraheerimislahusti valiku ja organosolv-ligniini koostise vahel, ning viimast iseloomustati NMR-i ja GC–MS meetodite abil. Lisaks demonstreeriti uuringus, et ligniini esterdamise viis on PLA-komposiitide omaduste kujundamisel määrava tähtsusega. Saadud tulemused pakuvad uusi teadmisi ligniini väärindamise kohta ning toetavad selle kasutamist kõrgema lisandväärtusega, majanduslikult atraktiivsete ja keskkonnasõbralike biopõhiste materjalide arendamisel.

Appendix 1

Publication I

Piia Jõul, T. Tran Ho, Urve Kallavus, Alar Konist, Kristiina Leiman, Olivia-Stella Salm, Maria Kulp, Mihkel Koel, and Tiit Lukk. Characterization of Organosolv Lignins and Their Application in the Preparation of Aerogels. Materials 2022, 15, 2861 https://doi.org/10.3390/ma15082861

materials

MDPI

Article

Characterization of Organosolv Lignins and Their Application in the Preparation of Aerogels

Piia Jõul [1,†], Tran T. Ho [1,†], Urve Kallavus [2], Alar Konist [3], Kristiina Leiman [1], Olivia-Stella Salm [1], Maria Kulp [1], Mihkel Koel [1] and Tiit Lukk [1,*]

[1] Department of Chemistry and Biotechnology, Tallinn University of Technology, Akadeemia tee 15, 12618 Tallinn, Estonia; piia.joul@gmail.com (P.J.); thihol@taltech.ee (T.T.H.); kristiina.leiman@taltech.ee (K.L.); olivia-stella.salm@taltech.ee (O.-S.S.); maria.kulp@taltech.ee (M.K.); mihkel.koel@taltech.ee (M.K.)

[2] Department of Mechanical and Industrial Engineering, Tallinn University of Technology, Ehitajate tee 5, 19086 Tallinn, Estonia; urve.kallavus@taltech.ee

[3] Department of Energy Technology, Tallinn University of Technology, Ehitajate tee 5, 19086 Tallinn, Estonia; alar.konist@taltech.ee

* Correspondence: tiit.lukk@taltech.ee

† These authors contributed equally to this work.

Abstract: The production of novel materials and value-added chemicals from lignin has received considerable attention in recent years. Due to its abundant occurrence in nature, there is a growing interest in utilizing lignin as a feedstock for functional materials production, for example aerogels. Much like in the synthesis of phenol-based resins, the vacant ortho positions of the aromatic rings in lignin can crosslink with formaldehyde and form polymeric gels. After drying the hydrogels with supercritical CO_2, highly porous aerogels are obtained. Current study focuses on the preparation and thorough parametrization of organosolv lignins from different types of lignocellulosic biomass (aspen, pine, and barley straw) as well as their utilization for the preparation of lignin-5-methylresorcinol-formaldehyde aerogels. The thorough structural characterization of the obtained aerogels was carried out by gas adsorption, IR spectroscopy, and scanning electron microscopy. The obtained lignin-based monolithic mesoporous aerogels had specific surface areas and total pore volumes in the upward ranges of 450 m^2/g and 1.4 cm^3/g, respectively.

Keywords: aerogel; lignin; hydrogels; functional polymer; biomass; supercritical drying

Citation: Jõul, P.; Ho, T.T.; Kallavus, U.; Konist, A.; Leiman, K.; Salm, O.-S.; Kulp, M.; Koel, M.; Lukk, T. Characterization of Organosolv Lignins and Their Application in the Preparation of Aerogels. *Materials* **2022**, *15*, 2861. https://doi.org/10.3390/ma15082861

Academic Editor: Debora Puglia

Received: 23 March 2022
Accepted: 11 April 2022
Published: 13 April 2022

1. Introduction

Lignocellulosic biomass is the most abundant renewable resource on Earth. This complex resource is composed of three major biopolymers-lignin, cellulose, and hemicellulose. Proportionally, lignin makes up 10–25% of its dry mass by weight, while the other counterparts–cellulose and hemicellulose, amount to approximately 40–50% and 20–30%, respectively. The topic has been thoroughly researched and many good review articles are available on this subject [1]. However, current biorefinery processes are focused primarily on the utilization of the carbohydrate fractions (cellulose and hemicellulose), while lignin remains underutilized [2]. Only a small percentage, less than 2%, of the approximately 70 million tons of lignin that are produced during pulping by the paper industry is utilized, primarily as concrete additives, stabilizing agents, or dispersants and surfactants. The remainder is simply discarded as waste or burnt as low-grade fuel. Similarly, only a fraction of the lignin portion that is considered a co-product of cellulosic ethanol production is used, and primarily for thermal energy production.

Lignin is an insoluble, highly branched, and randomly structured amorphous polymer. The typical lignin content in softwoods is 24–33%, 19–28% in hardwoods, and 15–25% in cereal straws, bamboo, and bagasse. Chemically speaking, lignin is a highly complex polyphenol, consisting of various methoxylated phenylpropane structures, which can be

considered as the most abundant natural source of aromatics [3]. Although the exact polymeric structure of lignin is not well defined, the key substructures and linkages are known, and on this basis possible structures can be proposed. There are three primary phenylpropanoid monomer units in lignin: syringyl-(S), guaiacyl-(G), and *p*-hydroxyphenyl-(H) units that are derived from the respective monolignols–sinapyl, coniferyl, and *p*-coumaryl alcohols (Figure 1). The ratio between these units, the molecular weight of lignin, and the proportion of lignin to cellulose and hemicellulose differ from species to species significantly [4].

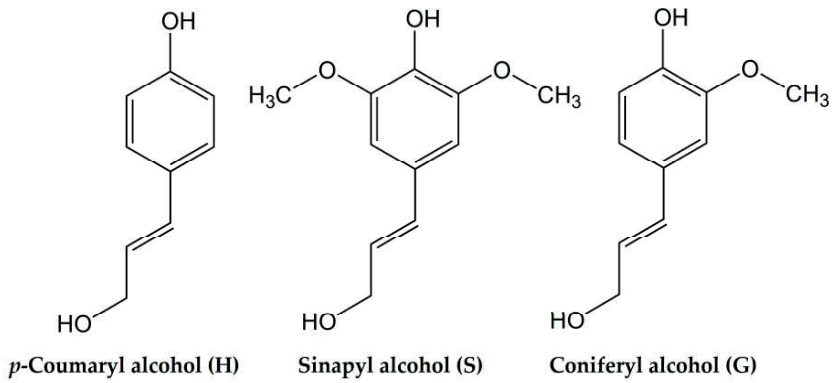

Figure 1. Structures of lignin monolignol units.

The effective extraction and separation of high purity lignin from lignocellulosic biomass is crucial for its efficient valorization. The rupture of bonds to separate lignin from carbohydrates and its partial depolymerization to make it extractable is required for its solubilization in proper solvents for further upgrading and processing. While the efficacy of lignin depolymerization is dependent on many different parameters (solvent, temperature, catalysts, etc.), the fragmentation of lignin is achieved primarily through the cleavage of β-O-4 and 4-O-5 aryl ether linkages.

Currently, the majority of lignin is produced by the pulp and paper-making industry–most commonly by Kraft, sulphite, or soda pulping, but also via hydrolysis/fractionation by hot water, dilute acid, or alkali, organic solvents or via enzymatic hydrolysis in a biorefinery process [2,5]. From these, soda, organosolv and hydrolysis lignins are sulfur-free materials [6].

Some technologies which are currently utilized primarily in research laboratories or in pilot plant reactors must be mentioned: (i) hydrolysis lignin that is obtained from the saccharification process of hemicellulose and cellulose during cellulosic ethanol production, and (ii) lignins from lignocellulose processing with molten salts (ionic liquids and deep eutectic solvents). Studies on using molten salts to develop more environmentally friendly processes for the fractionation of lignocellulosic biomass are gaining more and more attention [7].

In general, isolated lignins vary in structure due to the source of feedstock (i.e., type of biomass), extraction methods, and processing severity. Additionally, controlled degradation of lignin that leads to uniform starting material is necessary to arrive at a desired product in downstream valorization processes [8–10].

Biopolymer-based materials are suitable for the fabrication of biopolymer-based gels [11]. Phenolic resins are well-known polymeric materials where by manipulating the phenolic (or substituted phenols) to aldehyde monomer ratio and the amount of solvent, pH, catalyst type, reaction temperature, and reaction time, give rise to a variety of resin structures with a wide range of possible properties. In 1989, Pekala performed the aqueous polycondensation of resorcinol (1,3-dihydroxybenzene) with formaldehyde (FA) as a synthetic route to organic aerogels-low-density, open-porous, solid framework of a

gel that was isolated intact from the gel's liquid component and have pores in the range of <1 to 100 nm in diameter. In this system, resorcinol acted as the multifunctional monomer and FA formed methylene and/or methylene ether bridges between the benzene rings [12]. Some advantage in the preparation process was achieved with the replacement of resorcinol with 5-methylresorcinol (5-MR) [13,14]. The phenolic and polymeric nature of lignins make them potent replacements for phenol/resorcinol in a multitude of industrial applications as biopolymers with considerable economic and environmental benefits.

The presence of a free hydroxyl group and the vacant ortho- or para-sites on the aromatic ring are a prerequisite to polycondensation reaction, which is necessary for gel formation. In lignin, the H- and G-units possess the ortho reactive site that is similar to resorcinol, which can crosslink with FA. Properties such as these can be useful for the effective utilization of lignin as a phenol replacement in lignin-phenol-formaldehyde resins [15].

Conversely, phenolic groups in lignin are often substituted in the para position by an aliphatic chain. Here, the H-type unit possess more than one activatable site, offering the potential to create highly crosslinked structures. In G-type units, one ortho position is already occupied by a methoxy group, whereas in S-type units both ortho-positions are occupied. This higher degree of substitution results in a significantly lower reactivity of lignin as compared to phenol [16]. It is clear that the H and G-units are able to react with FA in the synthesis of lignin-based resins while the S- (no activatable site is present) unit is not [17]. In this sense, softwood lignins (containing mainly G-units) are a better choice for lignin-based resin synthesis than hardwood lignins (containing S-units and some H-units). Alkali and organosolv lignins with a higher number of G-units, a free ortho position, and moderate molecular weight seem to be better candidates for the synthesis of 100% lignin-based resins [16]. Therefore, in the synthesis of lignin-based aerogels, due to the nature of the reaction between lignin and FA, the sub-structures within lignin play a more important role than either molecular weight or polydispersity of lignin [18]. Despite that, lignins are less reactive towards addition/substitution reactions due to the lack of reactive sites [19]. The replacement of phenol with lignin would provide a cost-effective and green alternative as phenolic resins are used in many industrial applications (e.g., automotive, computing, aerospace, and construction), but also in the manufacturing of engineered wood products [16]. The control over lignin functionality appears to be one of the most important challenges for the development of lignin-based materials, and a multitude of analytical chemistry and spectroscopic tools (e.g., IR and NMR) are needed to parametrize the particular lignin sample structure.

Similar to the synthesis of phenol-based resins, the vacant ortho positions of the aromatic rings in lignin can react with FA to yield polymeric gels. Multiple examples of utilizing different types of lignin have been described in the literature for preparing gels, that, depending on the drying process, will yield aerogels [20], xerogels [16], or cryogels [17]. The evaporation of liquids from gels at normal atmospheric conditions results in xerogels with a higher density. To obtain lighter materials, sublimation of a frozen solvent via lyophilization results in cryogels. The most effective technique for preserving the porous structure utilizes the extraction of liquid at supercritical conditions where, typically, prior to the process, the solvent is exchanged with CO_2 [21]. However, supercritical CO_2 extraction is technically demanding, and despite the widespread use of this method, simpler and more economical methods for material drying are actively researched.

While phenolic resins and resorcinol aerogels are mainly considered as a useful source of porous carbon material, these materials do have some additional distinct advantages—a high carbon yield and high microporosity of the carbonized fibers without activation [22–24]. The latter is true also for lignin-derived materials [18,25].

The structure of lignin is highly dependent on its isolation method. The present study concentrated on the organosolv process for lignin extraction, utilizing two different solvent systems. There are not very many studies on using organosolv lignins for the preparation of gels and respective aerogels. Furthermore, the availability of structural information

on this type of lignin remains scarce. The current study focused on the preparation and thorough parametrization of organosolv lignins from different types of lignocellulosic biomass as well as their utilization for the preparation of aerogels in different ratios to phenolic compounds. A thorough structural characterization of the obtained aerogels and their properties was carried out.

2. Materials and Methods

2.1. Chemicals

Ethanol, dioxane, hydrochloric acid, acetic acid, sodium hydroxide, tetrahydrofuran, sulfuric acid, and chloroform-d were purchased from Sigma-Aldrich (Taufkirchen, Germany). All the chemicals were of analytical grade and were used as received. Deionized water from a Milli-Q water purification system (Millipore S. A., Molsheim, France) was used throughout the study. 5-MR with a reported purity of >99% was provided by AS VKG (Kohtla-Järve, Estonia).

2.2. Raw Materials and Methodology

Aspen wood chips were provided by Estonian Cell AS, longitudinally sawn pine timber sawdust was provided by Prof. Jaan Kers (Tallinn University of Technology, Tallinn, Estonia), and barley straw was provided by Prof. Timo Kikas (Estonian University of Life Sciences, Tartu, Estonia). All feedstocks were dried in a convection oven at 50 °C up to 8% moisture, followed by grinding to a fine powder, and stored in plastic bags at room temperature.

Organic solvent extraction under reflux conditions was used for the isolation of lignin from biomass and for that, ethanol and dioxane were used. The obtained lignin was further characterized for purity and structural properties by different analytical methods and used for the preparation of lignin-based aerogels, followed by their characterization.

2.3. Organosolv Extraction of Lignin

Ground and dried biomass (50 g) was refluxed with 1.5 L of solvent in a 2.0 L round bottom flask with a mechanical stirrer and a reflux condenser for 6 h. The solvent mixture contained 0.28M HCl and 5% v/v water in ethanol or 0.28M HCl and 2% v/v water in dioxane. The mixture was filtered through Whatman filter paper, and the solids were washed three times with 50 mL of ethanol or dioxane, depending on the extraction solvent. The combined filtrate and washes were concentrated to about 100 mL by rotor evaporation. Lignin recovery from the pretreatment liquor was performed by precipitation with ultrapure water. For this purpose, the pretreatment liquor was dissolved in 100 mL of acetone and introduced into 2 L of vigorously stirred cold ultrapure water to reduce the solubility of lignin. The mixture was stirred for 60 min, and then the precipitated lignin was separated by centrifugation at 4200 rpm. The recovered lignin was washed with 1 L of ultrapure water three times, centrifuged, dried in a convection oven at 30 °C for 24 h, weighed, and stored for further analysis and use. The lignin extraction yields were calculated according to the following equation:

$$\%\ Lignin\ yield = \frac{W_{Extracted\ lignin}}{W_{Lignin\ in\ biomass}} \times 100, \quad (1)$$

2.4. Characterization of Lignin

2.4.1. Moisture and Ash Content

For moisture analysis, 0.2 g of organosolv lignin was introduced into the moisture analyzer (Ohaus, Parsippany, NJ, USA) and heated at 105 °C until a constant weight. The ash content was determined by keeping of 0.2 g of the dry lignin in muffle furnace at 550 °C for 4 h and recording the weight of ash [26].

2.4.2. Determination of Lignin and Carbohydrate Content

The analysis of Klason lignin and carbohydrate content involved a two-stage acid hydrolysis of the lignin samples to solubilize and hydrolyze the carbohydrates that were present in the extracted lignin. For that, 200 mg of dry lignin was dissolved in 3 mL of 72% sulfuric acid. The mixture was incubated in a water bath at 30 °C for 1 h. Next, 72 mL of ultrapure water was added to the mixture, and the mixture was autoclaved at 121 °C for 60 min. The solution that was obtained was filtered while hot. The precipitate that retained in the filter was acid insoluble lignin (AIL), which was washed with water, followed by drying in a hot air oven, and weighing. Some amount of lignin was dissolved in the acidic solution (filtrate). That portion of lignin was quantified spectrophotometrically by recording the absorbance of the filtrate at 205 nm. The filtrate was analyzed by a UV–visible spectrophotometer (Cary 50 Bio, Varian, Palo Alto, CA, USA) and the acid soluble lignin (*ASL*) was quantified with the following formula of the Biorefinery test method L2:2016:

$$ASL = \frac{A * D * V}{a * b * M}, \quad (2)$$

Different notations are: A = absorption at 205 nm, D = dilution factor, V = volume of filtrate, L; a = extinction coefficient of lignin, g/L (110 g/L as per TAPPI UM 250), b = cuvette path length, cm; M = weight of dry sample (in g).

The carbohydrate content of the filtrate that was obtained from lignin hydrolysis was analyzed by an optimized capillary electrophoresis (CE) method. The direct UV-detection of carbohydrates at the 270 nm is possible due to in-capillary reaction of the carbohydrates in the alkali medium, which leads to the formation of UV-absorbing carbohydrate enediolate anion [27,28]. The alkaline electrolyte solution was made up of 136 mM sodium hydroxide and 46 mM disodium hydrogen phosphate dihydrate. The filtrate samples were neutralized with calcium carbonate and injected to CE instrument (7100 CE system, Agilent Technologies, Santa Clara, CA, USA) with a pressure of 35 mbar for 10 s. The applied separation voltage was 19.4 kV. The CE separation was carried out in uncoated fused-silica capillaries of 50 µm id and length 70/80 cm (effective length/total length). Both the capillary and samples were held at 17 °C. New capillaries (Molex, Polymicro Technologies, Phoenix, AZ, USA) were conditioned by rinsing with 1 M sodium hydroxide (30 min), ultrapure water (5 min), and the electrolyte solution (5 min). Between analyses, the capillaries were flushed with 5% v/v acetic acid for 3 min, with 1 M sodium hydroxide for 3 min, with ultrapure water for 3 min, and finally with electrolyte solution for 5 min.

A total of eight sugars raffinose, fucose, cellobiose, galactose, glucose, mannose, arabinose, xylose, and 5-hydroxymethylfurfural were quantified in the linear range of 0.1–4.0% dw with determination coefficients around 0.99.

2.4.3. FTIR Spectroscopy

The infrared (IR) absorption spectra of lignins were obtained using a FTIR spectrometer IRTracer-100 (Shimadzu, Kyoto, Japan). A spectrum of the blank KBr tablet and the scan of the KBr tablet with test substance (100:1) were recorded in the range 400–4000 cm^{-1} with a resolution of 4 cm^{-1}. The IR absorption spectrum of the lignin was obtained by subtraction of the test substance scan with the scan of the blank. A total of 32 spectra were averaged per sample and analyzed using the Lab Solutions software (Shimadzu, Kyoto, Japan).

2.4.4. NMR Characterization

For the sample preparation, about 35.0 mg of lignin was dissolved in 600 µL of DMSO-d_6. The full assignment of 2D-Heteronuclear Single Quantum Coherence (HSQC) was based on the spectra that were obtained from a 500 MHz Agilent DD2 spectrometer that was equipped with an inverse detection probe. HSQC experiment was recorded at 25 °C by applying the standard multiplicity edited HSQC pulse sequence with adiabatic pulses in ^{13}C channel. The 2D data were acquired in 256 increments (64 scans/increment) in f1 dimension with 20,000 Hz spectral width. The acquisition of the f2-dimension was zero

filled to 2000 points, while the f1 dimension was linear predicted to 512 points, followed by zero filling to 1000 points. Prior to Fourier transformation, a gaussian window function was applied in both dimensions. The resulting free induction decays were processed using MestReNova software. The HSQC cross signals were assigned by comparing with the literature [29–34].

2.4.5. ^{31}P-NMR Quantitative Analysis

Free hydroxyl group concentrations of the six organosolv lignin samples were estimated by using ^{31}P NMR, based on the derivatized OH groups with an appropriate phosphitylation reagent. Sample preparation for ^{31}P NMR analysis was carried out according to the procedure from Balakshin et al. [15]. Particularly, organosolv lignin (about 25.0 mg) was weighed into an Eppendorf tube, followed by adding 500.0 μL of pyridine/$CDCl_3$ with ratio 1.6:1 (solution I). Then, 100.0 μL of internal standard (IS) (20.0 mg/mL) that was prepared in solution I, was added. Subsequently, approximately 5.0 mg/mL of chromnium (III) acetylacetonate as a relaxation agent was pipetted into the same tube. Finally, the mixture was derivatized with 70.0 μL of 2-chloro-4,4,5,5-tetramethyl-1,3,2-dioxaphospholane (TMDP). The tube was closed tightly and manually shaken to obtain a homogeneous mixture. About 600 μL of the phosphitylated lignin was transferred into an NMR tube and analyzed. After phosphitylation (Figure 2), the signals of the hydroxyl groups from aliphatic, syringyl, guaiacyl, *p*-hydroxyphenyl, and carboxylic acid were identified from the NMR spectra. Their quantification was based on the peak integral of the targeted OH group relative to an IS endo-N-hydroxy-5-norbornene-2,3-dicarboximide. The data were obtained on a Bruker 400 MHz spectrometer that was equipped with 5 mm BBO BB-1H/D probe. The ^{31}P spectra were acquired at 25 °C with an inverse gated decoupling pulse sequence (zgig) with 768 number of scans, 10s for relaxation delay. The data were then processed by using Topspin 4.0.8.

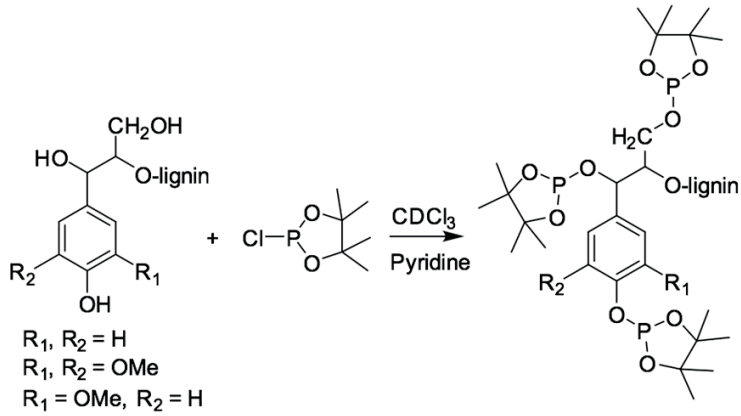

Figure 2. Phosphitylation of hydroxyl groups in lignin with TMDP reagent.

All the ^{31}P spectrum were calibrated by the signal from IS at 151.8 ppm; and the integration as well as assignment were based on the study by Balakshin et al. [15].

2.4.6. Lignin Molecular Weight Distribution

As a routine, the weight-averaged molecular weight (M_W) and weight distributions (M_WD) are determined by size exclusion chromatography (SEC), where the M_W data are related to calibration standards of known M_W. The lignin samples were dissolved in tetrahydrofuran (THF, 1 mg/mL) and analyzed on a Prominence LC-20A Modular HPLC System (Shimadzu, Japan) that was equipped with a photodiode array detector. All lignins that were prepared in this study were soluble in THF at 1 mg/mL. The columns that were used

were a series of two 300 mm × 7.5 mm i.d., 3 µm, MesoPore, with a 50 mm × 7.5 mm i.d. guard column of the same material (Agilent Technologies). The samples were eluted at 40 °C with 1 mL/min THF stabilized with 250 ppm butylated hydroxytoluene (BHT) and detected at 254 nm. The system was calibrated using polystyrene GPC/SEC calibration standards (EasiVial PS-L, Agilent Technologies) in the range of molecular weight at peak top (Mp) 46 380−162 Da. Mp, number-averaged molecular weight (Mn), M_W, and polydispersity (M_W/Mn) were determined by the Lab Solutions software (Shimadzu).

2.5. Preparation and Characterization of Lignin-Based Aerogels

The organosolv lignins that were obtained (Table 1) were used to prepare the lignin-5-methylresorcinol-formaldehyde (L-5-MR-FA) aerogels. Aerogels with partly replaced 5-MR with lignin were prepared according to previously published protocols [14,35], which were combined and improved as needed.

Table 1. Physicochemical characterization of organosolv lignin that was extracted from different sources of biomass with two different solvents (ethanol organosolv lignin- EOL and dioxane organosolv lignin—DOL).

Lignin ID	Biomass Source	Solvent Used	Lignin Yield %	Klason Lignin * %	Total Sugars %	M_W	Mn	PI
EOL-Aspen	Aspen wood	Ethanol	15 ± 2	95 ± 5	nd	2601	3743	1.4
DOL-Aspen	Aspen wood	Dioxane	44 ± 6	104 ± 5	nd	1925	2670	1.4
EOL-Barley straw	Barley straw	Ethanol	24 ± 3	96 ± 5	nd	2187	3211	1.5
DOL-Barley straw	Barley straw	Dioxane	49 ± 7	102 ± 5	nd	1809	2469	1.4
EOL-Pine	Pine wood	Ethanol	21 ± 3	89 ± 4	0.27 ± 0.05	2343	3391	1.4
DOL-Pine	Pine wood	Dioxane	61 ± 9	101 ± 5	0.57 ± 0.09	1959	3450	1.8

nd–not detected (content of each of eight sugars is below LOD 0.1% dw). ± expanded uncertainty (95% confidence interval). * Klason lignin includes both acid soluble and acid insoluble.

Firstly, the lignins were homogenized in ultrapure water and stirred at 85 °C for 90 min with 0.09 % (wt. % based on lignin) of NaOH, pH of mixture was close to 10. After that, a water solution of 5-MR and FA, prepared according to the mass ratios: (5-MR+L)/FA = 1.25; 5-MR/L = 1/3 (75% 5-MR is replaced by lignin); water content equal to 80%, was added to the cooled mixture of lignin and homogenized by mixing on a vortex. The mixture was kept at 85 °C to allow gelation, where the time of the gelation was determined visually. The gels were kept at room temperature for curing in 1% of acetic acid for 12 h, and then placed in acetone, which was changed every 24 h for four days. After the solvent exchange step, the gels were dried using supercritical CO_2, dynamic drying (100 bar 1.5 h 25 °C, 120 bar 2.5 h 45 °C).

The surface morphology of the L-5-MR-FA aerogels were examined with a high resolution scanning electron microscope (SEM) Zeiss EVO MA 15 SEM at an accelerating voltage of 10 kV. For imaging, pieces of aerogel samples were fractured into smaller parts to open the internal structure and view the particles close morphology. The fractured pieces were attached with double adhesive tape to the stub and coated with the Ag/Pd conductive layer in the Fine Coat Ion Sputter JFC-1100.

The pore structures of the aerogel samples were investigated by using the N_2 adsorption-desorption method at 77 K with Quantachrome Autosorb iQ apparatus in the relative pressure range of 0.005 to 0.995. Prior to analysis, aerogel powder was degassed at 105 °C for 24 h to remove surface impurities and moisture. The N_2 adsorption-desorption method at 77 K was used in the relative pressure P/P_0 range of 0.025 to 0.995. The specific surface area (S_{BET}) was calculated by applying the BET (Brunauer-Emmett-Teller) method and the total pore volume was determined by the volume of N_2 that was adsorbed at relative pressure P/P_0 = 0.99. Pore size distribution was determined using density functional theory (DFT).

Ground samples of aerogels were spotted on a diamond crystal and analyzed on an IRTracer-100 FTIR spectrophotometer (Shimadzu, Kyoto, Japan) in attenuated total

reflection (ATR) mode. The spectra were recorded over 400–4000 cm^{-1} range by averaging 20 scans at a maximum resolution of 2 cm^{-1} and analyzed using Lab Solutions software (Thermo Scientific, Waltham, MA, USA).

3. Results and Discussion

3.1. Lignin Structural Characterization

3.1.1. Purity and SEC Analysis

A total of three types of lignocellulosic biomass were organosolv-pretreated with two different solvents (ethanol and 1,4-dioxane) under reflux conditions as mentioned in the experimental section. Aspen, pinewood, and barley straw biomass had an initial lignin content ca. 27, 33, and 21% per dry weight, respectively. As can be seen in Table 1, the overall lignin recovery yield is around 20% for ethanol extraction. This low yield could be partially attributed to the formation of colloidal suspensions of lignin in the water washes that would not clear even after prolonged centrifugation. Also, for the ethanol solvent system, the lower yield is probably due to the lower extraction temperature (82–85 °C) compared to the dioxane systems (~95 °C) that led to less lignin fragmentation and less lignin solvolysis and therefore less overall lignin yield. The higher temperature and better solubilization ability of dioxane resulted in a maximum lignin yield of 61% for untreated pine wood.

The purity of the obtained lignins was evaluated by the ash, sugar, and Klason lignin contents. The lignin was treated with sulfuric acid to obtain Klason lignin content and release sugars that were present in the lignin. The acid solution was then filtered and neutralized, and the filtrate was analyzed by capillary electrophoresis (CE). Klason lignin contents varied between 95–100% (Table 1). The lowest value was observed for the lignin of pine due to the increased proportion of residual carbohydrates (0.3–0.6%), mainly mannose. Differences in the composition of carbohydrate impurities suggest that lignin-carbohydrate complexes in softwoods [36] are structurally distinct when compared to hardwoods and grassy biomass. The results show that no sugar was released from aspen and barley straw lignin after acid treatment. The ash contents for all lignins were insignificant (below 0,1% dw).

SEC was used to determine the $M_W D$ and polydispersity index (PI) of the obtained lignin. The Mn, weight average molecular weight (M_w), and polydispersity (M_w/Mn) of ethanol organosolv (EOL) and dioxane organosolv (DOL) lignins were calculated from SEC chromatograms. The results are shown in Table 1. For lignins that were isolated with ethanol, slightly higher values of M_W and Mn were observed when compared with lignin samples that were isolated with dioxane. Notably, EOL and DOL lignins that were obtained from different biomasses had similarly narrow polydispersity of 1.4–1.5, indicating homogeneity of the polymeric material.

A peak at longer retention time (around 1060 s) was present in the EOL-barley straw lignin and was remarkably abundant in the EOL-pine lignin (data not shown). This peak had a calculated molecular weight $\approx$ 0.2 kDa, was absent in all DOL-lignins. It was shown by Faleva et al. that a high ethanol concentration could favor the formation of ethylesterified compounds that were derived from either lignin or hemicellulose [29]. Due to their low water solubility, these derivatives could coprecipitate together with the larger lignin compounds.

3.1.2. FTIR Analysis

The IR absorption spectra of the six lignins that were studied were recorded in the 400–4000 cm^{-1} region (Figure 3). Absorption bands corresponding to bond vibrations in the FT-IR spectra were assigned based on previously reported data [37,38]. The IR spectral profiles are similar in all the isolates, which indicates that the "core" of the structure of organosolv lignins is similar for different kinds of biomass. The band at 3428 cm^{-1}, which is attributed to O-H stretching absorption due to the phenolic and aliphatic hydroxyl groups, had a similar absorption intensity in all lignins. However, the relative intensities

of the absorption bands at 2938 and 2849 cm^{-1}, assigned to C-H stretching vibrations in the methyl and methylene groups were quite different. These bands, which are mainly attributed to methoxy groups, were substantially higher for the EOL lignins and presented relatively lower absorbance bands for DOL lignins. The carbonyl stretching vibration at 1710 cm^{-1}, which is caused by stretching of unconjugated ketones, conjugated aldehydes, and carboxylic acids aromatic ring appeared in all spectra with different intensity. The bands at 1595 and 1516 cm^{-1} are caused by aromatic skeletal C=C vibrations, while the band at 1464 cm^{-1} corresponds to asymmetrical C-H deformations in methyl (-CH_3) and methylene (-CH_2-) groups. The band at 1424 cm^{-1}, which also corresponds to aromatic skeletal vibrations (C=C) (guaiacyl-syringyl) combined with C-H in-plane deformation, has lowest intensity in barley straw lignin spectra, and the band at 1330 cm^{-1} corresponding to C-O stretching (S) was clearly observed only on the aspen (hard wood) lignin spectra. The bands between 1300 and 1000 cm^{-1} are attributed to stretching of the C-O ether or ester linkage. Aliphatic ethers give a strong asymmetric stretch at 1122 cm^{-1} in aspen OL, while for the barley straw lignin, its intensity is negligible.

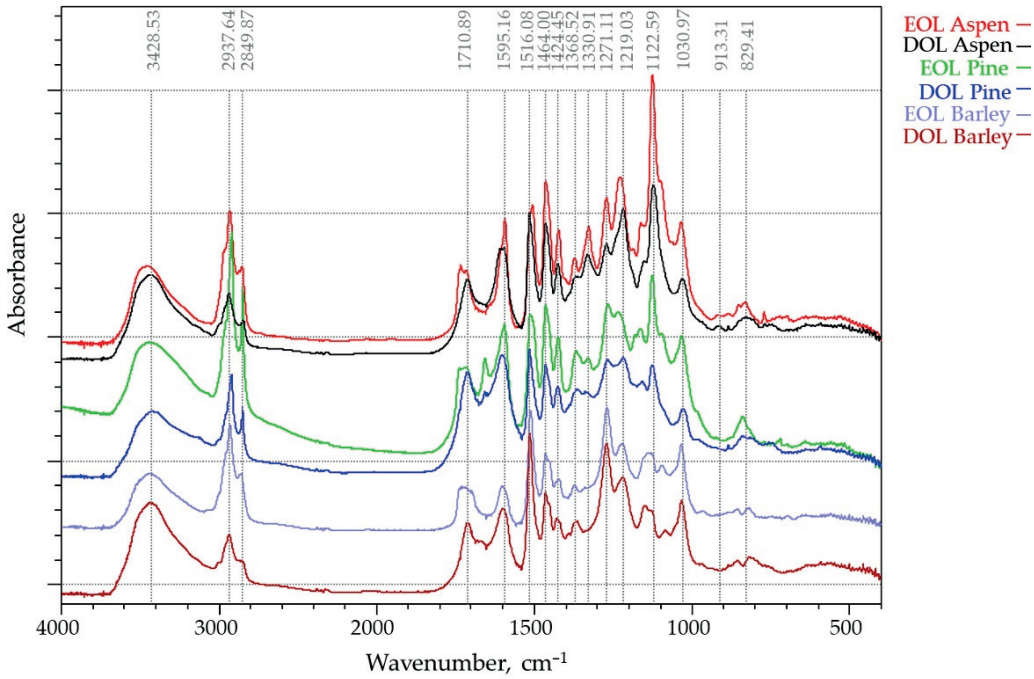

Figure 3. FT-IR spectra of EOL and DOL lignins that were isolated from three different biomass feedstocks (aspen, pine, and barley straw).

FTIR spectroscopy showed that the lignins under investigation had some structural differences that were caused by the used extraction solvent as well as biomass source, which will be covered in further detail in this study.

3.1.3. ^{31}P-NMR Quantitative Analysis

In the present study, the results only assigned for syringyl OH instead of combining its peak area with condensed phenolic units in lignin. Therefore, the additional aromatic OH region was taken into account from 144.0 to 137.0 (ppm) containing not only OH from H-/G-/S-units but also from the condensed units in lignin. The contribution of signals from specific hydroxyl groups were integrated and calculated quantitatively on the basis of the IS (Table 2). In general, the distribution of hydroxyl content from aliphatic chains and

p-hydroxyphenyl groups were higher when using ethanol to extract lignin from all types of biomass. In contrast, 1,4-dioxane gave better extraction yield as evidenced by a significant amount of phenolic compounds, including OH groups from the three main components in lignin H-, G- (uncondensed/condensed unit), and S-units.

Table 2. Six organosolv lignin samples and their hydroxyl contents (mmol OH/g of dried lignin) that were determined by ^{31}P NMR according to their integration for specific type of OH group.

Chemical Shift (ppm)	Types of OH	EOL-Aspen	EOL-Barley Straw	DOL-Aspen	DOL-Barley Straw	EOL-Pine	DOL-Pine
149.0–145.5	Aliphatic OH	2.38	2.08	1.50	0.94	1.90	1.61
143.5–142.0	Syringyl OH	0.35	0.11	1.32	0.53	0	0
140.2–139.0	Guaiacyl OH	0.47	0.48	0.55	0.62	0.73	1.35
138.0–137.5	*p*-Hydroxyphenyl	0.23	0.23	0.12	0.16	0.08	0.07
134.7–134.5	Carboxylic acid	0.05	0.02	0.20	0.25	0.04	0.15
144.0–137.0	Aromatic OH	1.14	0.92	2.49	1.76	0.97	2.59

The amounts of syringyl OH were found significantly higher in organosolv lignin from hardwood (i.e., aspen) than from softwood (i.e., pine). The highest amount was attributed to DOL-Aspen with 1.32 (mmol OH g^{-1} of dried lignin). Approximately one tenth of the amount of phenolic hydroxyls were attributed to the *p*-hydroxyphenyl functional group that was present in DOL-Aspen (0.12 mmol OH g^{-1} of dried lignin) compared to the OH groups from S-units. By contrast, phenolic OH groups from G moieties in organosolv lignin from pine were predominant, especially in DOL-Pine with 1.35 (mmol OH g^{-1} of lignin) while phenolic OH groups from the S-units were not detected. Barley straw was classified as a member of the grassy biomass family, therefore, its ^{31}P NMR showed all three phenolic OH groups in which the content from G-OH was slightly higher than the other two. The results showed a strong agreement with a previous study on lignin composition that described the monolignol distributions in different biomasses– S/G ratio is greater in hardwoods than softwood, while the lignins from grassy biomass contain all three components (H, G, S) [39].

It is clear that H- and G-units are able to react with FA to synthesize the lignin-based resins while the S (no active site is present) unit is not. This was seen in Table 2 where softwood and grass showed higher potential for forming good aerogels because of a higher content of G- and H-units.

3.1.4. 2D HSQC Characterization

In addition to the results that were obtained from phosphorous NMR, six organosolv lignin samples were further structurally characterized by 2D Heteronuclear Single Quantum Coherence (HSQC) NMR spectroscopy. HSQC is a powerful technique that shows the correlation of hydrogen atoms that are bonded directly to a carbon atoms, giving detailed information about inter-unit linkages in lignin [40,41]. In this study, HSQC was only employed for qualitative analysis to acquire more information about lignin substructures.

It was reported that the region of aliphatic side chain (δ_C/δ_H 50–10/3.0–1.1 ppm) was not informative compared to others in terms of lignin linkages [31]. Therefore, only two regions from the HSQC spectrum were considered: (i) oxygenated aliphatic side chain region (δ_C/δ_H 100–40/6.0–2.5 ppm), and (ii) aromatic/unsaturated region (δ_C/δ_H 150–100/8.0–6.0 ppm).

(i) The oxygenated aliphatic side chain region of organosolv lignins and its correlations are shown in Figure 4 and Table S1, respectively. As expected, the methoxy groups are present in all the lignin spectra. Under acidic hydrolysis condition, the cleavage of α-aryl ether bonds are favored over the cleavage of β-O-4′ bonds, resulting in the formation of intermediate α-carbocation. This active carbon with the presence of a nucleophile source from ethanol would lead to the substitution at C_α [42,43]. As a consequence, a strong signal for α-ethoxylation in the β-O-4′ substructure (A′) can

be observed (δ_C/δ_H 63.60/3.32 ppm) in all the ethanol organosolv lignin samples (EOL) [29].

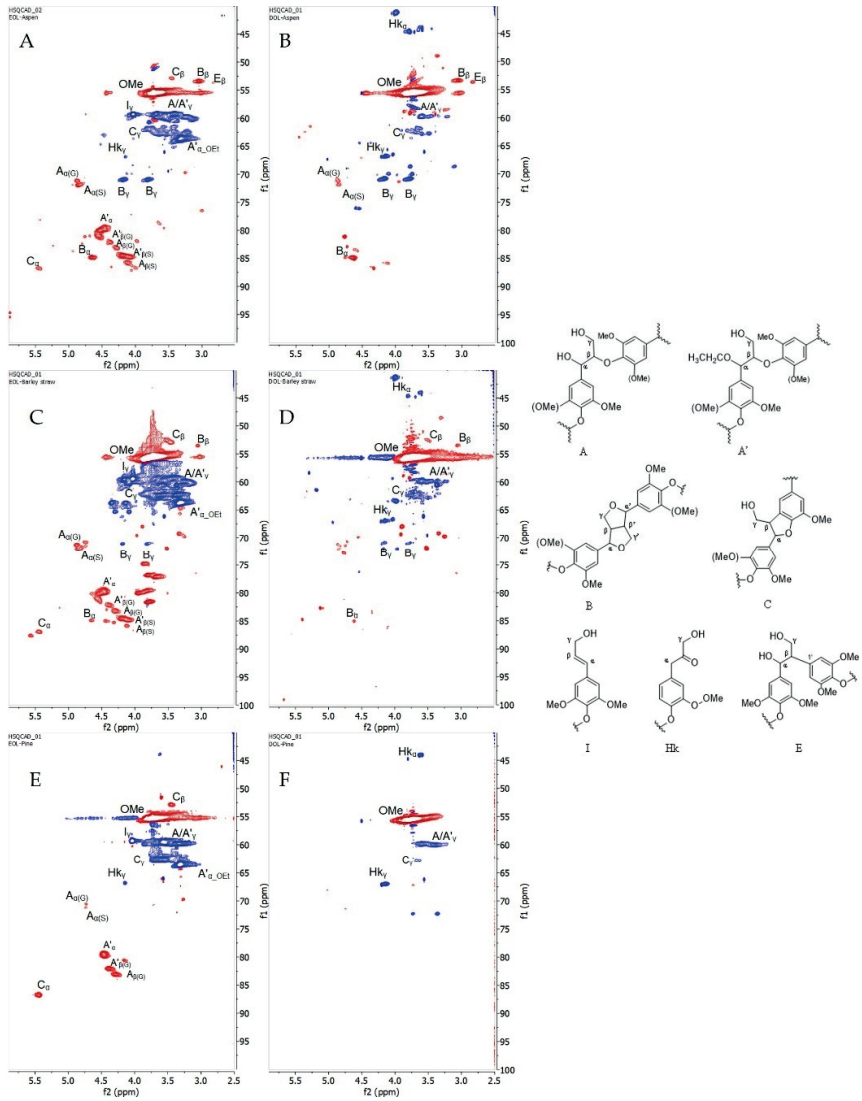

Figure 4. (**Left**) HSQC spectra that were presented in the oxygenated aliphatic side chain region from six organosolv lignins, (**A**) EOL-Aspen, (**B**) DOL-Aspen, (**C**) EOL-Barley straw, (**D**) DOL-Barley straw, (**E**) EOL-Pine, and (**F**) DOL-Pine. Red cross peaks are CH_3 and CH; blue cross peaks are CH_2. (**Right**) (**A**) β-O-4′ alkyl-aryl ethers; (**A′**) β-O-4′ alkyl-aryl ethers with ethoxylated α-OH; (**B**) resinols; (**C**) phenylcoumarans; (**I**) cinnamyl alcohol-end groups; (**Hk**) Hibbert's ketone (end-group); (**E**) β-1′ linkage.

The presence of other dominant substructures, such as β-O-4′ (A), resinol (B), phenylcoumarans (C), and cinnamyl alcohol end-groups (I) were found in all types of EOL, except in lignin from pinewood where resinol fragment was not detectable (Figure 4E). Surprisingly, the cross peak intensity from β-aryl ether bond in A/A′ was significantly reduced in

dioxane organosolv lignin (DOL), indicating vigorous cleavage of this bond to release lignin from the lignocellulosic matrix when using dioxane as the solvent. This phenomenon could be explained by the higher boiling point of dioxane (95 °C vs. 85 °C of ethanol) [9], which leads to a higher temperature during the extraction process, assisting in the breakdown of more aryl ether bonds. Additionally, $C_{\alpha,\gamma}$-$H_{\alpha,\gamma}$ Hibbert's ketone (Hk) structures were seen in all the DOL spectrums, while only C_{γ}-H_{γ} was observed in EOL. The occurrence of Hk in organosolv lignins must be one of the consequences of using an acid catalyst in the solvolysis process [9]. The low intensity of Hk_{α} in EOL can be explained by the fact that its formation likely competes with the ethoxylation reaction in the excess of ethanol. It has been noted that cinnamyl alcohol end-groups (I) can be observed only in EOL, while β-1′ linkage (E) has only been described for hardwood lignins (Figure 4A,B) [6].

(ii) Figure 5 shows the aromatic/unsaturated region in six lignin samples from different biomasses. Cross peaks from S-units and its oxidized-C_{α} (S′) were more pronounced in the aspen and barley straw, while there was no signal in the spectra from pine. In contrast, the G-unit was present in all the lignins, whereas H was only observed in all EOL-s. These results are in good agreement with the data from the analysis of the hydroxyl contents that were obtained from phosphorous NMR where the functional OH groups from the S-unit were not detected in organosolv lignin from pine.

In most of the cases, Hk-signals were frequently assigned for $C_{\alpha,\gamma}$-$H_{\alpha,\gamma}$ in many ways thanks to the past efforts by Miles-Barrett et al. [11] who synthesized an Hk analog from S-/G-units as well as Hibbert's ketone bound to a lignin structure that resulted from the cleavage under acidic organosolv treatment. As a result, it enabled us to extract more information from the HSQC spectrum. In the studied lignins, aromatics of syringyl/guaiacyl that were bound to Hk ($S_{2,6}$-LBHK, G_2-LBHK, G_5-LBHK, G_6-LBHK) were assigned at δ_C/δ_H 106.67/6.53, 113.31/6.84, 112.89/6.90, and at 121.36/6.64, respectively. Furthermore, other fragments from methyl-substituted phenylcoumaron (P) were successfully confirmed by Faleva et al. [8] and were present in DOL-Aspen/barley straw spectra in our studied cases. It can be seen that barley straw lignin (Figure 5C,D) contains ferulate (Fer) and *p*-coumarate (pCA) substructures as a result of acylation of lignin side chains [5]. Along with Fer and pCA, tricin (T) is well distributed in grasses/straw, therefore their signals were strongly observed and assigned according to a previous study [7]. Interestingly, the presence of *p*-benzoate (PB) was only seen in aspen with the assignment of $C_{2,6}$-$H_{2,6}$ at δ_C/δ_H 131.13/7.69 as reported previously [10].

From the point of view of gel-forming reactions, the most valuable elements are aromatic rings with hydroxyl group in ortho-or para-position-pCA, Fer, T, PB.

3.2. Characterization of the Obtained Aerogels

3.2.1. Drying Shrinkage, Bulk Density, and Gelation Analysis

Drying shrinkage, bulk density, and gelation time of AG-5-MR-FA and aerogels, where 75–85% of the 5-MR was replaced by lignin, are presented in Table 3. The drying shrinkages of lignin-based aerogels were higher than 45%, but the bulk densities were still quite low (0.15–0.46 g/cm^3), compared to dense structured AG-5-MR-FA, which had low shrinkage (37%), but a bulk density of 0.20 g/cm^3.

The solubility of lignin in water is important because when not fully dissolved, its reactivity is low and could act as aerogel filler, not as one of the precursors. This was the case for EOL-Pine lignin. The gelation time at 85 °C for lignin-based gels was relatively long, up to seven hours for lignin from aspen. While longer gelation times are characteristic for AG-EOLs, then AG-DOL gelation times are more comparable to the gelation times for common 5-MR-FA gels. SEC analysis of the obtained lignins (Table 1) reveals that using dioxane as the solvent for the extraction of lignin gives products with a higher yield and lower molecular weight. This could be explained by the higher temperature boiling point of dioxane compared to ethanol, which can assist the cleavage of aryl-ether bonds in lignin [7]. Furthermore, the results from 2D-HSQC (Figure 4) show that the peak intensities of the corresponding β-O-4′ linkages in lignin decreased significantly

when using dioxane, compared to ethanol under the same extraction condition. It can, therefore, be concluded, that the delignification of biomass with dioxane gives smaller fragments of lignin, which increases their solubility and increases the aerogel formation ability. Consequently, AG-DOL show shorter gelation time compared to AG-EOL (Table 3).

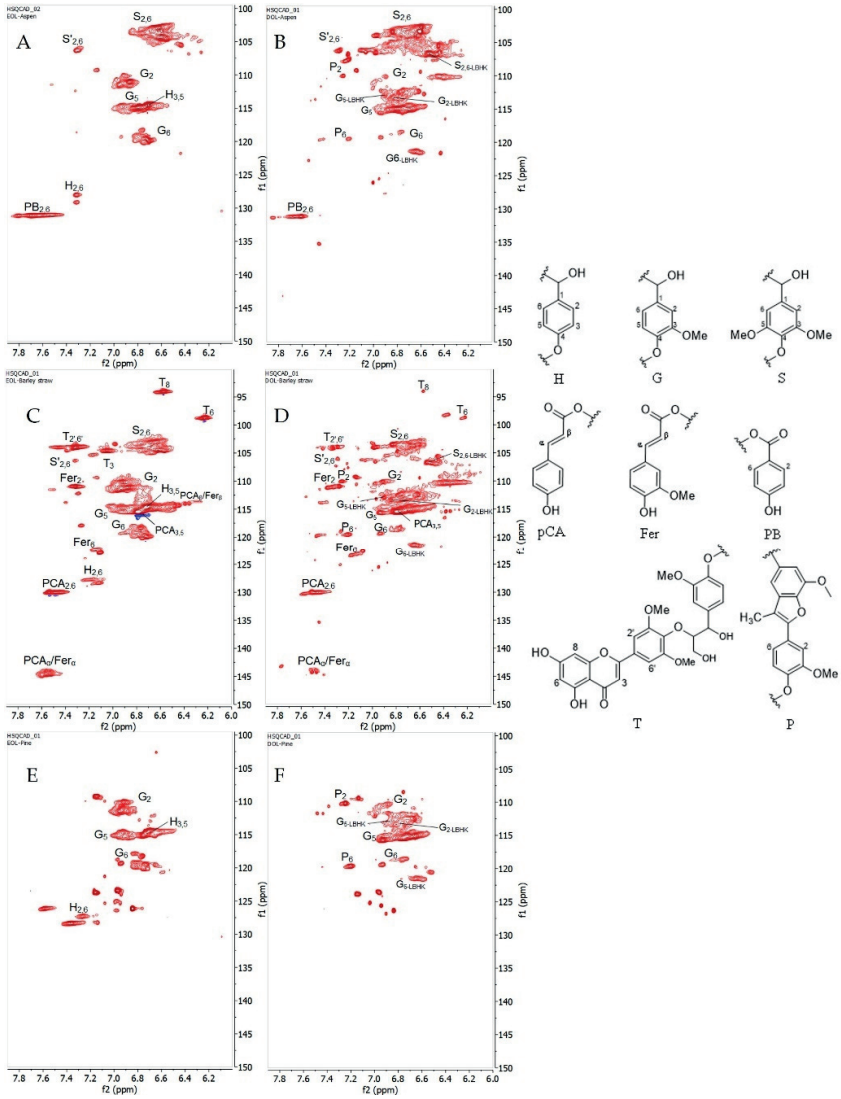

Figure 5. (Left) HSQC spectra that were presented in aromatic/unsaturated region from six organosolv lignins, (**A**) EOL-Aspen, (**B**) DOL-Aspen, (**C**) EOL-Barley straw, (**D**) DOL-Barley straw, (**E**) EOL-Pine, and (**F**) DOL-Pine. Red cross peaks are CH_3 and CH. (Right) (**H**) *p*-hydroxyphenyl unit; (**G**) guaiacyl unit; (**S**) syringyl unit; (**pCA**) *p*-coumarates; (**Fer**) ferulates; (**PB**) *p*-benzoate; (**T**) tricin; (**P**) methyl-substituted phenylcoumaran.

Table 3. The drying shrinkage, bulk density, and gelation time of lignin- based and 5-MR-FA aerogels.

Sample ID	AG-EOL Aspen		AG-DOL Aspen		AG-EOL Barley		AG-DOL Barley		AG-EOL Pine		AG-DOL Pine		AG-5-MR-FA
Amount of 5-MR replaced by lignin, %	75	85	75	85	75	85	75	85	75	85	75	85	0
Drying shrinkage, %	77.7	45.9	61.8	73.9	70.9	72.6	61.4	50.4	63.4	47.1	65.1	51.8	37.0
Bulk density, g/cm^3	0.36	0.15	0.24	0.28	0.33	0.46	0.35	0.19	0.28	0.18	0.33	0.20	0.20
Gelation time, h at (85 °C)	7	13.5	2	2	4	18	1.5	10	2	3.5	1	3.5	<1

In comparison, the shrinkage at the drying state of the material that was obtained from EOLs was higher than the ones from DOLs (except DOL Pine with similarity in their shrinkage). A lesser extent of shrinkage of AG-DOLs was likely due to the higher degree of cross-linkage in the material. The overall higher signal from phenolic groups (Table 2) in DOL gave more possibility to form an aerogel with FA.

The experiments of replacing more than 75% of 5-MR were also performed and these demonstrated that it is possible to replace even up to 85% of the 5-MR with lignin (Table 3). In the experiments where 95% of 5-MR was substituted with lignin showed no gelation of the mixture during 24 h at 85 °C for all the lignins that were used.

3.2.2. Measurement of Porosity and Surface Area

Aerogels are porous materials and the two parameters that characterize this type of material best are porosity and surface area. The common technique that is used for the determination of these parameters is N_2 adsorption/desorption analysis, which allows the calculation of average pore sizes and distribution as well as the surface area of the material. The N_2 adsorption-desorption isotherms of the prepared aerogels (lignin-based, where 75% of the 5-MR was replaced by lignin and AG-5-MR-FA) are depicted in Figure 6.

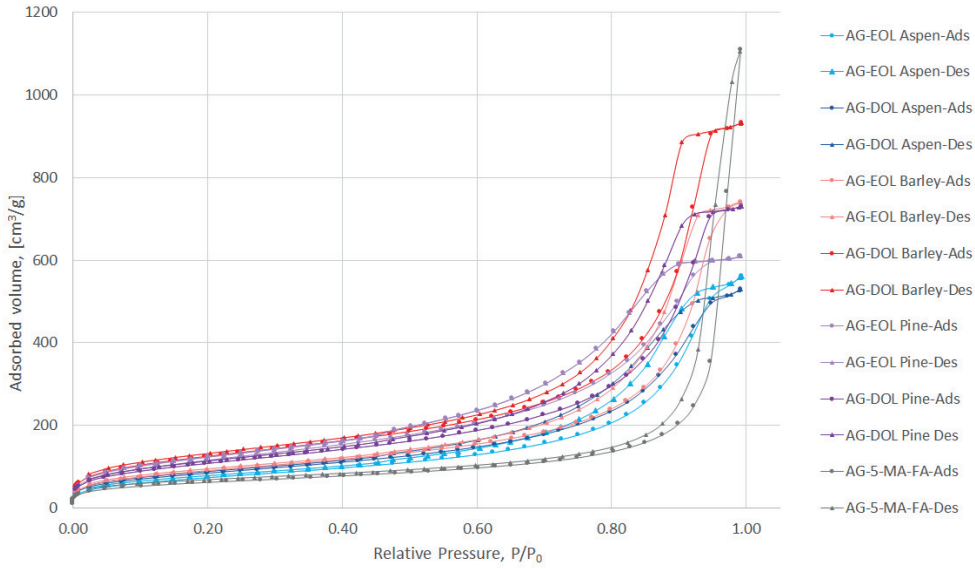

Figure 6. N_2 adsorption/desorption isotherms of lignin-based (75% of the 5-MR was replaced by lignin) and 5-MR-FA aerogels.

According to International Union of Pure and Applied Chemistry (IUPAC) classification, the obtained N_2 adsorption/desorption isotherms for aerogels are characteristic of adsorbents that are mesoporous (types IV and V). The adsorption hysteresis is clearly seen and can be utilized to find correlations between the shape of the hysteresis loop and the texture (e.g., pore size distribution, pore geometry, and connectivity) of a mesoporous material.

The initial region of the isotherms at low P/P_0, which indicates the presence of micropores in addition to mesopores in the gel structure, is very similar to all samples and not characteristic for these aerogels specifically. It is well-known that organic resorcinol-FA aerogels do not show microporosity in their structure. Hysteresis loops for gels in the P/P_0 range 0.2–1.0 show that mesoporosity is dominant in their structures.

The hysteresis loop of 5-MR-FA is of type H1, coinciding with the network structure of agglomerates of uniform spherical particles. The addition of lignin into the structure of aerogel tends to change the loop shape from type H1 to H2, suggesting that the primary particle shape is not well defined and some disordering with a partial opening of the network structure has taken place.

According to IUPAC, pores with diameters larger than 50 nm should be called macropores, while pores with diameters in the range of 2–50 nm should be called mesopores, and pores with diameters smaller than 2 nm should be called micropores [44].

All of the aerogels that were obtained during the study contained mainly mesopores with an average pore diameter in the range of 8.90–13.97 nm, while the 5-MR-FA aerogel, which does not contain lignin, had average pore volume of 30.60 nm. The pore size distributions of the prepared aerogels are depicted in Figure S1. The specific surface area (S_{BET})values were in the range of 271.3–452.9 m^2/g, which are even higher, compared to the aerogel, which does not contain lignin (224.3 m^2/g). The specific surface area, total pore volume, average pore diameter of lignin-based (75% of the 5-MR was replaced by lignin) and 5-MR-FA aerogels are presented in Table 4. We found no correlation between the average pore volumes or S_{BET}, and the extraction solvent, but the solubility of EOLs was always lower than DOLs (both pretreated with NaOH). However, there were similarities of aspen- and barley-based lignin aerogels, where the S_{BET} values were considerably higher for DOLs. For AG-EOL Pine, this might be due to the fact that EOL Pine was not completely solubilized and there was even a small amount of precipitation, which meant that the bottom layer of the aerogel was darker and not homogeneous. For the characterization experiments, this insoluble bottom layer was removed from the samples.

Table 4. The specific surface area, total pore volume, and average pore diameter of lignin-based (75% of the 5-MR was replaced by lignin) and 5-MR-FA aerogels.

Sample ID	BET Surface Area, m^2/g	Total Pore Volume, cm^3/g	Average Pore Diameter, nm
AG-EOL Aspen	271.3	0.87	12.81
AG-DOL Aspen	304.7	0.82	10.73
AG-EOL Pine	424.1	0.94	8.90
AG-DOL Pine	393.2	1.13	11.47
AG-EOL Barley	328.1	1.15	13.97
AG-DOL Barley	452.9	1.44	12.73
AG-5-MR-FA	224.3	1.72	30.60

3.2.3. FTIR Analysis

The Fourier transform infrared spectroscopy technique is sensitive to differences in the structure of lignin-based and AG-5-MR-FA aerogels. AG-5-MR-FA and all the aerogels, where 75% of the 5-MR was replaced by lignin were investigated by ATR FTIR spectroscopy (Figure 7).

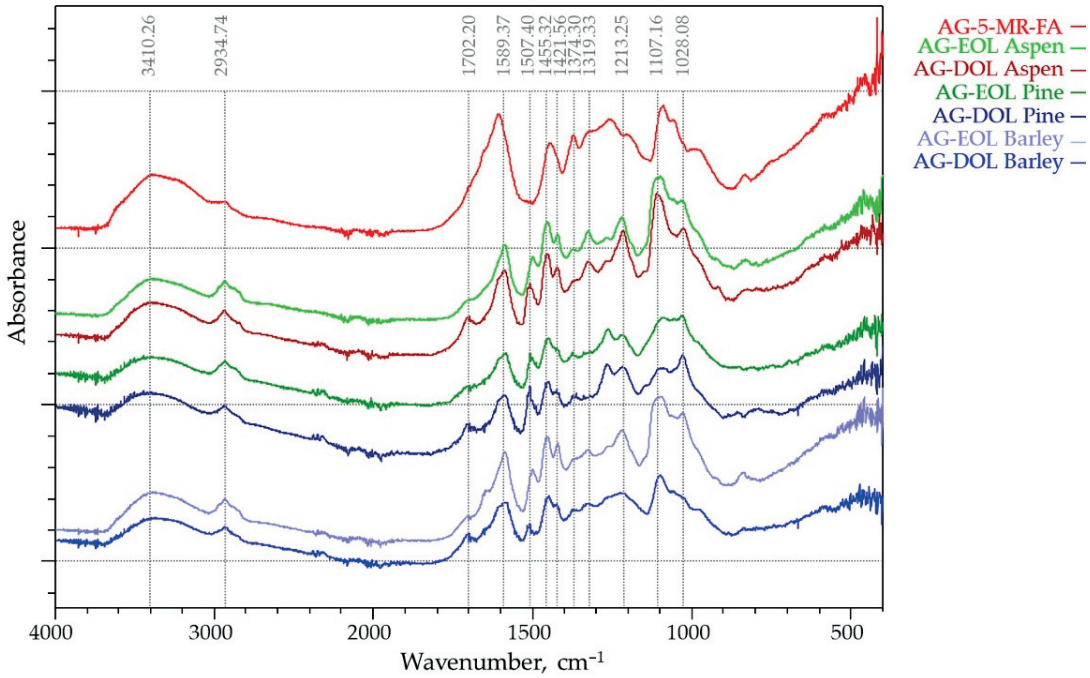

Figure 7. ATR FTIR spectrums of lignin-based (75% of the 5-MR was replaced by lignin) and AG-5-MR-FA aerogels.

The main bands that were located at 1589, 1455, and 1110 cm^{-1} have been described in the literature for resorcinol-FA aerogels that were studied by FTIR [45], which were confirmed by the AG-5-MR-FA spectra shown in Figure 7. The band around 1455 cm^{-1} is associated with the formation of methylene bridges between the aromatic rings as described in the literature earlier. The main band in the region of 1589 cm^{-1} is due to the C-C stretching in the aromatic rings, while the bands at around 1110 cm^{-1} can also be assigned to the C-OH stretching and deformation in phenolic groups. These bands are seen in both lignin-based and 5-MR-FA aerogels.

The main differences are observed in the region around 2900 to 2950 cm^{-1}, where the band intensities are increased from CH stretching in the aromatic methoxy groups and in the methyl and methylene groups of side chains. They are intensified in lignin spectra but less seen in lignin aerogels.

Also, in the FTIR spectra of lignin-based aerogels, there is an observable peak at 1507.40 cm^{-1}, which is a characteristic peak for lignin and does not exist in AG-5-MR-FA spectra. Another proof of the participation of lignin in polycondensation reactions leading to gelation is the decreasing intensity of bands corresponding to methoxy groups and primary alcohols, whereas bands that are related to C=O bond are still noticeable in the spectra of lignin-based aerogels in comparison with AG-5-MR-FA [46].

3.2.4. SEM Analysis

SEM images of the obtained lignin-based aerogel samples, where 75% of the 5-MR was replaced by lignin, are similar with characteristic features of 5-MR-FA aerogel, with particle sizes of 10–50 nm and uniformly distributed pores. However, a porosity assessment with SEM showed the differences from 5-MR-FA aerogels, which confirmed the N_2 adsorption/desorption analysis results. The morphology of the aerogels that were obtained during the study are presented in Figure 8.

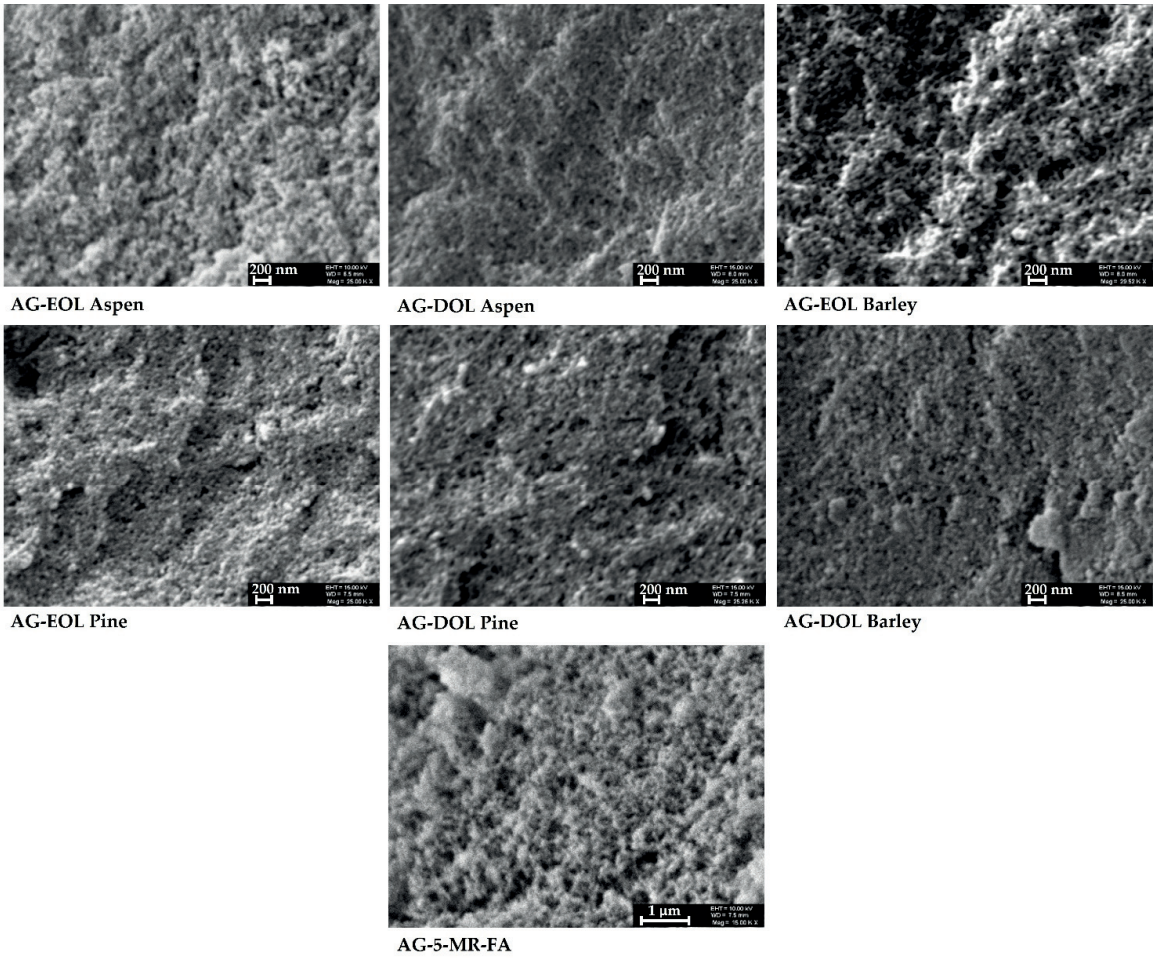

Figure 8. Examples of the SEM images of lignin-based (75% of the 5-MR was replaced by lignin) and 5-MR-FA aerogels.

4. Conclusions

It is possible to produce FA aerogels from lignin with the small addition of 5-MR (25% to 15%) using aspen, pine, and barley lignins that were obtained by organosolv extraction. It shows that the organosolv lignin extraction process gives material that has good reactivity to form gels with FA resulting in monolithic mesoporous aerogels with relatively high surface area –from 350 to 450 m^2/g. The primary particle shape in aerogels is not uniformly spherical but loosely defined and somewhat disordered with a partial opening of the network structure when compared to 5-MR-FA aerogels. Pretreatment of the precursor lignin with NaOH allows increased the solubility of the lignin and its further use in the base catalyzed synthesis of 5-MR-FA-Lignin aerogels. The obtained lignin-based organic aerogels will be further studied as adsorbents and raw material for porous carbon aerogels.

Supplementary Materials: The following supporting information can be downloaded at: https://www.mdpi.com/article/10.3390/ma15082861/s1, Table S1: The detailed HSQC assignment of six organosolv lignin samples. Figure S1: Pore-size distributions of lignin-based (75% of the 5-MR was replaced by lignin) and 5-MR-FA aerogels.

Author Contributions: Conceptualization, P.J., M.K. (Maria Kulp), M.K. (Mihkel Koel) and T.L.; methodology, formal analysis and investigation, P.J., T.T.H., U.K., A.K., K.L. and O.-S.S.; resources, T.L.; data curation, P.J. and M.K. (Maria Kulp); writing—original draft preparation and writing—review and editing, P.J., T.T.H., M.K. (Maria Kulp), M.K. (Mihkel Koel) and T.L.; visualization, P.J.; supervision, M.K. (Maria Kulp) and T.L.; project administration, T.L.; funding acquisition, T.L. All authors have read and agreed to the published version of the manuscript.

Funding: This study was supported by ERDF and Estonian Research Council via project RESTA11.

Institutional Review Board Statement: Not applicable.

Informed Consent Statement: Not applicable.

Data Availability Statement: The data that are presented in this study are available upon request from the corresponding author.

Acknowledgments: The authors would like to thank Marina Kudrjašova and Indrek Reile for valuable discussions on NMR data analysis.

Conflicts of Interest: The authors declare that they have no known competing financial interest or personal relationship that could have appeared to influence the work reported in this paper.

References

1. Bychkov, A.; Podgorbunskikh, E.; Bychkova, E.; Lomovsky, O. Current achievements in the mechanically pretreated conversion of plant biomass. *Biotechnol. Bioeng.* **2019**, *116*, 1231–1244. [CrossRef] [PubMed]
2. Wang, H.; Pu, Y.; Ragauskas, A.; Yang, B. From lignin to valuable products–strategies, challenges, and prospects. *Bioresour. Technol.* **2019**, *271*, 449–461. [CrossRef] [PubMed]
3. Chakar, F.S.; Ragauskas, A.J. Review of current and future softwood kraft lignin process chemistry. *Ind. Crop. Prod.* **2004**, *20*, 131–141. [CrossRef]
4. Ragauskas, A.; Beckham, G.; Biddy, M.; Chandra, R.; Chen, F.; Davis, M.; Davison, B.; Dixon, R.; Gilna, P.; Keller, M. GA Tuskan ja CE Wyman. *Science* **2014**, *344*, 1246843. [CrossRef] [PubMed]
5. Usmani, Z.; Sharma, M.; Awasthi, A.K.; Lukk, T.; Tuohy, M.G.; Gong, L.; Nguyen-Tri, P.; Goddard, A.D.; Bill, R.M.; Nayak, S.C.; et al. Lignocellulosic biorefineries: The current state of challenges and strategies for efficient commercialization. *Renew. Sustain. Energy Rev.* **2021**, *148*, 111258. [CrossRef]
6. Schutyser, W.; Renders, T.; Van den Bosch, S.; Koelewijn, S.F.; Beckham, G.T.; Sels, B.F. Chemicals from lignin: An interplay of lignocellulose fractionation, depolymerisation, and upgrading. *Chem. Soc. Rev.* **2018**, *47*, 852–908. [CrossRef]
7. Chen, Z.; Ragauskas, A.; Wan, C. Lignin extraction and upgrading using deep eutectic solvents. *Ind. Crop. Prod.* **2020**, *147*, 112241. [CrossRef]
8. Garlapati, V.K.; Chandel, A.K.; Kumar, S.J.; Sharma, S.; Sevda, S.; Ingle, A.P.; Pant, D. Circular economy aspects of lignin: Towards a lignocellulose biorefinery. *Renew. Sustain. Energy Rev.* **2020**, *130*, 109977. [CrossRef]
9. Kai, D.; Tan, M.J.; Chee, P.L.; Chua, Y.K.; Yap, Y.L.; Loh, X.J. Towards lignin-based functional materials in a sustainable world. *Green Chem.* **2016**, *18*, 1175–1200. [CrossRef]
10. Frankowski, K.J.; Wang, C.; Patnaik, S.; Schoenen, F.J.; Southall, N.; Li, D.; Teper, Y.; Sun, W.; Kandela, I.; Hu, D.; et al. Metarrestin, a perinucleolar compartment inhibitor, effectively suppresses metastasis. *Sci. Transl. Med.* **2018**, *10*, eaap8307. [CrossRef]
11. Tabani, H.; Alexovič, M.; Sabo, J.; Ramos Payán, M. An overview on the recent applications of agarose as a green biopolymer in micro-extraction-based sample preparation techniques. *Talanta* **2021**, *224*, 121892. [CrossRef] [PubMed]
12. Pekala, R.; Kong, F.-M. A synthetic route to organic aerogels-mechanism, structure, and properties. *J. Phys. Colloq.* **1989**, *50*, C4-33–C4-40. [CrossRef]
13. Peikolainen, A.-L.; Volobujeva, O.; Aav, R.; Uibu, M.; Koel, M. Organic acid catalyzed synthesis of 5-methylresorcinol based organic aerogels in acetonitrile. *J. Porous Mater.* **2012**, *19*, 189–194. [CrossRef]
14. Pérez-Caballero, F.; Peikolainen, A.-L.; Uibu, M.; Kuusik, R.; Volobujeva, O.; Koel, M. Preparation of carbon aerogels from 5-methylresorcinol–formaldehyde gels. *Microporous Mesoporous Mater.* **2008**, *108*, 230–236. [CrossRef]
15. Balakshin, M.; Capanema, E. On the quantification of lignin hydroxyl groups with 31P and 13C NMR spectroscopy. *J. Wood Chem. Technol.* **2015**, *35*, 220–237. [CrossRef]
16. Raj, A.; Devendra, L.P.; Sukumaran, R.K. Comparative evaluation of laccase mediated oxidized and unoxidized lignin of sugarcane bagasse for the synthesis of lignin-based formaldehyde resin. *Ind. Crop. Prod.* **2020**, *150*, 112385. [CrossRef]
17. Lin, K.-T.; Ma, R.; Wang, P.; Xin, J.; Zhang, J.; Wolcott, M.P.; Zhang, X. Deep Eutectic Solvent Assisted Facile Synthesis of Lignin-Based Cryogel. *Macromolecules* **2018**, *52*, 227–235. [CrossRef]
18. Yang, B.S.; Kang, K.-Y.; Jeong, M.-J. Preparation of lignin-based carbon aerogels as biomaterials for nano-supercapacitor. *J. Korean Phys. Soc.* **2017**, *71*, 478–482. [CrossRef]

19. Sen, S.; Patil, S.; Argyropoulos, D.S. Thermal properties of lignin in copolymers, blends, and composites: A review. *Green Chem.* **2015**, *17*, 4862–4887. [CrossRef]
20. Chen, F.; Xu, M.; Wang, L.; Li, J. Preparation and characterization of organic aerogels by the lignin-resorcinol-formaldehyde copolymer. *Bioresources* **2011**, *6*, 1262–1272.
21. García-González, C.; Camino-Rey, M.; Alnaief, M.; Zetzl, C.; Smirnova, I. Supercritical drying of aerogels using CO_2: Effect of extraction time on the end material textural properties. *J. Supercrit. Fluids* **2012**, *66*, 297–306. [CrossRef]
22. Petričević, R.; Reichenauer, G.; Bock, V.; Emmerling, A.; Fricke, J. Structure of carbon aerogels near the gelation limit of the resorcinol–formaldehyde precursor. *J. Non-Cryst. Solids* **1998**, *225*, 41–45. [CrossRef]
23. Wu, D.; Fu, R.; Sun, Z.; Yu, Z. Low-density organic and carbon aerogels from the sol–gel polymerization of phenol with formaldehyde. *J. Non-Cryst. Solids* **2005**, *351*, 915–921. [CrossRef]
24. Jõul, P.; Vaher, M.; Kuhtinskaja, M. Carbon aerogel-based solid-phase microextraction coating for the analysis of organophosphorus pesticides. *Anal. Methods* **2021**, *13*, 69–76. [CrossRef]
25. Saha, D.; Li, Y.; Bi, Z.; Chen, J.; Keum, J.K.; Hensley, D.K.; Grappe, H.A.; Meyer, H.M., III; Dai, S.; Paranthaman, M.P. Studies on supercapacitor electrode material from activated lignin-derived mesoporous carbon. *Langmuir* **2014**, *30*, 900–910. [CrossRef]
26. *ISO18122*; Solid biofuels—Determination of Ash Content. ISO: Geneva, Switzerland, 2015.
27. Rovio, S.; Yli-Kauhaluoma, J.; Sirén, H. Determination of neutral carbohydrates by CZE with direct UV detection. *Electrophoresis* **2007**, *28*, 3129–3135. [CrossRef]
28. Vaher, M.; Helmja, K.; Käsper, A.; Kurašin, M.; Väljamäe, P.; Kudrjašova, M.; Koel, M.; Kaljurand, M. Capillary electrophoretic monitoring of hydrothermal pre-treatment and enzymatic hydrolysis of willow: Comparison with HPLC and NMR. *Catal. Today* **2012**, *196*, 34–41. [CrossRef]
29. Bauer, S.; Sorek, H.; Mitchell, V.D.; Ibáñez, A.B.; Wemmer, D.E. Characterization of Miscanthus giganteus lignin isolated by ethanol organosolv process under reflux condition. *J. Agric. Food Chem.* **2012**, *60*, 8203–8212. [CrossRef]
30. Del Río, J.C.; Rencoret, J.; Prinsen, P.; Martínez, Á.T.; Ralph, J.; Gutiérrez, A. Structural characterization of wheat straw lignin as revealed by analytical pyrolysis, 2D-NMR, and reductive cleavage methods. *J. Agric. Food Chem.* **2012**, *60*, 5922–5935. [CrossRef]
31. Faleva, A.V.; Kozhevnikov, A.Y.; Pokryshkin, S.A.; Falev, D.I.; Shestakov, S.L.; Popova, J.A. Structural characteristics of different softwood lignins according to 1D and 2D NMR spectroscopy. *J. Wood Chem. Technol.* **2020**, *40*, 178–189. [CrossRef]
32. Greco, A.; Brunetti, D.; Renna, G.; Mele, G.; Maffezzoli, A. Plasticizer for poly(vinyl chloride) from cardanol as a renewable resource material. *Polym. Degrad. Stab.* **2010**, *95*, 2169–2174. [CrossRef]
33. Miles-Barrett, D.M.; Neal, A.R.; Hand, C.; Montgomery, J.R.; Panovic, I.; Ojo, O.S.; Lancefield, C.S.; Cordes, D.B.; Slawin, A.M.; Lebl, T. The synthesis and analysis of lignin-bound Hibbert ketone structures in technical lignins. *Org. Biomol. Chem.* **2016**, *14*, 10023–10030. [CrossRef] [PubMed]
34. Wang, P.; Fu, Y.; Shao, Z.; Zhang, F.; Qin, M. Structural changes to aspen wood lignin during autohydrolysis pretreatment. *BioResources* **2016**, *11*, 4086–4103. [CrossRef]
35. Grishechko, L.I.; Amaral-Labat, G.i.; Szczurek, A.; Fierro, V.; Kuznetsov, B.N.; Celzard, A. Lignin–phenol–formaldehyde aerogels and cryogels. *Microporous Mesoporous Mater.* **2013**, *168*, 19–29. [CrossRef]
36. Faleva, A.V.; Belesov, A.V.; Kozhevnikov, A.Y.; Falev, D.I.; Chukhchin, D.G.; Novozhilov, E.V. Analysis of the functional group composition of the spruce and birch phloem lignin. *Int. J. Biol. Macromol.* **2021**, *166*, 913–922. [CrossRef]
37. El Mansouri, N.-E.; Salvadó, J. Analytical methods for determining functional groups in various technical lignins. *Ind. Crop. Prod.* **2007**, *26*, 116–124. [CrossRef]
38. Yáñez-S, M.; Matsuhiro, B.; Nuñez, C.; Pan, S.; Hubbell, C.A.; Sannigrahi, P.; Ragauskas, A.J. Physicochemical characterization of ethanol organosolv lignin (EOL) from Eucalyptus globulus: Effect of extraction conditions on the molecular structure. *Polym. Degrad. Stab.* **2014**, *110*, 184–194. [CrossRef]
39. Katahira, R.; Elder, T.J.; Beckham, G.T. A brief introduction to lignin structure. In *Lignin Valorization: Emerging Approaches*; Energy and Environment Series; Royal Society of Chemistry: London, UK, 2018; pp. 1–20. [CrossRef]
40. Constant, S.; Wienk, H.L.; Frissen, A.E.; de Peinder, P.; Boelens, R.; Van Es, D.S.; Grisel, R.J.; Weckhuysen, B.M.; Huijgen, W.J.; Gosselink, R.J. New insights into the structure and composition of technical lignins: A comparative characterisation study. *Green Chem.* **2016**, *18*, 2651–2665. [CrossRef]
41. Wen, J.-L.; Sun, S.-L.; Xue, B.-L.; Sun, R.-C. Recent advances in characterization of lignin polymer by solution-state nuclear magnetic resonance (NMR) methodology. *Materials* **2013**, *6*, 359–391. [CrossRef]
42. Li, J.; Henriksson, G.; Gellerstedt, G. Lignin depolymerization/repolymerization and its critical role for delignification of aspen wood by steam explosion. *Bioresour. Technol.* **2007**, *98*, 3061–3068. [CrossRef]
43. Sannigrahi, P.; Ragauskas, A.J.; Miller, S.J. Lignin structural modifications resulting from ethanol organosolv treatment of loblolly pine. *Energy Fuels* **2010**, *24*, 683–689. [CrossRef]
44. Sing, K.S. Reporting physisorption data for gas/solid systems with special reference to the determination of surface area and porosity (Recommendations 1984). *Pure Appl. Chem.* **1985**, *57*, 603–619. [CrossRef]
45. Jirglova, H.; Perez-Cadenas, A.F.; Maldonado-Hodar, F.J. Synthesis and properties of phloroglucinol− phenol− formaldehyde carbon aerogels and xerogels. *Langmuir* **2009**, *25*, 2461–2466. [CrossRef] [PubMed]
46. Pekala, R. Organic aerogels from the polycondensation of resorcinol with formaldehyde. *J. Mater. Sci.* **1989**, *24*, 3221–3227. [CrossRef]

Appendix 2

Publication II

T.Tran Ho, Olivia-Stella Salm, Tiit Lukk, and Maria Kulp. Utilization of phenolic lignin dimer models for the quantification of monolignols in biomass and in its derived organosolv lignins via thioacidolysis and GC-MS analysis. Analytical Methods 2025, 17, 3283–3289, https://doi.org/10.1039/D5AY00073D

Analytical Methods

ROYAL SOCIETY OF CHEMISTRY

PAPER

View Article Online
View Journal | View Issue

Cite this: *Anal. Methods*, 2025, **17**, 3283

Utilization of phenolic lignin dimer models for the quantification of monolignols in biomass and in its derived organosolv lignins *via* thioacidolysis and GC-MS analysis†

T. Tran Ho, * Olivia-Stella Salm, Tiit Lukk and Maria Kulp

A thorough understanding of lignin's fundamental chemistry in lignocellulosic materials is essential for maximizing the efficiency of biorefineries. Thioacidolysis, followed by gas chromatography-mass spectrometry (GC-MS), has emerged as a reliable method for quantifying uncondensed monolignols, which are linked by labile aryl ether bonds within lignin network. However, the lack of commercially available pure thioethylated lignin monomers for GC analysis poses a challenge. This necessitates a multi-step synthesis process, which may not be feasible for all laboratories. We propose a novel approach that utilizes readily available phenolic lignin model dimers to establish a calibration curve for thioacidolysis quantification. These dimers, guaiacylglycerol-β-guaiacyl ether (GGE) and syringylglycerol-β-guaiacyl ether (SGE), upon thioacidolysis, yield thioethylated non-condensed guaiacyl (G) and syringyl (S) monomers. The GC-MS responses of these monomers are compared to those of bisphenol E, an internal standard (IS) to generate the calibration curve. This methodology exhibits excellent performance characteristics and was successfully employed to determine the thioethylated monomer contents and calculate of S/G ratios in three representative biomasses: aspen, barley straw, pine, and their organosolv lignin extracts.

Received 14th January 2025
Accepted 3rd April 2025

DOI: 10.1039/d5ay00073d

rsc.li/methods

1. Introduction

Lignin, a major constituent of plant biomass (15 to 36%), serves as a protective barrier against biological and chemical degradation by covalently crosslinking cellulose and hemicellulose.[1] Lignin's backbone is primarily formed of three monolignols, each with varying methoxylation levels: *p*-hydroxyphenyl (H), guaiacyl (G), and syringyl (S) units. These monolignols are polymerized by radical coupling mechanism from the three fundamental monomers, *p*-coumaryl, coniferyl, and sinapyl alcohols, respectively (Fig. 1).[1] The composition of lignin significantly differs based on botanical origin. Softwood lignin primarily derives from coniferyl and a minor portion of *p*-coumaryl and sinapyl monolignols,[2] while hardwood lignin is synthesized from coniferyl and sinapyl units, with the latter being more prevalent. In contrast, non-woody biomass is characterized as an H–G–S type lignin, indicating the presence of all three monolignols.[3]

Lignin's macromolecular structure is crosslinked by distinct bonding motifs, including β-O-4′, β-β′, β-5′, and dibenzodioxocin, as illustrated in Fig. 1. The β-O-4′ aryl–ether bond, present in approximately 50% of spruce (softwood), and 60% of birch or eucalyptus (hardwood), is the most common of these linkages.[4] During the fractionation of lignocellulosic biomass, lignin fragments are primarily released from the breakdown of these interunit linkages, altering the lignin structure.[5–7] One of the consequences of this modification is the irreversible repolymerization or condensation in isolated lignin, leading to a higher proportion of condensed structures (C–C bond) compared to its native form.[8,9] This undesirable reaction hampers the selective depolymerization of residual lignin into valuable phenolic monomers.[10–12] Although organosolv delignification is a mild method for fractionating lignocellulose, it unavoidably alters lignin's structure.[13,14] Considering lignin's variable composition and the inevitability of structural changes under specific pulping conditions, chemical analysis is an essential step prior to lignin valorization.

In recent decades, lignin chemistry has gathered significant attention from scientists seeking to decipher its complex structural network using a variety of analytical techniques. Among these, thioacidolysis followed by gas chromatography-mass spectrometry (GC-MS) has emerged as a prominent method for quantifying uncondensed monolignols. This technique, initially introduced by Lapierre in 1985 as a diagnostic test,[15] employs a mixture of ethanethiol dissolved in 1,4-dioxane

Department of Chemistry and Biotechnology, Tallinn University of Technology, Akadeemia tee 15, 12618 Tallinn, Estonia. E-mail: thihol@taltech.ee; olivia-stella.salm@taltech.ee; tiit.lukk@taltech.ee; maria.kulp@taltech.ee

† Electronic supplementary information (ESI) available. See DOI: https://doi.org/10.1039/d5ay00073d

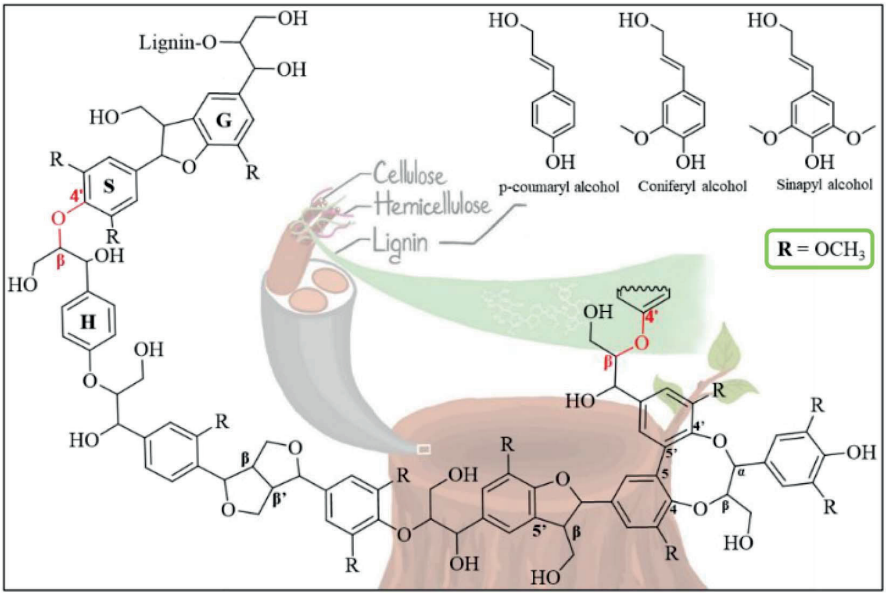

Fig. 1 Lignin monolignol compositions and interunit bonding motifs.

and boron trifluoride (BF_3) etherate to efficiently and selectively depolymerize lignin into its constituent phenolic monomers (H, G, and S) which lack condensed structures and are interconnected by β-O-4′ bonds (Fig. 2a).[15–17] The obtained non-condensed H/G/S ratios provide crucial information for the lignin-first strategy, which aims to preserve the aryl–ether bond for the subsequent conversion of lignin into valuable chemicals.[11]

Since its inception, the original thioacidolysis protocol has undergone progressive refinement.[18–23] Robinson and colleagues' modified the protocol by reducing the initial mass and thioacidolysis reagent by tenfold compared to the conventional method. This modification allowed for the processing of multiple samples simultaneously by facilitating the purification of thioehtylated monomers in a 5 mL screw-capped glass vial instead of a separatory funnel.[18] Further advancements focused on miniaturizing the workup processes, including derivatization and liquid–liquid extraction, and replacing chlorinated solvents with ethyl acetate or diethyl ether.[19,21] Harman-Ware introduced the innovative approach of Low Thermal Mass Modular Accelerated Column Heater (LTM MACH) coupled with gas chromatography-flame ionization detector (GC-FID), enabling results within five minutes per analysis.[20] Additionally, the multi-reaction monitoring (MRM) mode of MS detectors has been developed, significantly enhancing the sensitivity for detecting monolignols down to the ppb concentration range.[23] While these improvements have been addressed various aspects, the recovery of thioacidolysis-derived monomers through liquid extraction remains time-consuming. Fortunately, F. Chen's protocol eliminates this step without compromising the results.[22]

However, it is challenging to obtain authentic standard of lignin. To address this challenge, Yue *et al.*[24] introduced a method that utilizes pure synthetic thioethylated monolignols and their relative response factors (RRFs) for GC-MS analysis. This approach allows for the quantification of lignin-derived

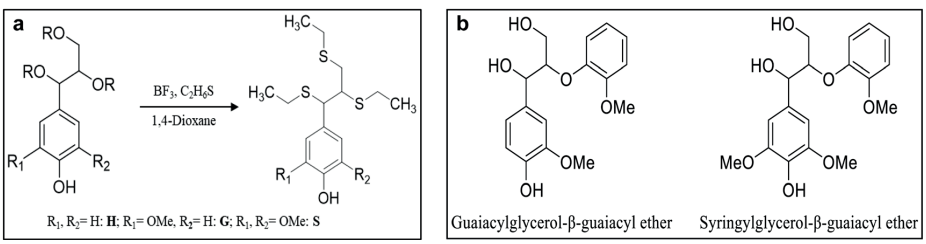

Fig. 2 Thioacidolysis reaction scheme (a) and phenolic lignin model compounds (b).

monomers without the need for commercial standards. The RRF is calculated by using the concentration of the analyte and internal standard together with their peak areas, as below:[24]

$$\mathrm{RRF} = \frac{\frac{W_S}{A_S}}{\frac{W_{IS}}{A_{IS}}} \quad (1)$$

where, W_S and W_{IS} represent the mass or concentration of the target thioethylated monolignol and the chosen internal standard (IS), respectively, while A_S and A_{IS} are their corresponding peak areas in chromatograms.[24] While the synthesis yielded high yields of three thioethylated monomers, each step required purification and characterization, which may not be feasible for all laboratories. In addition, the RRF is a conditionally dependent factor that can fluctuate due to small changes in the analytical process, such as instrument, operation parameters, IS selection, or other factors, leading to increased uncertainty in the measurement results.[25,26] As a result, pre-determined RRFs cannot be applied across laboratories for quantitative analysis without the availability of pure compounds.

In this study, we propose phenolic lignin model compounds (LMCs) as the alternatives to authentic standards for thioacidolysis analysis that has not yet covered in literature.[27] They are guaiacylglycerol-β-guaiacyl ether (GGE) and syringylglycerol-β-guaiacyl ether (SGE) (Fig. 2b), which closely mimic the non-condensed G and S subunits in lignin, respectively. Moreover, each of these LMCs is linked to another aromatic subunit *via* a β-O-4′ bond, a key structural feature of lignin. This structural resemblance and the thioacidolysis depolymerization selectivity (Fig. 2a) suggest that these chosen molecules can effectively represent a substantial portion of lignin during thioacidolysis reaction. By submitting the LMCs with varying concentrations to thioacidolysis without purification, the ratio of initial molar concentrations between GGE/SGE and IS are employed as the independent variable. Simultaneously, the peak areas of thioethylated monomers obtained from GC-MS are utilized as dependent variables to construct calibration curves. These calibration curves, in this instance, incorporate measurement uncertainty components including thioacidolysis depolymerization and derivatization reaction efficiency. As a result, they provide more reliable quantitative outcomes. Based on this approach, we predicted the non-condensed monolignols of lignin in three lignocellulosic biomass types: softwood (pine sawdust), hardwood (aspen chips), and non-woody (barley straw). We also examined those in organosolv lignin samples. Furthermore, the method was validated by evaluating its linearity range, limit of detection, precision, accuracy, and combined uncertainty parameters.

2. Materials and methods

2.1. Chemicals and materials

Guaiacylglycerol-β-guaiacyl ether (GGE, 97%, TCI, Tokyo), syringylglycerol-β-guaiacyl ether (SGE, 96%, BLDpharm, Germany). Pyridine (99.8%, anhydrous), bisphenol E (≥98%, analytical grade), boron trifluoride diethyl etherate (BF_3), and ethanethiol (97%) were purchased from Sigma-Aldrich. 1,4-Dioxane (analytical grade, ≥99.8%, Fisher). *N*,*O*-Bis(-trimethylsilyl)trifluoroacetamide containing 1.0% trimethylchlorosilane (BSTFA, 1.0% TMCS) was from Thermo Fisher Scientific, Germany.

The biomass and organosolv lignin preparations were identical to those used in our previous study.[28] In this study, the biomass was comminuted to a target size and sized by a 1 mm metal mesh. Both lignin samples that extracted by ethanol and 1,4-dioxane were investigated.

2.2. Thioacidolysis

2.2.1 Reagent preparation. 25.0 mL of thioacidolysis reagent was prepared fresh by firstly adding 10 mL of 1,4-dioxane in a 25 mL volumetric flask. After that, 6.25 mL of BF_3 and 2.5 mL of ethanethiol were added. IS was added into the same mixture, containing 1.5 mL of bisphenol E from the stock solution (concentration at 2.0 mg mL^{-1}, prepared in 1,4-dioxane). Finally, the mixture was brought to 25 mL as the final volume with the addition of 1,4-dioxane.

2.2.2 LMCs preparation. The stock solutions of two LMCs (GGE and SGE) were prepared by dissolving 10.0 mg of each LMC in 5.0 mL of 1,4-dioxane. Then, the series of working solutions were accurately prepared (with the volumes of 10, 20, 50, 100, 150, 200, 250 μL from stock solution) into 1.5 mL vials, followed by drying under a stream of nitrogen gas prior to subjecting it to thioacidolysis reaction.

Thioacidolysis protocol was adapted from F. Chen's publication with some changes in the use of glassware.[22] Briefly, 2.0–3.0 mg of biomass or organosolv lignin (analytical balance, accuracy of 0.01 mg) was weighed into a 1.5 mL aluminum sealed-cap vial. Next, 1.0 mL of thioacidolysis reagent was pipetted into each vial and tightly sealed. These vials were placed in a preheated MULTIVAP (model JXDC-10, China) at 100 °C for 4 hours reaction, a quick vortex required every 1 hour. The mixture was left to cool down at room temperature. In the meantime, a set of 1.5 mL vials was prepared with 190.0 μL of saturated $NaHCO_3$. The reaction was quenched by transferring 400.0 μL of reaction mixture into the vials containing $NaHCO_3$ solution and mixing by pipette for two times. Prior to derivatizing with silylation agent for GC-MS analysis, these vials were dried under nitrogen gas stream at 55 °C on the same MULTIVAP assisted with gas distribution system. For preparation of calibration using LMCs, the same volume of thioacidolysis reagent was added into the vials containing the known amount of dried matter of LMCs and all the steps were carried out as identical to sample preparation. Each standard point was prepared with three parallels, while samples from lignocellulosic materials and their corresponding organosolv lignins were duplicated.

2.3. GC-MS analysis

The ready-made dried samples were each derivatized with 200.0 μL of BSTFA (1.0% TMCS) : pyridine (1 : 1, v/v), at 55 °C for 30 min, a quick vortex required in the end. The volume of silylated sample was transferred by Pasteur pipette into the GC-

vial containing a 400 μL micro insert, then, sealed. The GC-MS analysis was carried out with an Agilent Technologies 7890A instrument equipped with an Agilent 5975C VL mass selective detector (MSD), using electron ionization (EI) mode together with quadrupole mass analyzer. An ultra-inert split liner (Agilent Technologies, 5190-2295) was used. A Phenomenex ZB-5plus capillary column (30 m × ID 0.25 mm, film thickness 0.25 μm) was used to achieve the separation of thioethylated monomers. Helium was used as carrier gas with a flowrate of 1.3 mL min^{-1}. The injection volume was 1.0 μL with a split ratio of 1 : 10.

The GC inlet temperature was kept at 250 °C. The oven temperature program started at 100 °C, held for 1 min, then increased to 300 °C at stepwise 25 °C min^{-1} and held for 3 min. The temperature of MSD transfer line, MS quadrupole, and ion source were set at 280 °C, 150 °C, and 230 °C, respectively. The ionization energy for EI mode operated at 70 eV. The signals were collected under a full scanning method in which the mass ranges from 30 to 500 *m*/*z* with solvent delay until 6.5 min. For quantification, the extracted ion chromatogram (EIC) was employed with characteristic fragments: 343 *m*/*z* for bisphenol E (IS), 269 *m*/*z* for thioethylated non-condensed G-derived monomers and 299 *m*/*z* for S-derived monomers. MSD ChemStation F.01.03.2357 software was used for integration.

2.4. Thioacidolysis method validation

The developed procedure was validated according to Eurachem validation guideline.[29] The GC-MS method was evaluated for selectivity, limits of detection and quantification (LOD and LOQ), linearity, precision, and accuracy. Measurement uncertainty of the quantitative results was also assessed at a confidence level of 95%.

Selectivity is defined as the ability of an analytical method to distinguish a target analyte from matrix components or other substances in the sample. Mass spectrometry is currently considered the most selective method for identifying compounds in complex mixtures using fragmentation patterns of their ions.[30] In the present study, the identity of S and G thioethylated monomers presenting in biomass and organosolv lignin samples were confirmed by comparing the relative retention times of the analytes to those of thioethylated monomers released from LMCs with a time window of ±0.5%.[30] The identity of the analytes was additionally approved by characteristic peak splitting due to the conformational isomer and mass fragments of G- and S-derived monomers.

Instrumental detection and quantification limits (IDL and IQL) were determined by calculating the ratio of the residual standard deviation of a regression line (the standard deviation of *y*-intercepts) and the slope, multiplied by 3.3 for IDL and 10 for IQL. Quantification limits of the thioacidolysis GC-MS procedure (LOQ) were calculated in μmol per g of lignin according to the methodology. For biomass analysis, LOQ was expressed per g of lignin, measured by Klason method.

Precision and trueness of the procedure were evaluated based on recovery of spiked samples ($n = 8$) on the barley straw matrix containing both G and S units. Trueness was expressed as the absolute difference (bias) between the experimental mean recovery and 100%, while precision was presented as relative standard deviation (RSD%). The recovery (*R*%) was calculated by taking the total concentration of analyte in spike sample ($C_{recovered}$, μmol) excluding the inherent amount of that in biomass matrix ($C_{non\text{-}spiked}$, μmol), followed by comparing to the initial known spiked concentration (C_{spiked}, μmol) of LMCs (eqn (2)). The mean recovery was the average of eight individual spiked samples. The un-spike and spike samples were prepared in the same way as described in Section 2.2.

$$R\% = \frac{C_{recovered} - C_{non\text{-}spiked}}{C_{spiked}} \times 100 \quad (2)$$

3. Results and discussions

3.1. Calibration using lignin model compounds (LMCs)

Instead of synthesizing pure thioethylated monolignols for the determination of their relative response factors (RRFs), we explored the feasibility of using commercially available reference models (GGE and SGE) to create calibration curves for GC-MS quantification of uncondensed G and S subunits in lignin. This approach eliminates the need for tedious synthesis, work-up, and characterization of pure thioethylated monolignols, as reported previously.[24] While the purification step of the final products can be bypassed by creating calibration curves rather than calculating absolute RRF values, the synthesis itself still requires certain expertise.[20,23] Instead, our proposed approach for constructing the calibrations using LMCs offers several advantages: (i) LMCs are white powders, making them easier to handle and prepare compared to viscous, oily thioethylated products that requires high precision and accuracy;[24] (ii) the conversion efficiency of LMCs is relatively stable or similar across the investigated dynamic range, ensuring consistent results; (iii) LMCs are dimers that mimic the β-O-4′ linking motif, making them more representative of lignin molecules for thioacidolysis depolymerization; (iv) this approach is readily applicable to various laboratories, particularly for routine analysis. In this study, the calculation of RRFs was not deemed favorable due to the inherent challenges of determining the precise thioacidolysis yield.

Fig. 3 represents chromatograms of two derivatized thioethylated monomers released from model compounds (GGE and SGE), biomass and lignin samples. The stacked TIC chromatograms of the individual model substance (Fig. 3a and b) demonstrate clear separation of the chosen IS, S- and G-monomers released from LMCs. The impurity of LMCs may give rise to the unknown peak (marked as an asterisk), however it does not interfere or overlap with the main compounds. The ability to yield analytes of interest *via* thioacidolysis and no interfering degraded products, the chosen compounds were proved to be the best fit for uncondensed monolignols quantification. From the reported data of pure lignin-derived thioacidolysis monomers, the identity of the substances was firmly confirmed by their characteristic splitting peak shape due to the mixture of diastereomers, erythro and threo; and *m*/*z* values for

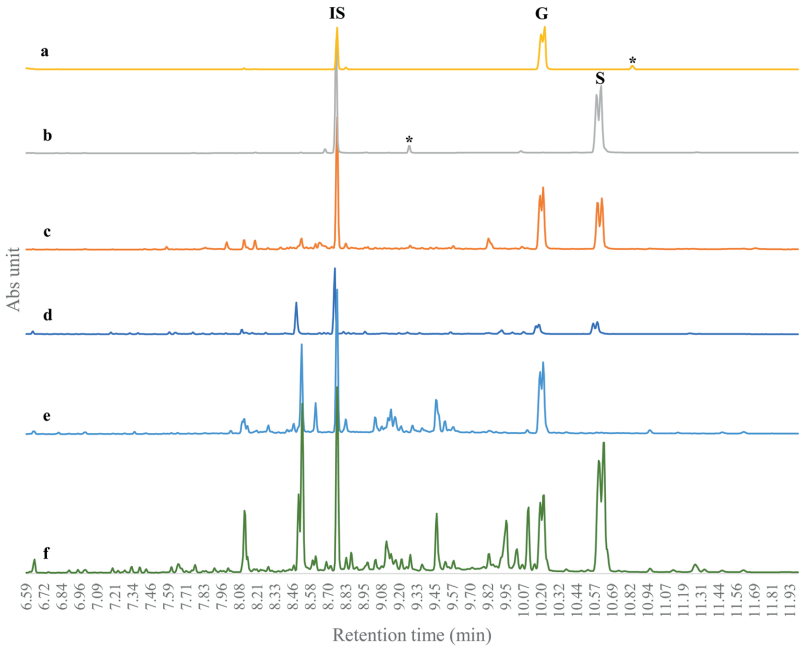

Fig. 3 TIC of: G – (a), and S – (b) derived thioacidolysis monomers, originated from phenolic lignin model compound, ethanol extracted lignin from barley straw (c), raw biomass barley straw (d), pine sawdust (e), aspen chips (f).

the main fragments of thioethylated non-condensed G- and S-derived monomers, 269 *m*/*z* and 299 *m*/*z*, from their mass spectra, respectively (Fig. S1a and b†).[24] The peak integration for quantitative analysis was relied on the extracted ion chromatogram (EIC) of these two quantitation ions for G- and S-units, with the relevance to the retention time on TIC. For the real samples, the relative retention times of the analytes (Fig. 3c–f) closely align those of the standards (Fig. 3a and b) with the average tolerances of 0.25 ± 0.02% for S-units and 0.11 ± 0.01% for G-units, satisfying the performance criteria requirements for confirmation GC-MS method (max. 0.5%).[30]

Table 1 summarizes thioacidolysis GC-MS method performance characteristics. The plots of peak area ratios (S- and G-monomers to IS) *versus* molarity of LMCs demonstrated adequate linearity for the studied analytes with acceptable statistical parameters: coefficients of determination greater than 0.99 and regression error less than 7.5%. The high correlation coefficients of two calibrations achieved from LMCs (Fig. S2 and S3†) were comparable to those established from aryl glycerol monomers ($R^2 \geq 0.99$).[20,23] These results confirm the feasibility of estimating monolignols by using the same sample preparation protocol.

The estimation of IDL, IQL was calculated based on the concentration range close to zero (0.2–1.2 μmol mL^{-1} for G-monomer and 0.1–0.6 μmol mL^{-1} for S- monomer). The LOQ was expressed per g of lignin and obtained LOQ values ensured the quantitation of both monomers in original biomass and lignin samples. The precision of the thioacidolysis procedure (Table 1), based on parallel measurements of eight spiked samples and expressed in RSD% were both less than or equal to 10.5% for S- and G-monomer. Herein, for the first time, the recovery test based on biomass matrix was examined. The mean recoveries ($n = 8$) were obtained for G, 88.9% and S, 97.1%, reflecting the accuracy of entire process including

Table 1 Thioacidolysis GC-MS method linearity, limits of quantification, and analytical reliability parameters

Compound	Linearity range (μm ml^{-1})	R^2	Regression error (%)	IQL[a] (μg ml^{-1})	LOQ (μm g^{-1} of lignin)	Precision (RSD, %)	Trueness (%)
G-Monomer	0.25–3.10	0.9900	7.1	48.11	30.0	9.0	11.1
S-Monomer	0.11–2.82	0.9970	5.4	43.58	25.0	10.5	2.9

[a] IQL was expressed in mass units based on the base fragments of GGE and SGE, which are 269, 299 *m*/*z*, respectively.

Table 2 Monomers yields from thioacidolysis (μmol g^{-1} of Klason lignin) in lignocellulosic materials and their organosolv lignin samples ($n = 2$)

Biomass	S (±SD)	G (±SD)	S/G	Organosolv lignin	S (±SD)	G (±SD)	S/G
Aspen	1334.7 (±86.8)	959.2 (±8.5)	1.39	EtOH	902.2 (±3.83)	339.1 (±23.9)	2.66
				1,4-Dioxane	379.9 (±14.11)	102.1 (±0.1)	3.72
Barley	538.4 (±111.6)	478.6 (±11.4)	1.12	EtOH	413.4 (±6.74)	491.3 (±13.7)	0.84
				1,4-Dioxane	109.1 (±1.66)	39.3 (±6.2)	2.77
Pine	39.3 (±0.3)	1037.4 (±201.5)	0.04	EtOH	36.5 (±3.9)	801.5 (±8.8)	0.05
				1,4-Dioxane	34.2 (±2.5)	174.7 (±14.4)	0.20

thioacidolysis and derivatization performance. Standard deviation and RSD% obtained from recovery test were shown in Table S2.† This yielded estimates of combined uncertainty of the procedure around 10.9% for S-units and 14.3% for G-units, which confirms the reliability of the developed method. The validity of the method eases the monolignols quantification for lignin in the absence of authentic standards, which require time and costly synthetic procedure. By that the application of such is broaden and feasible for all the lignin-related analytical testing laboratories.

3.2. Thioacidolysis analysis of uncondensed monolignols in biomass and lignin

The developed calibrations were used to quantitatively determine the amount of uncondensed S and G monomers in three representative lignocellulosic biomasses: hardwood (aspen), softwood (pine), non-woody (barley straw), and their organosolv lignins. As expected, the lignin compositions vary depending on biomass type and change accordingly under specific pulping conditions, all of which are reflected in the results of thioacidolysis monomers yields, summarized in Table 2. As typical lignin's components for softwood, S-derived thioacidolysis monomers were quantified at small amount in pine (39.28 μmol g^{-1} of Klason lignin). Instead, the recovery yield of characteristic G units was detected at 1037 (μmol g^{-1} of Klason lignin), which was close to the reported value obtained by calculating based on the RRF, 1020 (μmol g^{-1} of Klason lignin).[24] The monolignols ratio in hardwood aspen (*P. tremula*) S/G was 1.39, which was lower than previously reported 1.81,[31] the variation was due to the difference in methodology, meanwhile the S-monomer content was 1334.7 (μmol g^{-1} of Klason lignin), which was in consistent with reported value 1260 (μmol g^{-1} of Klason lignin).[31] In contrast, thioethylated S and G monomers were detected in lignin from barley biomass and are reported here for the first time with the ratio of S/G being 1.12. Notably, the abundance of these monomers was observed in aspen about 2300 μmol g^{-1} of Klason lignin, which was twice higher than in barley, 1017 μmol g^{-1} of Klason lignin. The difference in thioacidolysis yield was also dependent on the Klason lignin content of biomass (Table S1†).

For comparison purposes, thioacidolysis analyses were also conducted on organosolv lignin extracted from the same lignocellulosic materials. The results (Table 2) support two key observations: (i) β-O-4′ cleavage is the primary mechanism driving organosolv delignification; (ii) repolymerization or condensation is unavoidable when organosolv pulping is performed in dilute acid environment.[32] As a result of these processes, the total amount of uncondensed monolignols (S and G) connected by aryl ether bonds decreases for both solvent systems. Additionally, it is noteworthy that the recovery rates of thioacidolysis S and G monomers were higher for all ethanol organosolv-based lignins compared to dioxane lignins. In other words, acidic ethanol pulping conditions proved to be more effective in preserving lignin's native structure (β-O-4′ bond) for subsequent chemical valorization. These thioacidolysis findings are consistent with our observations of 2D-heteronuclear single quantum coherence (HSQC) data where the abundance of aryl–ether bond cross peaks drastically decreased when using 1,4-dioxane as solvent.[28] It was evident that the thioacidolysis protocol was efficient to analyze highly condensed lignin structure as it was in the case of 1,4-dioxane-extracted lignins.

4. Conclusions

This study introduces the use of lignin model compounds as reference substances for thioacidolysis analysis of uncondensed monolignols, offering an alternative to the traditional method of synthesizing the pure aryl glycerol monomers. This approach is highly adaptable to various laboratories, as it eliminates the need for elaborate synthesis and characterization steps. The obtained calibration curves exhibit efficient linear regression coefficients within the dynamic range, demonstrating the suitability of lignin model compounds for analysis. Applying the calibrations enabled the quantification of thioacidolysis non-condensed S and G monomers contents in three lignocellulosic biomasses and their corresponding organosolv lignin products, yielding results that are consistent with our previous study and literature. These quantification outcomes provide a comprehensive understanding of the variation in lignin composition and unveil the relationship between lignin' structural behavior under various treatment conditions. Nevertheless, our study was unable to verify some unknown degraded products released from LMCs, which could be further investigated for a better understanding whether it comes from the intrinsic impurity of the standards themselves or other causes.

Data availability

The data supporting this article has been included as part of the main article and the ESI.†

Author contributions

Tran T. Ho: methodology, investigation, formal analysis, visualization, writing – original draft preparation, writing – review and editing. Olivia-Stella Salm: investigation, writing – review and editing. Tiit Lukk: writing – original draft preparation, funding acquisition, supervision. Maria Kulp: conceptualization, methodology, supervision, validation, writing – original draft preparation, writing – review and editing. All authors read and approved the final manuscript.

Conflicts of interest

The authors declared there are no competing interests.

Acknowledgements

This study was supported by ERDF and Estonian Research Council *via* RESTA11 and TemTA49.

References

1 R. Whetten and R. Sederoff, *Plant Cell*, 1995, **7**, 1001–1013.
2 A. V. Faleva, A. Y. Kozhevnikov, S. A. Pokryshkin, D. I. Falev, S. L. Shestakov and J. A. Popova, *J. Wood Chem. Technol.*, 2020, **40**, 178–189.
3 L. Yao, H. Yang, X. Meng and A. J. Ragauskas, *Front. energy res.*, 2022, **9**, 804086.
4 J. Zakzeski, P. C. A. Bruijnincx, A. L. Jongerius and B. M. Weckhuysen, *Chem. Rev.*, 2010, **110**, 3552–3599.
5 E. I. Evstigneyev and S. M. Shevchenko, *Wood Sci. Technol.*, 2020, **54**, 787–820.
6 H. Yang, C. G. Yoo, X. Meng, Y. Pu, W. Muchero, G. A. Tuskan, T. J. Tschaplinski, A. J. Ragauskas and L. Yao, *Bioresour. Technol.*, 2020, **295**, 122240.
7 M. R. Sturgeon, S. Kim, K. Lawrence, R. S. Paton, S. C. Chmely, M. Nimlos, T. D. Foust and G. T. Beckham, *ACS Sustain. Chem. Eng.*, 2014, **2**, 472–485.
8 V. Patil, S. Adhikari, P. Cross and H. Jahromi, *Renewable Sustainable Energy Rev.*, 2020, **133**, 110359.
9 K. H. Kim and C. S. Kim, *Front. Energy Res.*, 2018, **6**, 1–7.
10 P. J. Deuss, C. S. Lancefield, A. Narani, J. G. De Vries, N. J. Westwood and K. Barta, *Green Chem.*, 2017, **19**, 2774–2782.
11 T. Renders, S. Van Den Bosch, S. F. Koelewijn, W. Schutyser and B. F. Sels, *Energy Environ. Sci.*, 2017, **10**, 1551–1557.
12 S. Wang, W. X. Li, Y. Q. Yang, X. Chen, J. Ma, C. Chen, L. P. Xiao and R. C. Sun, *ChemSusChem*, 2020, **13**, 4548–4556.
13 R. El Hage, N. Brosse, P. Sannigrahi and A. Ragauskas, *Polym. Degrad. Stab.*, 2010, **95**, 997–1003.
14 C. G. Yoo, X. Meng, Y. Pu and A. J. Ragauskas, *Bioresour. Technol.*, 2020, **301**, 122784.
15 C. Lapierre, B. Monties, C. Rolando, C. Lapierre, B. Monties and C. Rolando, *J. Wood Chem. Technol.*, 1985, **5**, 277–292.
16 C. Lapierre, B. Monties and C. Rolando, *Holzforschung*, 1986, **113**, 113–118.
17 C. Rolando, B. Monties and C. Lapierre, *Res. Chem. Intermed.*, 1995, **21**, 397–412.
18 A. R. Robinson and S. D. Mansfield, *Plant J.*, 2009, **58**, 706–714.
19 M. Yamamura, T. Hattori, S. Suzuki, D. Shibata and T. Umezawa, *Plant Biotechnol.*, 2012, **29**, 419–423.
20 A. E. Harman-Ware, C. Foster, R. M. Happs, C. Doeppke, K. Meunier, J. Gehan, F. Yue, F. Lu and M. F. Davis, *Biotechnol. J.*, 2016, **11**, 1268–1273.
21 Q. Qi, J. Hu, L. Qu, X. Jiang, Y. Gai, S. A. Valenzuela and L. Qi, *MethodsX*, 2019, **6**, 2592–2600.
22 F. Chen, C. Zhuo, X. Xiao, T. H. Pendergast and K. M. Devos, *Biotechnol. Biofuels*, 2021, **14**, 1–9.
23 L. Yang, J. Wang, C. Wang, F. Yue and F. Lu, *Holzforschung*, 2022, **76**, 604–610.
24 F. Yue, F. Lu, R. C. Sun and J. Ralph, *J. Agric. Food Chem.*, 2012, **60**, 922–928.
25 T. Capoun and J. Krykorkova, *J. Anal. Methods Chem.*, 2020, (1), DOI: **10.1155/2020/8857210**.
26 A. Korban, R. Čabala, V. Egorov, Z. Bosáková and S. Charapitsa, *Talanta*, 2022, **246**, 123518.
27 C. W. Lahive, P. C. J. Kamer, C. S. Lancefield and P. J. Deuss, *ChemSusChem*, 2020, **13**(17), 4169–4770.
28 J. Piia, T. T. Ho, U. Kallavus, A. Konist, K. Leiman, O. Salm, M. Kulp, M. Koel and T. Lukk, *Materials*, 2022, **15**(8), 2861.
29 In *Eurachem Guide: The Fitness for Purpose of Analytical Methods: A Laboratory Guide to Method Validation and Related Topics*, ed. B. Magnusson and U. Örnemark, 2nd edn, 2014.
30 European Commission, *Off. J. Eur. Communities*, 2002.
31 M. Christiernin, A. B. Ohlsson, T. Berglund and G. Henriksson, *Plant Physiol. Biochem.*, 2005, **43**, 777–785.
32 J. Bergrath, J. Rumpf, R. Burger, X. T. Do, M. Wirtz and M. Schulze, *Macromol. Mater. Eng.*, 2023, **308**, 2300093.

Appendix 3

Publication III

Mahendra Kothottil Mohan, T. Tran Ho, Carmen Köster, Oliver Järvik, Maria Kulp, Yevgen Karpichev. Tuning ester derivatives of organosolv vs technical lignin for improved thermoplastic materials. Faraday Discussions 2026, https://doi.org/10.1039/D5FD00068H

Faraday Discussions
Cite this: DOI: 10.1039/d5fd00068h

PAPER

Tuning ester derivatives of organosolv *vs.* technical lignin for improved thermoplastic materials†

Mahendra Kothottil Mohan, ‡[a] T. Tran Ho, ‡[a] Carmen Köster,[a] Oliver Järvik, [b] Maria Kulp [a] and Yevgen Karpichev *[a]

Received 4th May 2025, Accepted 30th June 2025
DOI: 10.1039/d5fd00068h

In this study, lignin from two different sources – organosolv pine and hydrolysis birch – were chemically modified through esterification of hydroxyl groups using octanoyl (C8), lauroyl (C12), and palmitoyl (C16) chlorides, as well as through chloromethylation followed by esterification with tetradecanoic acid (C14) and benzoic acid. Modification of lignin was confirmed by FTIR and NMR spectroscopy. The esterified lignin samples were loaded into polylactic acid (PLA) at loadings of 10%, 20%, and 30% using a solvent casting method. Thermal and mechanical properties of PLA/lignin composites revealed that esterification significantly affected the polymer matrix properties. PLA could sustain as much as 30% lignin ester loading without affecting the film integrity. Among the variations, hydrolysis lignin ester (HLE) and benzoic acid ester (BAEP) enhanced the heat stability of PLA, while esterification with palmitoyl chloride (OHLE_C16) increased its elasticity through plasticization.

1. Introduction

Despite its abundance (up to 35%) and aromatic-rich structure, lignin receives much less attention in biorefineries compared to sugar derivatives in lignocellulosic biomass.[1,2] For instance, the downstream process primarily utilizes black liquor, which contains mostly lignin, for electricity production, a common scenario for every pulp and paper industry worldwide.[3] The difficulties arise in lignin's valorisation due to its heterogeneity of structure and properties that drastically change depending on the botanical origin, as well as the severity of the fractionation process. Lignin's chemistry significantly varies in the compositions of the three main monolignols, *p*-hydroxyphenyl (H), guaiacyl (G), and syringyl (S) (Fig. 1).[4] As

[a]*Department of Chemistry and Biotechnology, Tallinn University of Technology (TalTech), Akadeemia tee 15, 12618 Tallinn, Estonia. E-mail: yevgen.karpichev@taltech.ee; Fax: +372 620 2994; Tel: +372 620 4381*
[b]*Department of Energy Technology, Tallinn University of Technology (TalTech), Ehitajate tee 5, 19086 Tallinn, Estonia*

† Electronic supplementary information (ESI) available. See DOI: **https://doi.org/10.1039/d5fd00068h**
‡ These authors contributed equally to the publication.

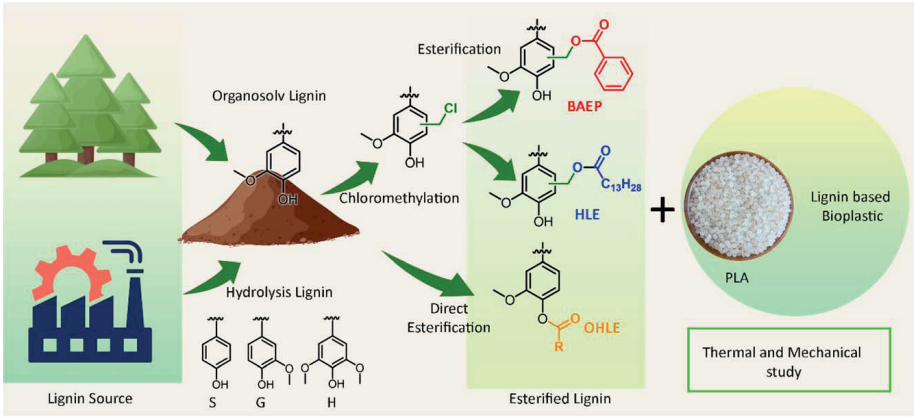

Fig. 1 Esterification of organosolv pine lignin and hydrolysis lignin in three different schemes and their compatibility study with PLA.

a conventional classification, softwood contains mostly guaiacyl units, and minor portions of *p*-hydroxyphenyl and syringyl; while, a hardwood's plant cell wall is predominantly composed of syringyl fragments, and a smaller quantity of guaiacyl; by contrast, all monolignols are present in non-woody biomass.[4,5] On an industrial scale, hydrolysis and organosolv pulping techniques are the two standard practices used to produce technical lignin. The former method focuses on using enzymatic treatment to liberate lignin from the recalcitrant biomass matrix, while the later employs aqueous organic solvents with or without a catalyst for the separation. The native lignin inevitably undergoes structural changes as a consequence of fractionation, which poses a challenge for its high-value-added applications.

Bio-derived polymers face several challenges, including poor interfacial adhesion with synthetic polymers, variations in purity due to differences in raw material sources, and complex extraction processes. These factors can hinder consistent material performance and limit broader applicability.[6] Lignin is a promising candidate for biocomposite production, due to its aromatic structure and high carbon content. The phenolic hydroxyl, carboxyl, and methoxy groups in lignin can be chemically modified to improve its compatibility with a variety of polymers. In recent decades, researchers have been focusing on potential application of lignin in various fields, including automotive components, bioplastics, adhesives, and antimicrobial packaging materials.[7–9] From a sustainability standpoint, lignin and its derivatives present a promising alternative to fossil-based plastics, helping to reduce reliance on petroleum-derived resources while promoting the development of bio-based materials.

Nevertheless, its structural complexity makes direct utilization challenging, which necessitates chemical modification to enhance its functionality and integration. Common modification strategies for lignin include depolymerization, the introduction of new reactive sites, and the functionalization of hydroxyl groups.[7] Techniques such as acetylation, esterification, and phenolation have been widely investigated.[8] Initial attempts to incorporate unmodified lignin into polypropylene often resulted in increased material stiffness but decreased tensile strength and elongation.[9] These drawbacks were primarily due to poor compatibility, specifically the weak adhesion between polar lignin and non-polar

polymers, which is attributed to strong self-interaction driven by inter- and intra-hydrogen bonding, causing lignin particles to agglomerate and act as stress concentrators within the composite.[10] Such limitations underscore the need for suitable chemical modifications to realize lignin's potential in polymer applications completely.[11,12] In contrast, acetylated lignin displays decreased hydrogen bonding because acetyl groups replace the hydroxyl groups during the acetylation. This modification makes acetylated lignin more hydrophobic and enhances its solubility in specific organic solvents.[13]

Esterification is the most frequently chosen pathway among different approaches to improve the thermoplasticity of lignin *via* chemical modification of hydroxy groups.[14] Those functional groups present as one of the significant active sites in lignin that can be functionalized with long-chain hydrocarbons, resulting in materials with improved thermoplasticity, flexibility of the polymer chain, hydrophobicity, and miscibility in nonpolar solvents as a consequence.[15] In a typical fashion, the synthesized material could be obtained by direct esterification with carboxylic acids,[16] acid anhydrides[17] or acid chlorides[18,19] in the presence of suitable catalysts. Recently, we have reported the development of a novel approach to esterify lignin *via* chloromethylation onto the aromatic rings at either the *ortho* or *meta*-position.[20] As an intermediate product, chloromethylated lignin (Fig. 1) offers highly reactive sites towards a variety of functionalization possibilities in which esterification using carboxylic acid is favourable. The obtained material has been successfully studied as a co-polymer blended with polylactic acid (PLA) for 3D printing purposes.[21]

In this work, we present a systematic comparison of two distinct esterification strategies for lignin modification: (i) direct esterification of hydroxyl groups using fatty acid chlorides, and (ii) a two-step process involving chloromethylation followed by reaction with carboxylic acids. The modified lignin samples were blended with polylactic acid (PLA) at varying ratios to assess compatibility and composite performance (Fig. 1). Additionally, the impact of hydrocarbon chain chemistry, such as saturated fatty acids and aromatic acids (*e.g.*, benzoic acid), on the physicochemical properties of the resulting lignin/PLA composites was examined. Two types of lignin were used: hydrolysis lignin from birch (a hardwood) and organosolv lignin from pine (a softwood) to highlight the broad potential of lignin for functionalization and application. The obtained materials were characterized using Fourier transform infrared spectroscopy (FT-IR), phosphorus nuclear magnetic resonance (^{31}P NMR), and 2D heteronuclear single quantum coherence (2D-HSQC). Additionally, the resulting biocomposites were characterized using differential scanning calorimetry (DSC), thermogravimetric analysis (TGA), and mechanical testing.

2. Materials and methods

2.1. Materials

PLA-Ingeo 3D850 from NatureWorks LLC-US, chloroform (99%), lauroyl chloride (98%), triethylamine, octanoyl chloride (99%), and palmitoyl chloride (98%) were purchased from Thermo Fischer Scientific. $CDCl_3$ and DMSO-d_6 from Eurisotop, as well as all reagents used, were of analytical reagent (AR) grade and were procured from Sigma-Aldrich (Taufkirchen, Germany). They were employed without further purification. Four distinct birch-derived hydrolysis lignin (HL)

samples were obtained from Fibenol OÜ (Estonia). The lignin was classified as hydrolysis lignin due to its production process, which involves enzymatic treatment. Longitudinally sawn pine timber sawdust was sourced from Prof. Jaan Kers (Tallinn University of Technology, Tallinn, Estonia).

The preparation of the biomass and organosolv lignin were carried out as described in an earlier study.[22]

2.2. Chloromethylation and esterification of lignin

The chloromethylation of organosolv lignin and hydrolysis lignin were carried out following our previously established procedure.[20] Esterification with benzoic acid was carried out by dissolving 2 g (1 eq.) of benzoic acid and 1.48 g (1 eq.) of K_2CO_3 in 20 mL of THF. The reaction mixture was heated to 70 °C and was maintained at this temperature for 1 hour. Subsequently, 66 mg of KI and 2 g of chloromethylated lignin (previously dissolved in 30 mL of THF) was added. The mixture was then refluxed overnight. After the reaction was completed, the mixture was cooled to room temperature, and the solvent was removed under reduced pressure. The residue was extracted using an ethyl acetate–water system. The organic layer was washed successively with a saturated $NaHCO_3$ solution, water, and brine, then dried over anhydrous Na_2SO_4. Finally, the solvent was removed under reduced pressure, and the product was precipitated in hexane. Esterification of the hydrolysis lignin with tetradecanoic acid was carried out following our previously published procedure.[21]

2.3. Chlorine content *via* XRF analysis

X-ray fluorescence (XRF) spectroscopy was used for the determination of chlorine content in chloromethylated lignin. Quantitation was performed using a Bruker S4 PIONEER wavelength-dispersive XRF spectrometer using an Rh anode under vacuum. Lignin samples were pressed into pellets to ensure homogeneity. Chlorine analysis was performed with a PET crystal and with Bruker's pre-calibrated methodology. The theoretical maximum chlorine content of 15.4 wt% was computed from the chloromethylated guaiacyl (G) unit (229.45 g mol^{-1}) to facilitate the evaluation of the efficiency of chloromethylation *via* mass-to-mass comparison with the XRF data.

2.4. Lignin–OH groups esterification

The direct esterification of organosolv lignin, *via* its hydroxyl groups, was prepared as reported.[23] 1 g of lignin was weighed and dissolved in a 100 mL round-bottom flask containing 10 mL of dry THF. Later, 300 μL of triethylamine (TEA, 1.5 eq. to total OH groups, 2.87 mmol g^{-1} of lignin[22]) was added and mixed for 10 minutes. The mixture was then kept in an ice bath for 10 minutes, and fatty acid chlorides (367 μL of octanoyl-C8, 506 μL of lauroyl-C12, or 657 μL of palmitoyl-C16 chlorides) (1.5 equivalents to the total OH groups) were added.[22] The reaction was carried out at room temperature for 4 hours, under vigorous stirring. Upon completion, 50 mL of chloroform was added, and the mixture was transferred to a separatory funnel for liquid–liquid extraction using 30 mL of a 5% sodium hydroxide solution. The organic layer was gathered, and the solvent was evaporated to collect the modified lignin. The final materials were washed three times with 50 mL of 100% ethanol to remove unwanted by-products. The esterified lignin samples were freeze-dried to remove all solvent residue.

2.5. PLA/lignin film preparation

PLA was separately dissolved in DCM in a 15 mL glass vial. Lignin was dissolved in THF at room temperature and then mixed to achieve a lignin content of 10% to 30% w/w. Our previous study[21] showed that at 40% lignin esters with PLA, a reduction in T_g was observed. Based on these results, we have considered only up to 30% as the maximum in this work. The dissolved components were combined in a Petri dish and allowed to dry overnight. After the initial drying phase, the composite material underwent further drying in a vacuum oven at 40 °C for an additional 12 hours.

2.6. Fourier transform infrared spectroscopy (FT-IR)

The infrared spectra of the lignins were recorded by IRTracer-100 (Shimadzu, Japan). The measurements were conducted in two modes: diffuse reflection and attenuated total reflection (ATR). All spectra were recorded in the range of 4000–400 cm^{-1} for 80 scans.

2.7. Nuclear magnetic resonance (NMR)

NMR analysis was measured as ^{31}P for determination of the hydroxyl contents and 2D-heteronuclear single quantum coherence (2D-HSQC) for structural characterization. For the ^{31}P experiment, approximately 30 mg of lignin was dissolved in 500 μL of pyridine and $CDCl_3$ (1.6 : 1 v/v). Upon solubilization, 100 μL of the internal standard (*N*-hydroxy-5-norbornene-2,3-dicarboximide, 20 mg mL^{-1}) and 100 μL of relaxation agent (chromium(III) acetyl-acetonate, 5 mg mL^{-1}), which were prepared in the same mixture of pyridine and chloroform, were added to the vial containing the solubilized lignin. Finally, 70 μL of 2-chloro-4,4,5,5-tetramethyl-1,3,2-dioxaphospholane, and a phosphorus derivatization reagent, were added. ^{31}P data were acquired at 25 °C using an inverse gated decoupling pulse sequence (zgig), with 1500 scans, on a Bruker Avance III 400 MHz spectrometer. Data acquisition for 2D-HSQC was carried out on the hydrolyzed lignin and its derivatives. 40 mg of the samples were dissolved in 600 μL of DMSO-d_6. Experimental data were achieved using a Bruker Avance III 800 MHz spectrometer with hsqcetgpsisp2.2 pulse sequence, four scans. Data analysis was assisted by the MestReNova software.

2.8. Differential scanning calorimetry

Differential scanning calorimetry (DSC) was performed using a PerkinElmer DSC 6000 calorimeter with an IntraCooler II as the cooling system at a constant heating rate of 10 °C min^{-1} in a pure nitrogen atmosphere (purity 99.999%, purge at 20 mL min^{-1}). A sample mass of 5 mg ± 2 mg was used for all materials. Samples were pressed into the aluminium crucible using the aluminium lid to improve contact between the material and the crucible.

2.9. Thermogravimetry

Thermogravimetric analysis (TGA) was performed using a NETZSCH STA 449 F3 Jupiter® apparatus. The samples were heated in a pure nitrogen atmosphere (purity 99.999%, purge at 40 mL min^{-1}) from 25 °C to 400 °C at a constant heating

rate of 10 °C min^{-1}. The mass of the samples was 4.8 ± 0.9 mg. Aluminium crucibles were used.

2.10. Mechanical testing

Biocomposites were tested mechanically using an Instron 5866 instrument (ASTM D638 standard) (Instron, US) and a load cell of 2.5 kN (force sensor capable of measuring up to 2.5 kN of force). A grip distance of 30 mm was used for a 10 mm wide film.

3. Results and discussion

3.1. Characterization of lignin and its modification

We previously demonstrated the esterification followed by chloromethylation of pine lignin, and the same methodology was applied to hydrolysis lignin. NMR proved the chloromethylation procedure to be as efficient for in-house lignin as it was for *in situ* extracted pine lignin. In the ^{1}H NMR spectra, the characteristic peak at 4.5–4.75 ppm (Fig. S1 and S2†) confirms the presence of CH_2–Cl. For further confirmation, 2D-HSQC measurement with a higher order in dimension that offers a deeper understanding of lignin structure (*e.g.*, inter-unit linkages, and subunits) was analysed for the hydrolysis of birch lignin.[24,25] As a rule of thumb for the 2D-HSQC interpretation of lignin, focused on two major informative areas: (i) the oxygenated aliphatic side chain (C/H 100–35/6–2.5 ppm), (ii) aromatic or unsaturated carbon (C/H 150–100/8.0–6.0 ppm). All the spectra were calibrated at the solvent signal of DMSO-d_6 (C/H 39.51/2.50 ppm). As a result, the new reactive groups were successfully introduced onto aromatic rings in lignin, as verified by two distinct cross-peaks appearing at C/H 37.97/4.8 and 40.61/4.63 ppm, marked as an asterisk in Fig. 2c, compared to those of the starting material (Fig. 2a). Since the introduction of new functional groups could occur at either the *ortho* or *meta*-position, it explains the emergence of two distinguishable signals in the HSQC spectra. This observation was consistent with the previous ^{1}H NMR data. Methoxy is one of the most abundant functional groups in lignin, which supply the intense and stable cross signal at C/H 55.62/3.77 ppm before and after chemical modification, however, the ether linkage (β-O-4′) peaks ($A_{\beta(S)}$: C/H 86.06/4.11) undergo substantial decrease in chloromethylation-modified lignin. This can be explained by the fact that the acidic media used in the chloromethylation step depolymerized lignin into smaller fragments by breaking down the labile bond, as also evidenced in our previous study.[20] Moving to the aromatic area of the HSQC spectra, they were strongly indicated by the cross signals of the S and G units as two main monolignols in the hardwood species at C/H 104.30/6.60 and 118.5–110.11/6.90–6.76 ppm, respectively[26] (Fig. 2b). After chloromethylation (Fig. 2d), the intensity of all these peaks drastically declines, confirming that the substitution occurred on the aromatic rings, as per our hypothesis. It is worth noting that, despite the higher degree of methoxylation in S than G units, steric hindrance was not a barrier for introducing new functional groups onto other positions on S-rings.

On the other hand, a ^{31}P NMR measurement was employed to investigate the impact of the esterification process on the –OH groups through the two pathways: using acid chlorides targeting hydroxy groups, and chloromethylation followed by

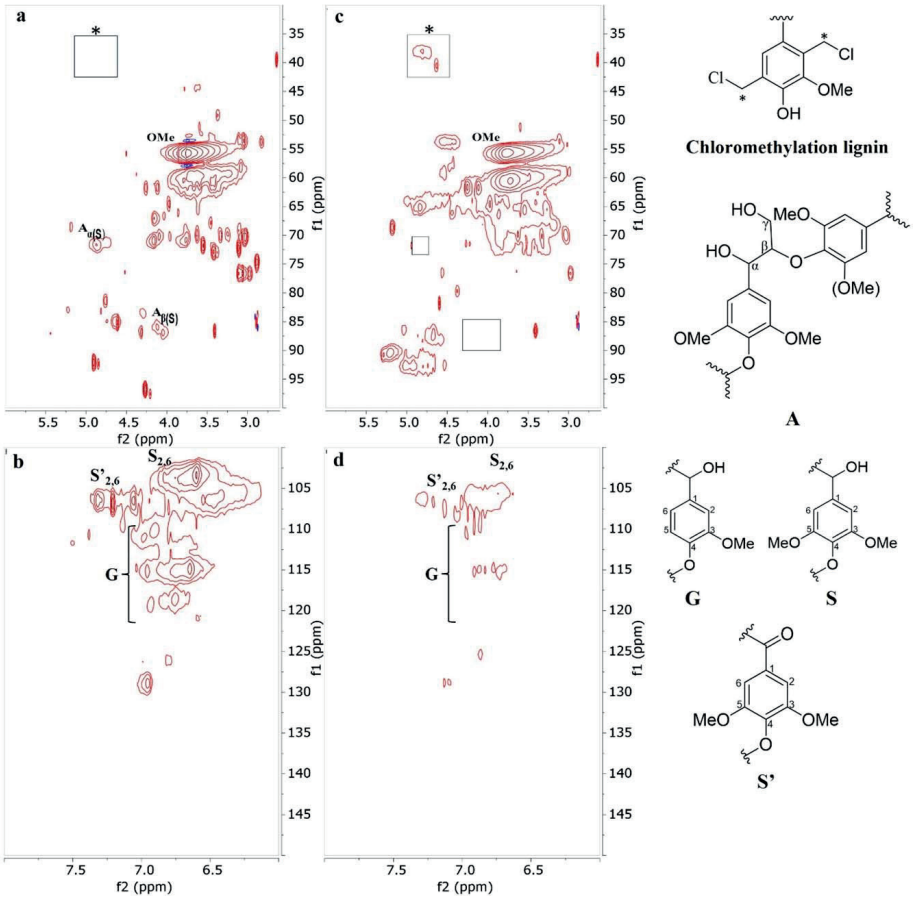

Fig. 2 2D-HSQC of hydrolysis lignin (a and b), chloromethylation lignin (c and d). Two regions of investigation: oxygenated aliphatic side chain (C/H 100–35/6.0–2.5 ppm) (top), aromatic/unsaturated region (C/H 150–100/8.0–6.0 ppm) (bottom). The lignin's subunits are shown on the right side.

esterification. All the spectra were referenced at the internal standard signal of 151.8 ppm before analysis. As a softwood species, phenolic hydroxy groups were predominantly found for G and H units (Fig. S3a†).[27] These functional groups were expected to be consumed in the direct esterification approach, as shown in Fig. S3b,† which shows a significant decrease. At the same time, aliphatic hydroxyl groups show a slight change. In the chloromethylated sample (Fig. S3c†), there is a profound shift of the origin of OH groups from G units towards the regions of condensed OH (from around 139.0 to 144.0 ppm). Still, it does not disappear, as observed in the first case. The shifting can be explained by two facts: (i) the attachment of chloromethyl to aromatic rings of lignin mimic a similar structure of condensed lignin, (ii) the electronegativity of chloride atoms contributes to the decrease of electron density on the aromatic rings, which causes the shifting towards lower field or higher chemical shift. Later, the grafting of benzoic acid was confirmed by the shift of the signal at approximately 144.0 ppm to a lower chemical shift of 142.4 ppm (Fig. S3d†), indicating that the electronegative groups

were replaced successfully, resulting in a balance in electron density due to the attachment of a conjugation system.

XRF analysis further confirms that 13.3% and 13.6% of chlorine is present in the chloromethylated hydrolysis lignin and organosolv pine lignin, respectively. The esterification reaction was confirmed through ^{1}H NMR. A comparison study revealed the disappearance of the chloromethylated peak (ph–CH_2–Cl) and the emergence of a new peak (ph–CH_2–O), corresponding to the methylene moieties, indicating the formation of the ester (HLE) (Fig. S1†).

The esterification of hydrolysis lignin with tetradecanoic acid (HLE) was confirmed by the enhanced intensity of the two bands around 2918 and 2846 cm^{-1}, which are attributed to CH_2 stretching vibrations in the methyl and methylene groups of the ester side chains (Fig. 3a). Additionally, a slightly merged absorption band at 1734 cm^{-1} corresponds to C=O stretching vibrations, while the band at 1575 cm^{-1} and 1541 cm^{-1} is associated with aromatic skeletal vibrations in lignin, as shown in Fig. 3a. The complex and heterogeneous structure of lignin, with aromatic moieties, makes it challenging to differentiate between peaks arising from native lignin and those introduced through esterification with benzoic acid. The absorption bands arising at 1740 cm^{-1} and 1464 cm^{-1} correspond to the ester C=O and aromatic stretching vibrations. The C–H deformation vibration absorption at 713 cm^{-1}, typical of monosubstituted benzene compounds, will confirm the benzoic acid ester (BAEP) in Fig. 3b.

For all the direct esterification samples using fatty acid chlorides (C8, C12, C16) (Fig. 3c), the successful modification was confirmed by the appearance of two characteristic signals at 1740 cm^{-1} and 1760 cm^{-1} representing aliphatic and

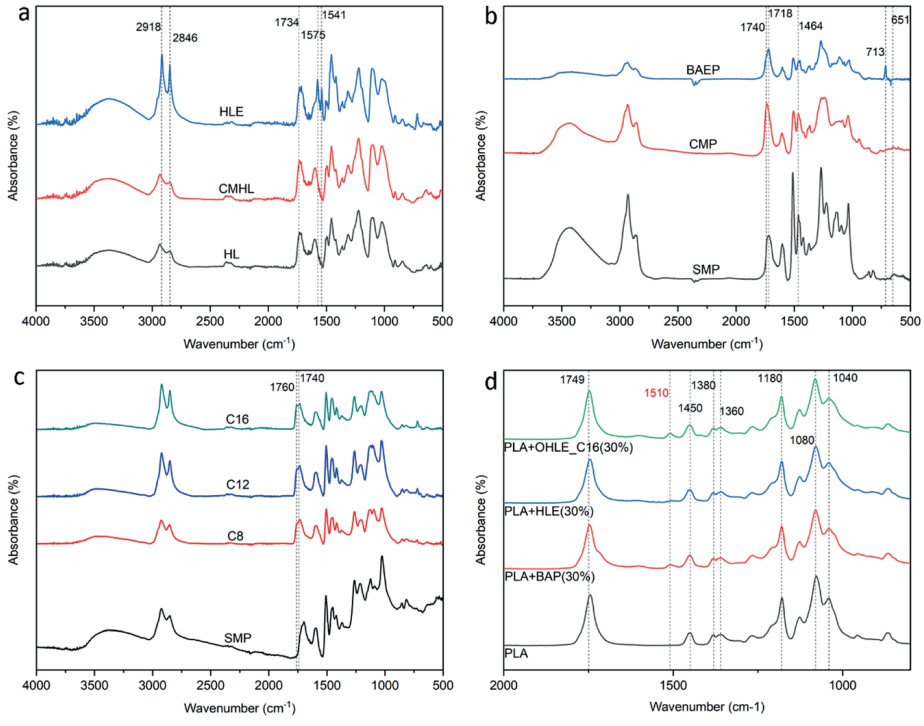

Fig. 3 FT-IR measurements for hydrolysis lignin esters (HLE) (a), lignin benzoic acid ester (BAEP) (b), direct esterified lignin (OHLE) derivatives (c), and PLA/lignin ester films (d).

aromatic esters, respectively.[28] Moreover, the OH stretching vibration band at 3440 cm^{-1} experienced an incremental decline, which further verifies the consumption of hydroxy groups during the esterification. The variation in attached hydrocarbon chain length (from C8 to C16) was observed as a slight increase within the region of aliphatic C–H stretching 2918–2846 cm^{-1}. The work-up procedure was proven to be efficient as the absence of a carbonyl chloride (Cl–C=O) signal at 1800 cm^{-1}, which originates from unreacted acid chloride,[29] indicated that no side products were detected.

The FT-IR spectra of PLA/lignin composites showed the characteristic band of neat PLA (Fig. 3d). The prominent peak at 1749 cm^{-1} is attributed to C=O stretching vibrations, and that at 1450 cm^{-1} is due to antisymmetric bending of CH_3 groups. Peaks associated with deformation and bending vibrations of CH groups appear at 1380 cm^{-1} and 1360 cm^{-1}. C–O–C stretching vibrations are present at 1180, 1080, and 1040 cm^{-1}. A weak band at 1510 cm^{-1} for C=C stretching of an aromatic ring was observed in the biocomposites with lignin.

3.2. Thermal behaviour: DSC, TG, and DTG of esterified lignin/PLA composite

The thermal properties of PLA can be systematically altered by incorporating modified lignin at different loadings. Our previous study explored changes in T_g of PLA loaded with organosolv pine lignin modified with fatty acids. Lignin tetradecanoic acid (C14) at 30% was found to provide the maximum improvement in the glass transition temperature.[21] Similarly, PLA with hydrolysis lignin esters (HLE) resulted in a gradual increase in the glass transition temperature (T_g) from 66 °C to 70 °C, as the concentration increases from 10% to 30%, while reducing C_p values, indicating enhanced thermal stability of the glassy phase and flexibility of the polymer matrix (Fig. 4a). In contrast, phenolic-OH esterified lignin (OHLE) mixed with PLA exhibited various trends depending on the alkyl chain length. OHLE_C8 and OHLE_C12 showed T_g values close to PLA but moderately increased ΔC_p, suggesting balanced flexibility. Remarkably, OHLE_C16 reduces both T_g (down to 55 °C) and ΔC_p, as shown in Fig. 4b, indicating a strong plasticization effect. Benzoic acid ester lignin (BAEP) with PLA exhibited an increase in T_g, reaching 70 °C at a 30% loading, accompanied by a moderately rising ΔC_p, indicating improved thermal properties at higher concentrations. Thus, the results of the present study suggest that HLE-30%, OHLE_C16-30%, and BAEP-30% should be chosen for further studies.

The thermogravimetric (TG) data (Fig. 4c) reveal the thermal stability of the PLA/lignin esters. All samples show a gradual decrease in mass with increasing temperature. Mass loss occurs in two separate temperature ranges, initiating at around 80 °C and again at approximately 245 °C. The mass loss observed at 80 °C is due to the evaporation of humidity and chemically bound water. Significant thermal decomposition begins at 245 °C, marking the onset of substantial degradation, with the degradation rate increasing with the temperature rise. Among them, PLA, BAP-30%, and HLE-30% exhibit a similar trend of degradation, while the OHLE_C16-30% sample shows the lowest thermal stability. However, BAP-30% shows a slightly higher mass loss at temperatures preceding thermal degradation onset. The differential thermogravimetric (DTG) analysis (Fig. 4d) reveals the differences in thermal degradation behavior. BAP-30% exhibits slightly higher DTG values at the intermediate temperature range of 80 °C

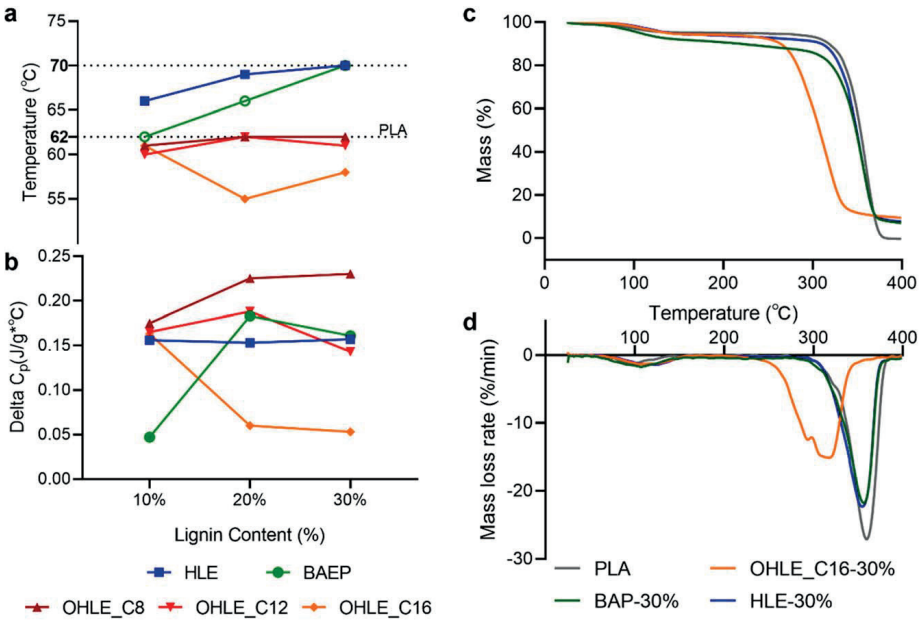

Fig. 4 Glass transition temperature (a), delta C_p (b), thermogravimetric (c), and differential thermogravimetric (d) studies for PLA/lignin film.

to 120 °C. OHLE_C16-30% exhibits an early degradation trend, whereas HLE-30% and BAP-30% display similar DTG trends to PLA. These results suggest that the OHLE_C16-30% is the least thermally stable, due to the lack of phenolic hydroxyl groups to form hydrogen bonds. In contrast, esterification through chloromethylation provides the free hydroxyl groups, which are likely to have stronger intermolecular interactions and result in a more thermally stable structure.

Overall, compared to the thermal properties of common fossil-based plastics like polyethylene terephthalate (PET, T_g 70–87 °C),[30] all esterified lignin/PLA composites show slightly lower glass transition temperatures (T_g 55–70 °C). The same applies to the selected loading at 30% of modified lignin (OHLE C16, BAP, and HLE) with PLA (T_g 58–70 °C).

3.3. Mechanical properties

Based on the DSC properties, neat PLA and its composites with 30 wt% lignin esters (HLE, OHLE_C16, and BAEP) were examined for tensile properties, and are listed in Fig. 5 and Table S1.† The neat PLA film exhibited the maximum load (15.2 ± 2 N) (Fig. 5a), indicating greater load-carrying capacity compared to other modified composites. Significantly, the PLA + HLE (30%) composite showed reduced maximum load (8.5 ± 2 N) yet the highest tensile stress among all other modified composites (Fig. 5b), which shows improvement in the strength of the material in terms of cross-sectional area after the addition of HLE. In contrast, PLA + OHLE_C16 (30%) and PLA + BAEP (30%) composites exhibited lower maximum loads and tensile stresses, with PLA + BAEP (30%) recording the lowest tensile stress, indicating a loss of strength.

Tensile extension to the maximum increased upon lignin ester addition (Fig. 5c), showing enhanced ductility of the composite materials. Maximum

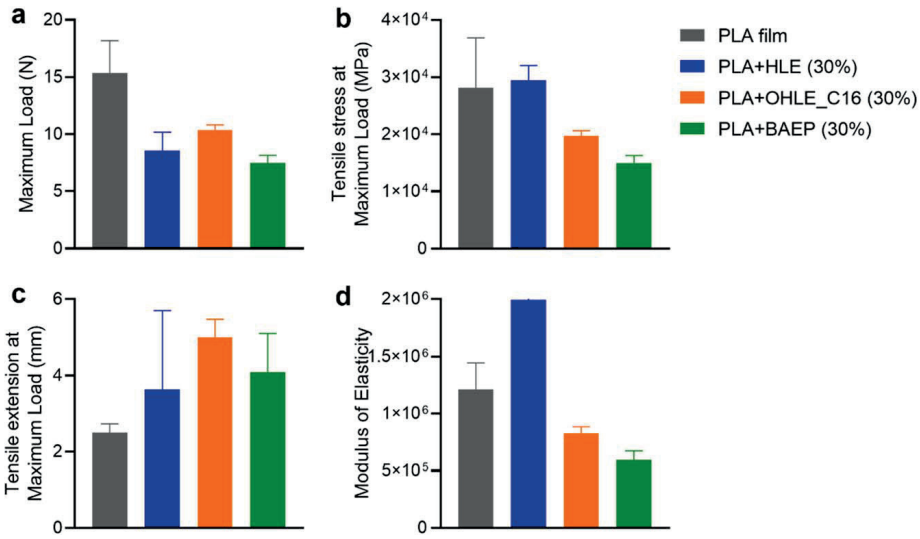

Fig. 5 (a) Maximum load, (b) tensile stress at maximum load, (c) tensile extension at maximum load, (d) Young's modulus of PLA/lignin film.

elongation was observed for PLA + OHLE_C16 (30%), followed by PLA + HLE and PLA + BAEP, while neat PLA had the minimum extension. This shows that the addition of lignin esters reduces the brittleness of the PLA matrix and enhances its flexibility. The most structurally similar commercial plastic derived from fossil fuel resources, polystyrene (PS), has tensile strength ranging from 35 to 51 MPa,[30] which is lower than PLA itself. This transitive comparison proves that the composite consists of PLA and 30% HLE is a promising material to replace fossil-based plastic.

The modulus of elasticity (Fig. 5d), being a measure of material stiffness, was greatly influenced by the form of lignin ester used. PLA + HLE (30%), followed by neat PLA, possessed the largest modulus, thereby indicating increased stiffness by incorporating HLE. Both the other composites, namely PLA + OHLE_C16 (30%) and PLA + BAEP (30%), exhibit a lower modulus, indicating a softening effect on the PLA matrix.

In conclusion, the mechanical characteristics of PLA composites depend to a great extent on the nature of the incorporated lignin ester. Among the under-examined samples, PLA + HLE (30%) exhibited higher tensile stress and stiffness, and is therefore most suitable for applications requiring enhanced mechanical strength and rigidity. PLA + OHLE_C16 (30%) improved ductility at the expense of strength and stiffness, making it ideal for more elastic applications. PLA + BAEP (30%) possessed the worst mechanical properties, suggesting minimal structural reinforcement. This result demonstrates the tunability of the mechanical properties of PLA through lignin ester modification and the potential of HLE as an effective reinforcing agent.

4. Conclusions

Lignin isolated by two different processes – organosolv and hydrolysis – were chemically modified through direct esterification at the hydroxyl groups and

esterification *via* chloromethylation. The resulting lignin esters were subsequently characterized and incorporated into PLA at varying concentrations (10%, 20%, and 30%) using the solvent casting technique. Thermal and mechanical analysis of the blended composites revealed that the introduction of ester moieties into lignin affects the thermal and mechanical behaviour of the polymer matrix. Notably, PLA was able to accommodate up to 30% of lignin esters. Among the modifications, HLE and BAEP modifications improve the thermal characteristics of PLA, whereas OHLE_C16 provides enhanced flexibility through plasticization. These results underscore that the overall characteristics of PLA composites strongly depend on the type of lignin ester introduced. The results demonstrate the potential for tailoring the thermal and mechanical properties of PLA through selective lignin esterification approaches, offering a promising avenue for the production of high-performance, sustainable bioplastics.

Data availability

The following data associated with this work can be found in the ESI.† ^{1}H NMR spectra of hydrolysis lignin (HL), chloromethylated hydrolysis lignin (CMHL), and hydrolysis lignin esters (HLE) (Fig. S1†); ^{1}H NMR spectra of organosolv pine lignin (OPL), chloromethylated pine lignin (CMPL), and benzoic acid ester pine (BAEP) (Fig. S2†); ^{31}P NMR spectra of organosolv pine lignin (a), C16 ester modified OH of pine lignin (b), chloromethylated pine lignin (c), and benzoic acid ester pine (d) (Fig. S3†); the tensile properties of neat PLA and its composites with 30 wt% lignin esters (HLE, OHLE_C16, and BAEP) (Table S1†).

Author contributions

The manuscript was written through the contributions of all authors. All authors have approved the final version of the manuscript. Mahendra K. Mohan: conceptualization; methodology; investigation – organosolv extraction, chemical modification, characterization, thermal and mechanical testing; validation; data curation; visualization; writing – original draft preparation. Tran Ho: methodology; investigation – organosolv lignin extraction, esterification, characterisation, NMR analysis; validation; data curation; writing – original draft preparation. Carmen Köster: investigation – technical lignin characterisation and modification; validation; data curation; writing – original draft preparation. Oliver Järvik: investigation – thermal analysis; validation; data curation; writing – reviewing and editing. Maria Kulp: methodology, writing – reviewing and editing. Yevgen Karpichev: conceptualization, methodology; resources; funding acquisition; writing – reviewing and editing; project administration.

Conflicts of interest

The authors declare that they have no known competing financial interests or personal relationships that could have appeared to influence the work reported in this paper.

Acknowledgements

The Estonian Research Council supported this work *via* project TEM-TA49. The valuable technical support of Dr Illia Krasnou, Dr Marina Kudrjašova, and Dr Indrek Reile is gratefully acknowledged. The authors acknowledge Muhammad Afaq Khan for organosolv lignin extraction.

References

1 R. Shorey, A. Salaghi, P. Fatehi and T. H. Mekonnen, *RSC Sustainability*, 2024, **2**, 804–831.
2 J. Ralph, C. Lapierre and W. Boerjan, *Curr. Opin. Biotechnol.*, 2019, **56**, 240–249.
3 S. Sethupathy, G. Murillo Morales, L. Gao, H. Wang, B. Yang, J. Jiang, J. Sun and D. Zhu, *Bioresour. Technol.*, 2022, **347**, 126696.
4 V. K. Ponnusamy, D. D. Nguyen, J. Dharmaraja, S. Shobana, J. R. Banu, R. G. Saratale, S. W. Chang and G. Kumar, *Bioresour. Technol.*, 2019, **271**, 462–472.
5 A. V. Faleva, A. Yu. Kozhevnikov, S. A. Pokryshkin, D. I. Falev, S. L. Shestakov and J. A. Popova, *J. Wood Chem. Technol.*, 2020, **40**, 178–189.
6 J. Sameni, S. A. Jaffer and M. Sain, *Composites, Part A*, 2018, **115**, 104–111.
7 P. Figueiredo, K. Lintinen, J. T. Hirvonen, M. A. Kostiainen and H. A. Santos, *Prog. Mater. Sci.*, 2018, **93**, 233–269.
8 F. Taleb, M. Ammar, M. ben Mosbah, R. ben Salem and Y. Moussaoui, *Sci. Rep.*, 2020, **10**, 11048.
9 R. Pucciariello, V. Villani, C. Bonini, M. D'Auria and T. Vetere, *Polymer*, 2004, **45**, 4159–4169.
10 D. Kun and B. Pukánszky, *Eur. Polym. J.*, 2017, **93**, 618–641.
11 C. Wang, S. S. Kelley and R. A. Venditti, *ChemSusChem*, 2016, **9**, 770–783.
12 E. A. Agustiany, M. Rasyidur Ridho, M. Rahmi D. N., E. W. Madyaratri, F. Falah, M. A. R. Lubis, N. N. Solihat, F. A. Syamani, P. Karungamye, A. Sohail, D. S. Nawawi, A. H. Prianto, A. H. Iswanto, M. Ghozali, W. K. Restu, I. Juliana, P. Antov, L. Kristak, W. Fatriasari and A. Fudholi, *Polym. Compos.*, 2022, **43**, 4848–4865.
13 U. Hwang, B. Lee, B. Oh, H. S. Shin, S. S. Lee, S. G. Kang, D. Kim, J. Park, S. Shin, J. Suhr, S.-H. Kim and J.-D. Nam, *Eur. Polym. J.*, 2022, **165**, 110971.
14 S. Laurichesse and L. Avérous, *Prog. Polym. Sci.*, 2014, **39**, 1266–1290.
15 A. Lisý, A. Ház, R. Nadányi, M. Jablonský and I. Šurina, *Energies*, 2022, **15**, 6213.
16 P. Hafezisefat, L. Qi and R. C. Brown, *ACS Sustain. Chem. Eng.*, 2023, **11**, 17053–17060.
17 S. N. Pawar, R. A. Venditti, H. Jameel, H.-M. Chang and A. Ayoub, *Ind. Crops Prod.*, 2016, **89**, 128–134.
18 O. Gordobil, E. Robles, I. Egüés and J. Labidi, *RSC Adv.*, 2016, **6**, 86909–86917.
19 O. Gordobil, I. Egüés and J. Labidi, *React. Funct. Polym.*, 2016, **104**, 45–52.
20 M. K. Mohan, O. Silenko, I. Krasnou, O. Volobujeva, M. Kulp, M. Ošeka, T. Lukk and Y. Karpichev, *ChemSusChem*, 2024, **17**, e202301588.
21 M. K. Mohan, I. Krasnou, T. Lukk and Y. Karpichev, *ACS Omega*, 2024, **9**, 44559–44567.
22 P. Jõul, T. T. Ho, U. Kallavus, A. Konist, K. Leiman, O.-S. Salm, M. Kulp, M. Koel and T. Lukk, *Materials*, 2022, **15**, 2861.

23 E.-L. Hult, J. Ropponen, K. Poppius-Levlin, T. Ohra-Aho and T. Tamminen, *Ind. Crops Prod.*, 2013, **50**, 694–700.
24 J.-L. Wen, S.-L. Sun, B.-L. Xue and R.-C. Sun, *Materials*, 2013, **6**, 359–391.
25 T.-Q. Yuan, S.-N. Sun, F. Xu and R.-C. Sun, *J. Agric. Food Chem.*, 2011, **59**, 10604–10614.
26 Z. Wang and P. J. Deuss, *ChemSusChem*, 2021, **14**, 5186–5198.
27 L. Lagerquist, A. Pranovich, I. Sumerskii, S. von Schoultz, L. Vähäsalo, S. Willför and P. Eklund, *Molecules*, 2019, **24**, 335.
28 K. A. Y. Koivu, H. Sadeghifar, P. A. Nousiainen, D. S. Argyropoulos and J. Sipilä, *ACS Sustain. Chem. Eng.*, 2016, **4**, 5238–5247.
29 R. Shorey and T. H. Mekonnen, *Int. J. Biol. Macromol.*, 2023, **230**, 123143.
30 F. Luzi, L. Torre, J. M. Kenny and D. Puglia, *Materials*, 2019, **12**, 471.

Curriculum vitae

Personal data

Name:	Hồ Thị Thùy Trân (T.Tran Ho)
Date of birth:	22/04/1995
Place of birth:	Ho Chi Minh city, Vietnam
Citizenship:	Vietnamese

Contact data

E-mail:	hothithuytran@gmail.com

Education

2021–2025	Tallinn University of Technology, Estonia, PhD
2019–2021	Umeå University, Sweden, MSc (Analytical Chemistry and Material Science)
2013–2017	Ho Chi Minh University of Industry and Trade, Vietnam, BSC (Analytical Chemistry)
2010–2013	Bui Thi Xuan high school, Ho Chi Minh, Vietnam

Language competence

Vietnamese	Native
English	Fluent
Mandarin Chinese	B1

Professional employment

2017–2019	Minh Long Ltd., Long An province, Vietnam, QA/QC

Short study visit

2022	LignoCOST CA17128 training school, Åbo Akademi, Finland
2022	International School of Chemometrics, University of Copenhagen, Denmark

Honours and awards

2022	Dora Plus short study visit scholarship (T1.1)
2019–2021	A selected candidate for MSc program, Umeå University, Sweden
2016–2017	Annual bachelor scholarship, Ho Chi Minh University of Industry and Trade, Vietnam
2013	Outstanding student, Bui Thi Xuan high school, Ho Chi Minh, Vietnam

Supervision

2022–2023	Co-supervision of Bioceb (Green line project for MSCs)
2024–2025	Supervision of Bachelor's thesis – 'Ash-free kraft lignin production technology development' – Hanna-Martha Heinla
Summer 2025	An internship adviser – 'Lignin valorization by sequential solvent fractionation' – Nemo Hennequart

Elulookirjeldus

Isikuandmed

Nimi:	Hồ Thị Thùy Trân (T.Tran Ho)
Sünniaeg:	22/04/1995
Sünnikoht:	Ho Chi Minh, Vietnam
Kodakondsus:	Vietnami kodakondsus

Kontaktandmed

E-post:	hothithuytran@gmail.com

Hariduskäik

2021–2025	Tallinna Tehnikaülikool, Eesti, PhD
2019–2021	Umeå University, Rootsi, MSc (Analüütiline keemia ja materjaliteadus)
2013–2017	Ho Chi Minhi Tööstuse ja Kaubanduse Ülikool, Vietnam, BSc (Analüütiline keemia)
2010–2013	Bui Thi Xuan gümnaasium, Ho Chi Minh, Vietnam

Keelteoskus

Vietnami keel	Emakeel
Inglise keel	Kõrgtase
Mandariini hiina keel	B1

Teenistuskäik

2017–2019	Minh Long Ltd., Long An maakond, Vietnam, QA/QC

Lühiajaline õppevisiit

2022	LignoCOST CA17128 õppepraktikakool, Åbo Akademi, Soome
2022	Rahvusvaheline kemomeetrika kool – Kopenhaageni Ülikool, Taani

Auhinnad ja tunnustused

2022	Dora Pluss lühiajalise õpirände stipendium (T1.1)
2019–2021	Valitud kandidaat magistriõppe programmi jaoks, Umeå Ülikool, Rootsi
2016–2017	Aastane bakalaureuseõppe stipendium, Ho Chi Minhi Tööstuse ja Kaubanduse Ülikool, Vietnam
2013	väljapaistev üliõpilane, Bui Thi Xuan gümnaasium, Ho Chi Minh, Vietnam

Järelevalve

2022–2023	Bioceb'I (Green Line projekti magistriõppe kaasjuhendamine)
2024–2025	Bakalaureusetöö juhendamine – 'Tuhavaba kraft ligniini tootmise tehnoloogia arendus' – Hanna-Martha Heinla
Suvi 2025	praktika nõustaja – 'Ligniini väärindamine järjestikuse lahusti fraktsioneerimise teel' – Nemo Hennequart

ISSN 2585-6901 (PDF)
ISBN 978-9916-80-456-8 (PDF)